Astrophysical Flows near Static, Spherically Symmetric Black Holes

by

Ayyesha Kanwal Ahmed

Supervised by

Dr. Mubasher Jamil

Submitted in the partial fulfillment of the

Degree of Master of Philosophy

In

Mathematics

School of Natural Sciences,

National University of Sciences and Technology,

H-12, Islamabad, Pakistan.

2016

And, when you want something, all the universe
conspires in helping you to achieve it.

-Paulo Coelho

Dedicated to
My Parents

for their infinite love, support
and encouragement.

Acknowledgements

First of all, I am sincerely thankful to Almighty Allah, the Most Gracious and the Most Merciful, who gave me the strength to carry out research on such an interesting field i.e., Mathematical Physics.

Secondly, I would like to present my heart-felt gratitude to Dr. Mubasher Jamil, my supervisor, for his patience, guidance and support throughout this research work. Without his valuable suggestions and motivation, I would not have reached to such extent. Despite of his busy schedules, he has always made himself available and helped me in every possible good manner. His kind attitude always encouraged me to move ahead. I feel myself fortunate enough to carry out research under his expert supervision. May Almighty Allah bless him with infinite happiness and good health.

I would also acknowledge my GEC members Dr. Umar Farooq and Dr. Adnan Aslam for their cooperation.

In the end I would like to thank especially my father for his endless love, support and encouragement throughout my career; I believe he is the driving force behind my hard work. Last but not the least, I wish to give loud cheers to my husband Arshad S. Awan and my younger sister Munazza K. Ahmed who gave me so much moral support throughout the research work.

Ayyesha Kanwal Ahmed

Abstract

The aim of the present work is to study the spherically symmetric accretion process and to explore its historical background. We have discussed the static spherically symmetric black holes. We have calculated the accretion rate for the Schwarzschild and Reissner-Nordström black holes. By considering the isothermal and polytropic equations of state, we have also explored the accreting properties of the black holes when they are surrounded by the perfect fluid (gas).

Further, to explore the above process, the speed of sound is taken into account; as sound wave is the most basic wave which can easily propagate through any fluid. We have assumed the variations in the density of a flow very small, which enabled us to make approximations for the simplicity of the calculations. Hence, we have found that the accretion rate is maximum, when the fluid is moving transonically in the medium. This transonic behaviour of the fluid leads us to the homoclinic orbits of the fluid, which is moving around the body having infinitesimal mass. Hence, we have found the homoclinic solutions for the Schwarzschild anti-de-Sitter black hole.

Preface

The first chapter is a brief review of the Reimannian geometry and General Relativity. We define the basic terms and definitions which are required to understand the further work of thesis.

The next two chapters are devoted for the literature review. In the second chapter we review the accretion process on Schwarzschild black hole and the homoclinic solutions to the Schwarzschild anti-de-Sitter black hole. We also discuss the general behaviour of flow when the process of accretion is carried out.

In the third chapter we review the transonic solutions for the Reissner-Nordström anti-de-Sitter black hole by assuming the isothermal equation of state. We consider the specific kind of fluids such as ultra-stiff, ultra-relativistic, radiation and sub-relativistic fluid. We also analyse the general behaviour of fluid by assuming the polytropic equation of state.

In the fourth chapter we analyse the same results as discussed in the second and third chapter for the general static spherically symmetric black hole.

In the last chapter, we conclude the thesis in correspondence to the literature review and its extensions.

Throughout the thesis, we use the common relativistic notations. The chosen metric signature is timelike i.e. (-,+,+,+) and the geometric units $G = c = 1$.

Contents

Chapter 1

Introduction

1.1 Review of General Relativity

In 1680*s* *Newton* gave a theory of universal gravitation, in which he showed that time passes uniformly without regard of the motion and speed of the object and in this way he gave the concept of absolute time. Later on, in 1905 *Einstein* determined that all the laws of physics are invariant for the non-accelerating observers in the theory of Special Relativity (SR) and showed that the speed of light in a vacuum is independent of the motion of the observer. He spent ten more years to include the accelerating observers in this theory and so published his theory of General Relativity (GR) in 1916, which is basically the relativistic theory of gravitation. In this theory, he determined that massive objects cause the distortion in spacetime, which is felt as gravity. So his theory of GR generalizes both SR and Newton's theory of gravitation. According to this theory, gravity is defined as the curvature of spacetime[1] and the curvature of a spacetime is directly related to energy and momentum of the matter. Furthermore, he gave the concept of curved spacetime. His theory depends on the following assumptions:

- The gravitational and inertial mass are equivalent, known as the weak equivalence principle whereas, the strong equivalence principle states that within the small regions of spacetime, no experiment can distinguish between an accelerating and gravitational frame of reference.

[1]Spacetime is the sum of all events which are endowed with physical properties and has temporal component as well as spacial components.

- The covariance principle, according to which field equations are generally covariant tensor equations and they remain invariant in all coordinate systems. In other words, it states that all coordinate systems are physically equivalent.

Einstein's theory has many astrophysical implications as it allows to examine the effects of gravity such as gravitational lensing, gravitational time dilation and gravitational redshift, etc. Mainly it implies the existence of black holes which play a very important role in GR. In order to understand the concept of black holes and curved spacetime we need Reimannian geometry. So we start this chapter by giving its short review.

1.1.1 Tensors

Tensors are geometrical objects which are entirely defined in terms of the properties under a coordinate transformation [1]. Usually tensors are involved when directions are required to specify a system like in the case of wind, moving with some velocity in any direction. In order to describe its physical field on the surface, we have to formulate our equations in such away that they will remain valid for all coordinate systems. Furthermore, in the calculation of stresses on a body, we require both the direction of force and the direction of the surface on which the force acts upon. Therefore, we can study stresses mathematically by using tensors. A tensor can be defined as a linear combination of direct product of basis vectors $\underline{e}_\mu$ and co-vectors $\underline{e}^\mu$ such that:

$$\begin{aligned} \mathbf{E} &= E^{\mu\nu}\underline{e}_\mu \otimes \underline{e}_\nu \qquad\qquad (\mu,\nu = 0,1,2,3) \\ \mathbf{F} &= F_{\mu\nu}\underline{e}^\mu \otimes \underline{e}^\nu \\ \mathbf{G} &= G_\mu{}^\nu \underline{e}^\mu \otimes \underline{e}_\nu \quad \text{or} \quad \mathbf{H} = H^\mu{}_\nu \underline{e}_\mu \otimes \underline{e}^\nu, \end{aligned} \tag{1.1.1}$$

where $\mathbf{E}$, $\mathbf{F}$, $\mathbf{G}$ and $\mathbf{H}$ are the tensors; $E^{\mu\nu}$, $F_{\mu\nu}$, $G_\mu{}^\nu$ and $H^\mu{}_\nu$ are their components respectively and $\otimes$ shows the direct product. Note that, a contravariant tensor $\mathbf{E}$ has all upper indices whereas, the covariant tensor $\mathbf{F}$ has all lower indices and mixed tensor has both upper and lower indices.

In other words, we can define a contravariant tensor of rank 2 in terms of geometrical object $\mathbf{T}$, where $T^{\mu\nu}$ under the coordinate transformation

$x^\mu \to x^{\mu'}$ obey the rule

$$T^{\mu'\nu'}(x^{\mu'}) = \frac{\partial x^{\mu'}}{\partial x^\mu}\frac{\partial x^{\nu'}}{\partial x^\nu}T^{\mu\nu}(x^\mu). \tag{1.1.2}$$

Similarly, the components of a covariant tensor of rank 2 transform as

$$T_{\mu'\nu'}(x^{\mu'}) = \frac{\partial x^{\mu}}{\partial x^{\mu'}}\frac{\partial x^{\nu}}{\partial x^{\nu'}}T_{\mu\nu}(x^\mu). \tag{1.1.3}$$

and the mixed tensor of rank 2 will be

$$T^{\mu'}_{\ \nu'}(x^{\mu'}) = \frac{\partial x^{\mu'}}{\partial x^{\mu}}\frac{\partial x^{\nu}}{\partial x^{\nu'}}T^{\mu}_{\ \nu}(x^\mu). \tag{1.1.4}$$

If these coordinates are regular (i.e. $\frac{\partial x^{\mu'}}{\partial x^\mu}$ is invertible), then the tensors defined in (1.1.2), (1.1.3) and (1.1.4) also obey the inverse transformation.

1.1.2 Metric tensor

In order to study the geometrical properties of any surface such as distance between two points, we define a useful quantity called the *metric tensor*. In general we define a metric tensor in terms of basis vectors $\{\underline{e}_\mu\}$ as:

$$\begin{aligned} & g_{\mu\nu} \equiv \underline{e}_\mu \cdot \underline{e}_\nu. \\ \text{Since} \quad & \underline{e}_\mu \cdot \underline{e}_\nu = \underline{e}_\nu \cdot \underline{e}_\mu \\ \text{Therefore,} \quad & g_{\mu\nu} = g_{\nu\mu}, \end{aligned} \tag{1.1.5}$$

i.e., $g_{\mu\nu}$ is a second rank symmetric tensor. The contravariant and mixed forms of metric tensor $\mathbf{g} = g^{\mu\nu}\underline{e}_\mu \otimes \underline{e}_\nu$ or $\mathbf{g} = g_{\mu\nu}\underline{e}^\mu \otimes \underline{e}^\nu$ are given by

$$g^{\mu\nu} = \underline{e}^\mu \cdot \underline{e}^\nu. \tag{1.1.6}$$

$$g^\mu_{\ \nu} = \underline{e}^\mu \cdot \underline{e}_\nu = \delta^\mu_{\ \nu}. \tag{1.1.7}$$

$$\text{Also} \quad g^{\mu\sigma}g_{\sigma\nu} = \delta^\mu_{\ \nu}, \tag{1.1.8}$$

$$\text{and} \quad g^{\mu\nu}g_{\mu\nu} = \delta^\mu_{\ \mu} = 4 \qquad \text{if } \mu,\nu = 0,1,2,3. \tag{1.1.9}$$

For instance, if we consider a 2-dimensional plane polar coordinate system i.e. $x^1 = r$ and $x^2 = \theta$ and the basis vectors are given by

$$\begin{aligned} \underline{e}_r &= \cos\theta\underline{e}_x + \sin\theta\underline{e}_y, \\ \underline{e}_\theta &= -r\sin\theta\underline{e}_x + r\cos\theta\underline{e}_y. \end{aligned} \tag{1.1.10}$$

Then by their dot products, we find that $\underline{e}_r \cdot \underline{e}_r = 1$, $\underline{e}_\theta \cdot \underline{e}_\theta = r^2$ and $\underline{e}_r \cdot \underline{e}_\theta = 0$. Thus, we get $g_{rr} = 1$, $g_{\theta\theta} = r^2$ and $g_{r\theta} = 0$ which can be written in the matrix form as $g_{\mu\nu} = \begin{pmatrix} 1 & 0 \\ 0 & r^2 \end{pmatrix}$. A *metric tensor* is also defined in terms of the arc-length to give the line element ds^2, which measures the distance between two points say $P(x^\mu)$ and $Q(x^\mu + dx^\mu)$ on a manifold[2] such that

$$ds^2 = g_{\mu\nu} dx^\mu \otimes dx^\nu, \tag{1.1.11}$$

which is also called the First Fundamental Form.

1.1.3 Covariant derivative

In order to define a *covariant derivative*, suppose we have a vector field $V(x^\mu)$ which represents a physical quantity. We can express it in terms of basis vector $\{\underline{e}_\mu\}$ or co-vector $\{\underline{e}^\mu\}$ as

$$\mathbf{V} = V^\mu \underline{e}_\mu = V_\mu \underline{e}^\mu. \tag{1.1.12}$$

In terms of the basis vector $\{\underline{e}_\mu\}$, the differential of Eq.(1.1.12) is given as

$$\begin{aligned} dV &= (dV^\mu)\underline{e}_\mu + V^\mu d\underline{e}_\mu \\ &= \Big(V^\mu_{\ ,\nu} dx^\nu\Big)\underline{e}_\mu + V^\mu\Big(\Gamma^\lambda_{\ \mu\nu} dx^\nu \underline{e}_\lambda\Big), \\ &= \Big(V^\lambda_{\ ,\nu} + V^\mu \Gamma^\lambda_{\ \mu\nu}\Big) dx^\nu \underline{e}_\lambda, \\ &= \nabla_\nu V^\lambda dx^\nu \underline{e}_\lambda, \end{aligned} \tag{1.1.13}$$

i.e., $\nabla_\beta V^\alpha = V^\alpha_{\ ,\beta} + \Gamma^\alpha_{\ \beta\mu} V^\mu$ [2]. Analogously, in terms of co-vector $\{\underline{e}^\mu\}$, the differential of Eq. (1.1.12) will be

$$\begin{aligned} dV &= (dV_\mu)\underline{e}^\mu + V_\mu d\underline{e}^\mu \\ &= \Big(V_{\mu,\nu} dx^\nu\Big)\underline{e}^\mu + V_\mu\Big(- \Gamma^\mu_{\ \lambda\nu} dx^\nu \underline{e}^\lambda\Big), \\ &= \Big(V_{\lambda,\nu} - V_\mu \Gamma^\mu_{\ \lambda\nu}\Big) dx^\nu \underline{e}^\lambda, \\ &= \nabla_\nu V_\lambda dx^\nu \underline{e}^\lambda, \end{aligned} \tag{1.1.14}$$

[2]A manifold is a set of points satisfying the covering property, smooth overlapping property and Hausdorff property which is topologically same as the locally Euclidean space (i.e. around every point there exists a neighbourhood which is topologically same as the unit ball).

i.e., $\nabla_\beta V_\alpha = V_{\alpha,\beta} - \Gamma^{\mu}_{\ \alpha\beta} V_\mu$. Here, $\Gamma^{\alpha}_{\ \beta\mu}$ is special kind of symbol known as the *Christoffel symbol*, which is said to define a connection on the manifold in such away that it is possible to connect a vector in the tangent space at a point (say P) with the vector parallel to it at another point (say Q) see figure 1.1 [3]. There is some degree of freedom in the specification of affine connection, i.e., $\Gamma^{\lambda}_{\ \mu\nu} = \Gamma^{\lambda}_{\ \nu\mu}$. They are given as

$$d\underline{e}_\lambda = \Gamma^{\gamma}_{\ \lambda\beta} \underline{e}_\gamma dx^\beta, \tag{1.1.15}$$

where $\Gamma^{\lambda}_{\ \mu\nu} = \frac{1}{2} g^{\lambda\alpha}(g_{\alpha\mu,\nu} + g_{\nu\alpha,\mu} - g_{\mu\nu,\alpha})$. We can explain it further by letting a curve γ and a tangent vector u^α which lies on a curve having the vector field A^α defined in the neighbourhood of the curve γ. If the point P has coodinates x^α and Q has coordinates $x^\alpha + dx^\alpha$ whereas, $A^\alpha(P)$ and $A^\alpha(Q)$ are the vectors on these coordinates respectively, then by the parallel transport of vectors, vector $A^\alpha(P)$ can be moved to the point Q so that $A^\alpha(P)$ is parallel to $A^\alpha_\parallel(Q)$. In this way, the difference between these vectors will be a covariant derivative as shown in the figure 1.1.

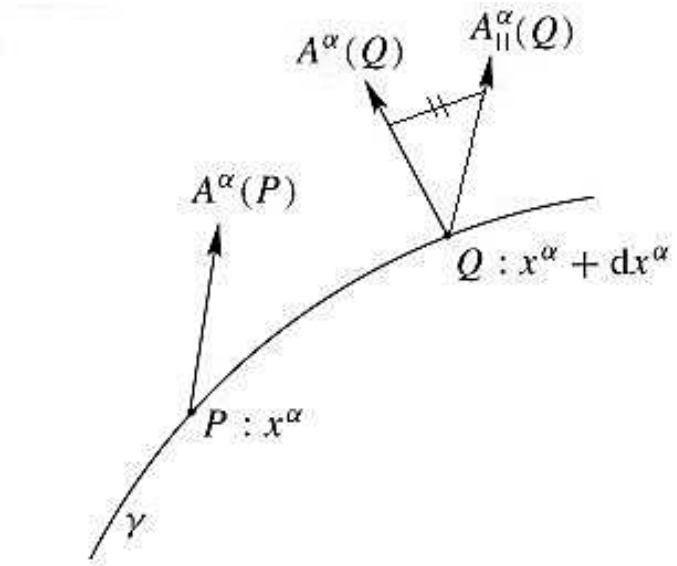

Figure 1.1: Vector field A^α on a curve in manifold [4].

1.1.4 Reimann, Ricci and Einstein tensor

In GR the presence of gravity is indicated by the curvature of spacetime. The curvature tensor or Reimann tensor provides a measure of this curvature [3]. It is defined as:

$$R^{\sigma}{}_{\mu\nu\lambda} = \Gamma^{\sigma}{}_{\mu\lambda,\nu} - \Gamma^{\sigma}{}_{\mu\nu,\lambda} + \Gamma^{\sigma}{}_{\alpha\nu}\Gamma^{\alpha}{}_{\mu\lambda} - \Gamma^{\sigma}{}_{\alpha\lambda}\Gamma^{\alpha}{}_{\mu\nu}. \tag{1.1.16}$$

In Reimannian geometry, *curvature invariants* are those scalar quantities which are usually constructed by the Reimann tensor and they represent the curvature of a spacetime. They are given by

$$\begin{aligned} I_1 &= R, \\ I_2 &= R^{\mu\nu}R_{\mu\nu}, \\ I_3 &= R^{\mu\nu\sigma\rho}R_{\mu\nu\sigma\rho}. \end{aligned} \tag{1.1.17}$$

These quantities are known as the first, second and third curvature invariants respectively, whereas R is the *Ricci scalar* and $R_{\mu\nu}$ is the *Ricci tensor* defined as

$$R = R^{\mu}{}_{\mu} = g^{\mu\nu}R_{\mu\nu}. \tag{1.1.18}$$

$$R_{\mu\nu} = g^{\lambda\sigma}R_{\lambda\mu\sigma\nu} = R^{\sigma}{}_{\mu\sigma\nu}. \tag{1.1.19}$$

In differential geometry, there is another type of tensor called the *Einstein tensor*, which is usually used to express the curvature of spacetime and is denoted by $G_{\mu\nu}$. The Einstein tensor is given by

$$G_{\mu\nu} = R_{\mu\nu} - \frac{1}{2}g_{\mu\nu}R. \tag{1.1.20}$$

Note that the Einstein tensor is symmetric, i.e., $G_{\mu\nu} = G_{\nu\mu}$.

1.1.5 Energy momentum tensor

The source of gravitational field is the energy momentum tensor denoted by $T^{\mu\nu}$. It represents the physical properties of material things in a specific spacetime. In component form T^{00} is the energy density; T^{10}, T^{20} and T^{30} are the momentum densities; T^{11}, T^{22} and T^{33} are the components of isotropic

pressure; T^{01}, T^{02} and T^{03} show energy flux and rest are the components of stress [1].

For instance, the *perfect fluid* is defined as the fluid for which there exists no such forces between the particles which oppose their motion, no heat conduction or viscosity in the instantaneous rest frame[3] (IRF) [5] and is represented as

$$T_{\mu\nu} = (e+p)u_\mu u_\nu + p g_{\mu\nu}, \tag{1.1.21}$$

where $T_{\mu\nu}$ is the energy momentum tensor, u^μ is the four-velocity, e and p are the density and pressure respectively. The trace T of Eq. (1.1.21) is given by

$$T = T^{\mu}_{\ \mu} = e + 3p. \tag{1.1.22}$$

Some other special cases for the perfect fluid are:

$$\begin{aligned}
\text{Dust (pressureless fluid):} \quad & T_{\mu\nu} = e u_\mu u_\nu \quad (p=0).\\
\text{Empty space (vacuum):} \quad & T_{\mu\nu} = 0 \quad (p=e=0).\\
\text{Cosmological constant:} \quad & T_{\mu\nu} = \Lambda g_{\mu\nu} \quad (p=-e=\Lambda).\\
\text{Radiation:} \quad & T_{\mu\nu} = \Big(\frac{4e}{3}\Big)u_\mu u_\nu + \frac{e}{3}g_{\mu\nu} \quad (p=\frac{e}{3}).
\end{aligned}$$

For instance, the energy-momentum tensor for an electromagnetic field is

$$T^{\mu\nu}_{(em)} = \frac{-1}{\mu_0}\Big[F^{\mu}_{\ \sigma}F^{\nu\sigma} - \frac{1}{4}g^{\mu\nu}F_{\sigma\rho}F^{\sigma\rho}\Big], \tag{1.1.23}$$

where μ_0 is the constant and $F^{\mu\nu}$ is the Maxwell or electromagnetic tensor.

1.1.6 Einstein field equations

Historically, *Einstein* and *Hilbert* separately found the gravitational field equations of GR in 1915. According to them, curvature of spacetime at any event is related to the energy momentum tensor of the matter content at that event [3]. These equations are given by

$$G_{\mu\nu} + \Lambda g_{\mu\nu} = \kappa T_{\mu\nu}. \tag{1.1.24}$$

[3]The frame of reference which is inertial at each instant i.e. the frame of reference where time and space varies homogenously.

Using Eq. (1.1.20) we obtain

$$R_{\mu\nu} - \frac{1}{2}Rg_{\mu\nu} + \Lambda g_{\mu\nu} \;\; = \;\; \kappa T_{\mu\nu}. \tag{1.1.25}$$

In vacuum, we have $T_{\mu\nu} = 0$ which implies $R_{\mu\nu} = 0$ and is known as vacuum Einstein field equations. In Einstein's theory, field equations is the set of 10 non-linear partial differential equations with 20 unknowns (10 components of $g_{\mu\nu}$ and 10 components of $T_{\mu\nu}$). In contrast to this, we have only one field equation in Newtonian theory, i.e., $\nabla^2\Phi = 4\pi G\rho$ (also called the Poisson's equation). A large number of solutions have been found by solving the Einstein's field equations [6]. They are usually obtained by imposing symmetries on the spacetime in such away that the metric coefficients can be calculated. The very first solution of these equations was obtained by Karl Schwarzschild in 1916 [7] which describes static, spherically symmetric black hole of mass M.

1.2 Black Hole

Black hole is a geometrical defined region of space-time. The term *black hole* was invented by R. Ruffini and J.A. Wheeler in 1967 [8]. The black holes are usually found at the center of galaxies. A massive star is made up of dust clouds and gases such as hydrogen and helium. This will undergo a gravitational collapse continuously throughout its life cycle. Generally, it happens when the star has totally consumed its nuclear fuel and there is no supporting force left behind which provides a balance against the internal pull of gravity. This is a situation when the whole matter collapses and shrinks due to its own gravity. Therefore, gravity overcomes the fundamental forces of nature, which eventually provides the pressure in a star that helps it to balance against the gravity pull. Hence, the final outcome of this collapse will depend on the initial mass of the star. If the mass of the star is such that $M \leq 1.44{M_\odot}^4$ (Chandrasekhar limit), then it is supported by the electron degeneracy pressure and is known as *White Dwarf*. On the other hand, if the mass of the star is such that $1.4M_\odot \leq m \leq 3.2M_\odot$, then the gravitational collapse overcomes the neutron degeneracy pressure and we call it a *Neutron*

[4] $M_\odot$ is the solar mass i.e. $1.9891 \times 10^{30} kg$.

Star whereas, the star whose mass is three times the mass of the sun or more and it collapse, it forms a black hole.

If the star is more massive, then there does not exist any force that can maintain the balance between the internal pressure and the gravitational pull, therefore the collapse continues and creates a spacetime singularity. It is a region where all the physical parameters such as mass, energy densities and spacetime curvatures reach to their extreme and blow up [9]. Within this singularity, the gravitational pull is so strong that it forms a one-way membrane from which nothing could escape, not even light and is known as *Event Horizon*. In other words, we can say that it is the point of no return. The size of event horizon is considered as the size of the black hole, which means the more massive the black hole is, the larger will be its event horizon. It is clear that the event horizon must form before the spacetime singularity, as if the event horizon forms after the spacetime singularity then nothing could be observable and all the matter is supposed to be squeezed into an infinite singularity at the center of the black hole. As we move away from the event horizon we get the *Naked Singularity* which is the final state of the gravitational collapse. Furthermore, there are two different types of singularities exists for a black hole. We can define them with the help of curvature invariants I_1, I_2 and I_3 (as mentioned in Eq. 1.1.17). At the point where singularity arises, if these curvature invariants are finite then we call it as a coordinate singularity which is not a physical singularity so we can remove it with the help of Eddington-Finkelstein coordinates, Kruskal coordinates etc. However, if any of these invariants become infinite then the singularity is called curvature singularity which is the physical singularity and hence cannot be removed.

In figure 1.2 we see that there is a matter which is continually collapsing and shrinks under the force of its own gravity. In the center there is a spacetime singularity and the region bounded by the singularity is the event horizon. Note that, the black hole is a space-time region which is characterized by the metric or line element. The speciality of this region is that it is disconnected from the rest of the space which means there is no influence of such events on it which are carried outside this region. There are different types of black hole. Some of them are discussed below.

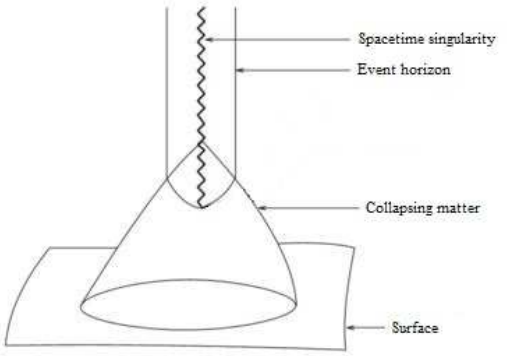

Figure 1.2: Event horizon and singularity of a black hole [9].

1.2.1 Schwarzschild solution

In 1916 Karl Schwarzschild gave the first solution of the Einstein field equations. It is the static spherically symmetric solution of the vacuum Einstein's field equations (EFE) given by [7]

$$ds^2 = -\Big(1-\frac{2M}{r}\Big)dt^2+\Big(1-\frac{2M}{r}\Big)^{-1}dr^2+r^2(d\theta^2+\sin^2\theta d\phi^2), \quad (1.2.1)$$

where M is the mass and r is the radial coordinate. The event horizon occurs where $g_{tt}\to 0$ and is given by

$$1-\frac{2M}{r_h} = 0 \quad \Rightarrow \quad r_h = 2M. \quad (1.2.2)$$

The metric given in (1.2.1) has two potential singularities at $r_h = 2M$ and $r = 0$. The curvature invariants for (1.2.1) are given as:

$$\begin{aligned} I_1 &= 0. \\ I_2 &= 0. \\ I_3 &= \frac{48M^2}{r^6}. \end{aligned} \quad (1.2.3)$$

So it is clear that $r_h = 2M$ is a coordinate singularity which is removable and $r = 0$ is a curvature singularity which cannot be removed because I_3 becomes divergent at $r = 0$ in Eq. (1.2.3).

1.2.2 Reissner-Nordström solution

The metric of Reissner-Nordström (RN) black hole was given by Hans Reissner and Gunnar Nordström [10, 11]. The RN metric is a static spherically

symmetric electrically charged solution of EFE(s). However, it is a non-vacuum solution, since the source has an electric charge Q and hence there is an electric field. The stress-energy momentum tensor ($T^{\mu\nu}$) for electromagnetic field is given in Eq. (1.1.23) and the metric is given by

$$\begin{aligned} ds^2 &= -\frac{\Delta}{r^2}dt^2 + \frac{r^2}{\Delta}dr^2 + r^2(d\theta^2 + \sin^2\theta d\phi^2), \\ \text{where,} \qquad \Delta &\equiv r^2 - 2Mr + Q^2. \end{aligned} \tag{1.2.4}$$

Here M is the mass and Q is the total electric charge on a black hole. The event horizon occurs where $g_{tt} \to 0$ (or $\Delta \to 0$) and is given as

$$\Delta = (r - r_-)(r - r_+), \tag{1.2.5}$$

where $r_\pm$ represents the radii of horizons i.e. $r_\pm = M \pm \sqrt{M^2 - Q^2}$. Here, r_+ denotes the event horizon because when $Q = 0$, it reduces to the Schwarzschild's horizon. In the limit $Q \to 0$, the RN black hole becomes a Schwarzschild black hole. The metric in (1.2.4) has three potential singularities at $r = 0, r_\pm$. The curvature invariants are given as:

$$\begin{aligned} I_1 &= 0. \\ I_2 &= \frac{4Q^4}{r^8}. \\ I_3 &= \frac{8(6M^2r^2 - 12MQ^2r + 7Q^4)}{r^8}. \end{aligned} \tag{1.2.6}$$

So it is clear that $r = 0$ is a curvature singularity which cannot be removed and $r = r_\pm$ is a coordinate singularity which can be removed by using the Eddington-Finkelstein coordinates or Kruskal coordinates.

1.3 Hamilton Jacobi Equations

The dynamical system which is described by the Hamiltonian is called the *Hamiltonian system*. If the state of the system is defined with the generalized coordinates, then the canonical form of Hamiltonian can be derived by using the Legendre transformation to the Lagrangian. If we consider Lagrangian as a function of $t, q, \dot{q}$ such that

$$\mathcal{L} = \mathcal{L}(t, q_1, ..., q_n, \dot{q_1}, ..., \dot{q_n}), \tag{1.3.1}$$

where t is the time coordinate, while q_i and $\dot{q}_i$ are the generalized coordinates and generalized velocities respectively. By applying the Lagendre transform, we know that the new function $\mathcal{H}$ will depend on t and q_i and the derivatives of $\mathcal{L}$ w.r.t $\dot{q}_i$ i.e.

$$\begin{aligned} \mathcal{H} &= \mathcal{H}\left(t, q_i, \frac{\partial \mathcal{L}}{\partial \dot{q}_i}\right), \\ \mathcal{H} &= \mathcal{H}(t, q_i, p_i), \end{aligned} \tag{1.3.2}$$

where $p_i = \frac{\partial \mathcal{L}}{\partial \dot{q}_i}$, the generalized momentum conjugate to q_i. Hence, by the Lengendre transform we can write

$$\mathcal{H}(t, q_i, p_i) = \sum_{i=1}^{n} p_i \dot{q}_i - \mathcal{L}(t, q_i, \dot{q}_i). \tag{1.3.3}$$

Further, Hamiltonian principle states that the action integral of a system in a certain time period is stationary i.e.

$$\delta I = \delta \int_{t_1}^{t_2} \mathcal{L} dt = 0. \tag{1.3.4}$$

In the Hamiltonian formulation both the coordinates and momentum lie on the same point, so by using Eq. (1.3.4) in (1.3.3) we get

$$\delta I = \delta \int_{t_q}^{t_2} \left[\sum_{i=1}^{n} p_i \dot{q}_i - \mathcal{H}(t, q_i, \dot{q}_i) \right] dt = 0. \tag{1.3.5}$$

Clearly, the term inside the square bracket is a fuction of $t, p_i, \dot{p}_i, q_i$ and $\dot{q}_i$. Therefore,

$$\delta I = \delta \int_{t_q}^{t_2} f(t, p_i, \dot{p}_i, q_i, \dot{q}_i) dt = 0. \tag{1.3.6}$$

Now the Euler-Lagrange equations for both generalized coordinates leads us to the following equations

$$\frac{d}{dt}\left(\frac{\partial f}{\partial \dot{q}_i}\right) - \frac{\partial f}{\partial q_i} = 0, \tag{1.3.7}$$

$$\frac{d}{dt}\left(\frac{\partial f}{\partial \dot{p}_i}\right) - \frac{\partial f}{\partial p_i} = 0. \tag{1.3.8}$$

We know that

$$\begin{aligned} \frac{\partial f}{\partial \dot{q}} &= p, \quad \frac{d}{dt}\frac{\partial f}{\partial \dot{q}} = \dot{p} \quad \text{and} \quad \frac{\partial f}{\partial q} = -\frac{\partial \mathcal{H}}{\partial q}. \\ \frac{\partial f}{\partial \dot{p}} &= q, \quad \frac{d}{dt}\frac{\partial f}{\partial \dot{p}} = \dot{q} \quad \text{and} \quad \frac{\partial f}{\partial p} = \frac{\partial \mathcal{H}}{\partial p}. \end{aligned} \tag{1.3.9}$$

Using these values in Eq. (1.3.7) and (1.3.8) we get

$$\frac{\partial \mathcal{H}}{\partial q} = -\dot{p}, \tag{1.3.10}$$

$$\frac{\partial \mathcal{H}}{\partial p} = \dot{q}, \tag{1.3.11}$$

which are known as the canonical forms of the Hamiltonian.

1.3.1 Conserved system and conservation laws

A dynamical system in which no change occurs in the quantities during the physical processes i.e. the system remain in a constant state is called *conserved system* and the quantities are called the *conserved quantities*. The conserved quantities are related to symmetries. For this we have the *Noether Theorem*, which states that whenever there is a continuous symmetry of Lagrangian, there is an associated conservation law. Here symmetry means the transformation of the generalized coordinates t, q_i and $\dot{q}_i$. We have two basic conservation laws for accretion which are discussed below.

(i) Particle conservation

In particle conservation, particles are neither created nor destroyed. In other words, the change in the flux is zero. Mathematically,

$$\nabla_\mu J^\mu = 0. \tag{1.3.12}$$

So, by using Eq. (1.1.13)

$$\nabla_\mu J^\mu = J^\mu{}_{,\mu} + \Gamma^\mu{}_{\mu\nu} J^\nu. \tag{1.3.13}$$

From the Reimanian geometry ($ds^2 > 0$), we have the identity $\Gamma^{\mu}_{\ \mu\alpha} = \frac{1}{\sqrt{-g}}(\sqrt{-g})_{,\alpha}$. So,

$$\begin{aligned}
\nabla_\mu J^\mu &= \frac{1}{\sqrt{-g}}\sqrt{-g}J^{\mu}_{\ ,\mu} + \frac{1}{\sqrt{-g}}(\sqrt{-g})_{,\nu}J^\nu \\
&= \frac{1}{\sqrt{-g}}[\sqrt{-g}J^{\mu}_{\ ,\mu} + (\sqrt{-g})_{,\mu}J^\mu] \\
&= \frac{1}{\sqrt{-g}}(\sqrt{-g}J^\mu)_{,\mu}. \qquad (1.3.14)
\end{aligned}$$

In the case of static spherically symmetric metric on equatorial plane ($\theta = \pi/2$), we know $\sqrt{\mid -g \mid} = r^2$, therefore by Eq. (1.3.12) and (1.3.13) we get

$$\nabla_\mu J^\mu = \frac{1}{r^2}(r^2 J^\mu)_{,\mu} = 0. \qquad (1.3.15)$$

(ii) Energy-momentum conservation

By the energy-momentum conservation, we mean that the rate of change of energy transfer is zero i.e.

$$\nabla_\mu T^{\mu}_{\ \nu} = 0. \qquad (1.3.16)$$

As we know that

$$\nabla_\mu T^{\mu}_{\ \nu} = T^{\mu}_{\ \nu,\mu} + \Gamma^{\mu}_{\ \mu\alpha}T^{\alpha}_{\ \nu} - \Gamma^{\alpha}_{\ \nu\mu}T^{\mu}_{\ \alpha}. \qquad (1.3.17)$$

Using the identity $\Gamma^{\mu}_{\ \mu\alpha} = \frac{1}{\sqrt{-g}}(\sqrt{-g})_{,\alpha}$ in Eq. (1.3.17) we have

$$\begin{aligned}
\nabla_\mu T^{\mu}_{\ \nu} &= \frac{1}{\sqrt{-g}}[\sqrt{-g}T^{\mu}_{\ \nu,\mu} + (\sqrt{-g})_{,\alpha}T^{\alpha}_{\ \nu}] - \Gamma^{\alpha}_{\ \nu\mu}T^{\mu}_{\ \alpha} \\
&= \frac{1}{\sqrt{-g}}(\sqrt{-g}T^{\mu}_{\ \nu})_{,\mu} - \Gamma^{\alpha}_{\ \nu\mu}T^{\mu}_{\ \alpha}. \qquad (1.3.18)
\end{aligned}$$

$$\begin{aligned}
\text{Since,} \qquad \Gamma^{\alpha}_{\ \nu\mu} &= g^{\gamma\alpha}\Gamma_{\gamma\nu\mu} \\
\Gamma^{\alpha}_{\ \nu\mu}T^{\mu}_{\ \alpha} &= \Gamma_{\gamma\nu\mu}g^{\gamma\alpha}T^{\mu}_{\ \alpha} \\
&= \Gamma_{\gamma\nu\mu}T^{\mu\gamma} \\
&= 0, \qquad (1.3.19)
\end{aligned}$$

as $\Gamma_{\gamma\nu\mu}$ is anti-symmetric and $T^{\mu\gamma}$ is symmetric in $(\gamma\mu)$ therefore, their product will be zero. In this way, Eq. (1.3.18) becomes

$$\nabla_\mu T^\mu_{\ \nu} = \frac{1}{\sqrt{-g}}(\sqrt{-g}T^\mu_{\ \nu})_{,\mu}. \tag{1.3.20}$$

Further, on having static spherical symmetry on equatorial plane, it can be written as

$$\nabla_\mu T^\mu_{\ \nu} = \frac{1}{r^2}(r^2 T^\mu_{\ \nu})_{,\mu} = 0. \tag{1.3.21}$$

Similarly, by the conservation of energy-momentum tensor of a perfect fluid, we can define the **relativistic Euler equation** as

$$(e+p)_{;\mu}u^\mu u^\nu + (e+p)(u^\mu u^\nu)_{;\mu} + p_{;\mu}g^{\mu\nu} = 0. \tag{1.3.22}$$

Multiplying by u_ν on both sides, Eq. (1.3.22) becomes

$$u^\mu(e+p)_{;\mu} + (e+p)(u^\mu_{\ ;\mu}) + p_{;\mu}u^\mu = 0. \tag{1.3.23}$$

After simplifying it and putting its value back in Eq. (1.3.22), we get

$$(e+p)(\nabla_\mu u^\nu)u^\mu = -[g^{\mu\nu}\nabla_\mu p + u^\mu u^\nu \nabla_\mu p], \tag{1.3.24}$$

which is the momentum-conservation or relativistic Euler equation of motion [12].

1.4 Astrophysical Fluid and Flows

Usually a material deforms when different forces act upon it. If the deformation continuously increases without limit, the phenomenon is known as *flow* and anything that can flow is called *fluid*. The *fluid element* is defined as a region over which we can define our local variables such as density, temperature etc. [13].

Astrophysical fluids are the fluids which flows anywhere in space. There are certain equations in astrophysics which provides the complete information about the flow mathematically and are known as *equations of state*. They show the relationship between pressure and other thermodynamical properties of the system. We can compute all the thermodynamic quantities

with the help of them. For instance, we have *isothermal fluid* which refers to the fluid flowing at a constant temperature. Its equation of state is $p = ke$, where p is the pressure, k is constant such that $0 < k \leq 1$ and e is the energy density. Another type of fluid is the *polytropic fluid*. Polytropic fluid refers to the solution of polytropes in which pressure depends on the density in the form $p = k\rho^{\Gamma}$, where k and Γ are the constants. Similarly, in case of *dust* (pressureless fluid) the equation of state is $p = 0$.

If the fluid is moving in adiabatic and reversible system i.e. the entropy of a fluid moving along a stream line[5] is constant, then we call it *isentropic flow*. Isentropic flow is an idealized flow in thermodynamics in which the system is frictionless. Neither heat transformation nor energy transformations occur due to friction or dissipative effects.

1.4.1 Homoclinic flow

Homoclinic flow corresponds to the motion of a fluid in the homoclinic orbit. Let $f(x,t)$ be a function and $O(x)$ be the orbit such that $O(x) = \{f(x,t) : t \in [\alpha, \beta]\}$. Let x^* be the fixed point such that $f(x,t) \to x^*$ as $t \to k \in \mathbf{R}$, then the orbit $O(x)$ is called a *homoclinic orbit*. Its solution guarantees that there exists only one critical point of a conserved system for a certain range of parameters and that critical point forms a trajectory of a flow that joins a critical point to itself [14]. For instance, if we consider a particle moving on the surface of a Mobius strip with $f(t,x,y) = (R+x)\cos t, (R+x)\sin t, y$ such that $t \in [0, 4\pi]$ then we see that the geometry of its motion defines a homoclinic orbit as shown in figure 1.3.

1.5 Review of Accretion

In astrophysics, *accretion* is a term which is usually used to describe the inflow of matter towards the center of the mass of a compact object (which has low volume and high density) such as white dwarfs, neutron stars and black holes. It is defined as "the process by which any compact object or a star gravitationally captures some ambient matter" [12], or in other words we can

[5]The path of particles which are flowing along the fluid.

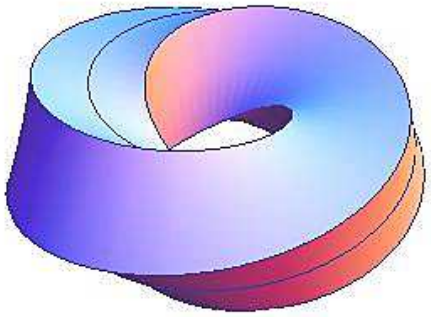

Figure 1.3: Mobius strip showing a homoclinic orbit.

define *accretion* as a process by which any gravitating object, gravitationally captures some matter towards its center due to which its mass increases. The rate at which matter is accreted is known as the *accretion rate*.

The history of research on accretion begins more than 60 years back with Bondi in 1952 [15]. He worked within the Newtonian framework and found that whether a transonic[6] solution is possible for the perfect fluid (gas) when accreting onto compact object. Its relativistic version was given by Michel in 1972 [16]. He studied the accretion using steady state spherically symmetrical flow of a test gas around a Schwarzschild black hole. His work attracted many other astrophysicists like Shapiro and Teukolsky [12] and they began to start work in this context.

Later on, the concept of *dark energy* was found. *Dark energy* is the energy that exerts a negative pressure, tending to accelerate the expansion of the universe. This *dark energy* represents the so-called *phantom energy*. These are the hypothetical form of energies. Phantom energy is more potent than the dark energy, as it expands the universe so quickly that the phenomenon of Big Rip (in which all spacetime would torn apart) would occur. Babichev et al [17], discussed the effect of accretion of dark energy onto Schwarzschild black hole and found that the mass of the black hole increases when the gas

[6]The point where the speed of the fluid approaches the speed of sound.

is accreted whereas, the accretion of phantom energy will reduce the mass of black hole and the mass of the black hole completely vanishes near Big Rip. The accretion of phantom energy onto Banados-Teitelboim-Zanelli (BTZ) black hole was studied by Jamil and Akbar [18]. In their work they showed that due to the accretion of phantom energy, the mass of black hole decreases. Phantom energy accretion onto Schwarzschild anti-de-Sitter black with topological defect was studied by Amani and Farahani [19]. They also showed that the mass of black hole decreased due to phantom energy, even with a topological defect (solution that exists on the boundary) in the black hole. Mach et al [20] discovered the homoclinic type solutions for the polytropic gas in anti-de-Sitter spacetime. Later on, they also investigated the stability of Michel-type accretion on it. Ganguly et al [21], discussed the effect of a string cloud parameter onto the Schwarzschild black hole when polytropic fluid is accreted and found that accretion rate in a string cloud background is higher than that of a simple black hole. Recently, Ficek has investigated the accretion process in the Reissner Nordstöm anti-de-Sitter spacetime [22].

In space there are billions of stars and compact objects which continuously lose their energy upon collisions with other compact objects. Due to this, these stars slowly start moving towards the center which actually gave rise to the concept of accretion which show different behaviours of flow. For instance, the accretion is sub-sonic (where speed of fluid is less than the speed of sound) when it occurs outside the black hole and at the horizon the accretion is transonic. We usually calculate the accretion rate at the sonic (critical) point because the velocity of the fluid is equal to the speed of sound at the sonic point and hence the accretion rate is maximum at this point. Furthermore, there is an important source of accretion which is known as *radiant energy*. It is the energy produced by electromagnetic radiation (light, X-rays etc.) emitted by the black hole. The basic types of accretion are:

(i) Spherically symmetric accretion: It occurs when the relative velocity of the fluid is much less than the speed of sound at the sonic (critical) point i.e. $v_{rel} \ll a_s$ and there is no significant amount of angular momentum in it [3].

(ii) Cylindrical accretion: The relative velocity of the fluid is either greater or equal to the speed of sound at the sonic point i.e. $v_{rel} \geq a_s$

having the small amount of angular momentum [3].
(iii) Disk accretion: There is a considerable amount of angular momentum [3]. The gases and dust rotate around the accretor (compact object) and forms a disk.

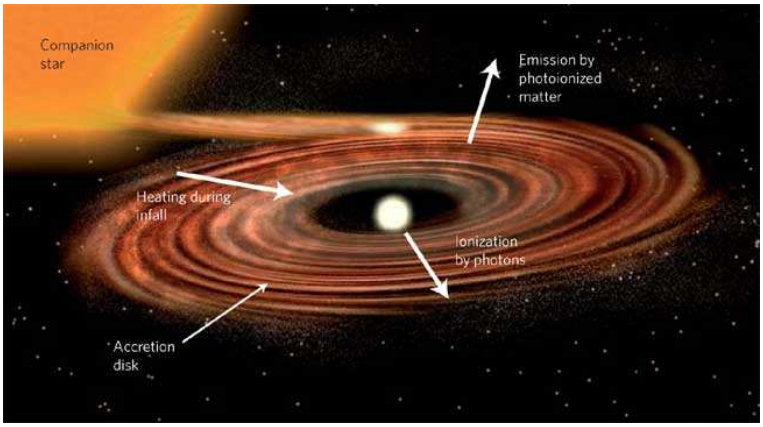

Figure 1.4: An overview of accretion onto a compact star.

The aim of studying the accretion is to obtain the net energy output which is emitted by the infalling gases when accreted onto compact objects. Mathematically, the accretion rate is given by [15]

$$\dot{M} = 4\pi r_s^2 n_s v_s m, \tag{1.5.1}$$

where $\dot{M}$ denotes the accretion rate, r is the radial coordinate, n, v and m are the number density, velocity and mass respectively of the flow and the subscript "s" denotes all these values at the sonic point. This concept further leads to the luminosity L (radiant energy per unit time) which is given as

$$L = \eta \dot{M}, \tag{1.5.2}$$

where L denotes the luminosity and η is the efficiency of conversion of matter into energy. From Eq. (1.5.2) it is clear that $L \propto \dot{M}$ which means the higher the accretion rate is, the higher will be the radiant energy and so luminosity. The luminosity will be maximum when the compact object achieves the hydrostatic equilibrium, which means both the outward force of radiation and the inward gravitational pull becomes equal. This is also called the *Eddington luminosity*.

1.5.1 Bondi accretion

In 1952 Bondi was the first astrophysicist who studied the steady state, spherically symmetric model of accretion under the Newtonian limit [15]. It is the simplest case of accretion. As there is no significant angular momentum in it therefore, the matter easily accrets inside the compact object. The model discussed by the Bondi was that in an infinite cloud of gas, there is a star of mass M having uniform density and pressure. The motion of the gas was steady and spherically symmetrical and the increase in the mass of the star ignored at first, so that the field of force of gravity remains constant [15]. The conservation equations for an ideal fluid in this state are

$$\frac{1}{r^2}\frac{d}{dr}(r^2\rho v) = 0 \tag{1.5.3}$$

$$v\frac{dv}{dr} + \frac{1}{\rho}\frac{dp}{dr} + \frac{M}{r^2} = 0, \tag{1.5.4}$$

where ρ, p, v be density, pressure and velocity of the gas particles respectively. If the gas particles satisfies the polytropic equation of state then the density and pressure are related as:

$$\frac{p}{p_\infty} = \left(\frac{\rho}{\rho_\infty}\right)^\gamma, \tag{1.5.5}$$

where ρ_∞ and p_∞ is the density and pressure of the gas at infinity, and γ is a constant such that $1 \leq \gamma \leq \frac{5}{3}$. For instance, $\gamma = 1$ and $\gamma = 5/3$ represent the isothermal and adiabatic flow respectively. Bondi considered all this in adiabatic system. By taking r the radial coordinate and v as the inward velocity of the gas, the continuity equation is obtained by integrating the Eq. (1.5.3) given by

$$4\pi r^2 \rho v = C_1, \tag{1.5.6}$$

where C_1 is a constant which is the accretion rate, $4\pi r^2$ is the area and ρv is the flux of the gas particles. On the other hand, if we integrate Eq. (1.5.4) we get the Bernoulli equation as

$$\frac{v^2}{2} + \int_{p_\infty}^{p} \frac{dp}{\rho} - \frac{M}{r} = C_2. \tag{1.5.7}$$

From Eq. (1.5.5) we have

$$p = p_\infty \Big(\frac{\rho}{\rho_\infty}\Big)^\gamma. \tag{1.5.8}$$

Taking differential of above equation and dividing by ρ on both sides we get

$$\frac{dp}{\rho} = \frac{\gamma p_\infty}{\rho_\infty^\gamma}\rho^{\gamma-2}d\rho. \tag{1.5.9}$$

Integrating both sides by taking boundary conditions at infinity so that

$$\begin{aligned}
\int_{p_\infty}^{p}\frac{dp}{\rho} &= \frac{\gamma p_\infty}{\rho_\infty^\gamma}\int_{\rho_\infty}^{\rho}\rho^{\gamma-2}d\rho, \\
&= \frac{\gamma p_\infty}{\rho_\infty^\gamma}\frac{\rho^{\gamma-1}}{\gamma-1}\Big|_{\rho_\infty}^{\rho}, \\
&= \frac{\gamma}{\gamma-1}\frac{p_\infty}{\rho_\infty^\gamma}\Big[\rho^{\gamma-1}-\rho_\infty^{\gamma-1}\Big], \\
&= \frac{\gamma}{\gamma-1}\frac{p_\infty}{\rho_\infty}\Big[\Big(\frac{\rho}{\rho_\infty}\Big)^{\gamma-1}-1\Big].
\end{aligned} \tag{1.5.10}$$

Using Eq. (1.5.10) in (1.5.7) we have

$$\frac{v^2}{2}+\frac{\gamma}{\gamma-1}\frac{p_\infty}{\rho_\infty}\Big[\Big(\frac{\rho}{\rho_\infty}\Big)^{\gamma-1}-1\Big] = \frac{M}{r}. \tag{1.5.11}$$

Now by using Eq. (1.5.9), we can find the speed of sound as

$$a^2 = \frac{dp}{d\rho} = \frac{\gamma p_\infty}{\rho_\infty^\gamma}\rho^{\gamma-1}, \tag{1.5.12}$$

$$= \frac{\gamma p_\infty}{\rho}\Big(\frac{\rho}{\rho_\infty}\Big)^\gamma, \tag{1.5.13}$$

$$= \frac{\gamma p}{\rho}, \tag{1.5.14}$$

by taking the boundary condition at infinity

$$a^2 = \frac{\gamma p_\infty}{\rho_\infty}. \tag{1.5.15}$$

To simplify the system further, Bondi introduced the dimensionless variables such that

$$x = \frac{ra^2}{M}\ ,\ y = \frac{v}{a} \quad \text{and} \quad z = \frac{\rho}{\rho_\infty}. \tag{1.5.16}$$

On putting these variables in Eqs. (1.5.6) and (1.5.11), we get

$$A = 4\pi\lambda M^2 a^{-3}\rho_\infty, \tag{1.5.17}$$

$$\frac{y^2}{2} + \frac{(z^{\gamma-1}-1)}{\gamma-1} = \frac{1}{x}, \tag{1.5.18}$$

where $\lambda = x^2yz$. Hence, the accretion rate given by Bondi was [15]

$$\dot{M} = \frac{dM}{dt} = 4\pi\lambda M^2 a^{-3}\rho_\infty, \tag{1.5.19}$$

where $\dot{M}$ is the accretion rate, M is the mass of the star, λ is the dimensionless parameter which determines the accretion rate, a is the speed of sound and ρ_∞ is the density of the gas cloud far from star.

Chapter 2

Accretion onto Schwarzschild Black Hole and Homoclinic Solutions in the Schwarzschild Anti-de-Sitter Black Hole

In this chapter, we review the accretion process for the Schwarzschild black hole [12] and the homoclinic accretion solutions for the Schwarzschild anti-de-Sitter black hole [14]. For Schwarzschild black hole, we study the hydrodynamical spherical accretion and calculate the accretion rate $\dot{M}$ by using the polytropic equation of state in the presence of ambient gas. For Schwarzschild anti-de-Sitter black hole we study the homoclinic solutions to the accretion for polytropic as well as isothermal equation of state and calculate an upper bound on the mass of the black hole which shows the accretion is transonic.

In sec I we derive the expression for accretion rate ($\dot{M}$) at the sonic (critical) point for Schwarzschild black hole and in sec II we do the homoclinic-type accretion for the Schwarzschild anti-de-Sitter black hole.

2.1 Accretion by the Schwarzschild Black Hole

For a typical gas, the accretion flow onto the compact objects is considered to be hydrodynamical in nature. The reason is the presence of macroscopically weak magnetic fields that they keep the moving particle's mean free path(average distance travelled by the particle) very very small. One of the

unique feature of accretion onto black hole is its regularity condition on the flowing fluid at small radii near horizon $r = 2M$ which serves to determine the accretion rate $\dot{M}$. As the accretion rate depends on the boundary conditions, therefore due to the presence of event horizon the black hole solution gives the maximum accretion rate.

2.1.1 General equations for spherical accretion

The line element and horizon for the Schwarzschild black hole are given in Eq. (1.2.1) and (1.2.2). Now we show the relationship of inflowing gas into the Schwarzschild black hole. The four-velocity of the fluid is given by $u^\mu = \frac{dx^\mu}{ds}$, which obeys the normalization condition for time-like vectors i.e. $u^\mu u_\mu = -1$. For adiabatic flow, we know that $p = p(n)$. So if we let n to be the baryon number [1] density, the baryon number flux J^μ will be given by $J^\mu = nu^\mu$ and the gas is considered as a perfect fluid whose energy momentum tensor will be $T^{\mu\nu} = (\rho + p)u^\mu u^\nu + pg^{\mu\nu}$. Now the accretion process is based on two conservation laws i.e. particle number conservation and total energy conservation given by

$$\nabla_\mu J^\mu = \nabla_\mu (nu^\mu) = 0. \tag{2.1.1}$$

$$\nabla_\mu T^\mu_{\ \nu} = 0. \tag{2.1.2}$$

We consider the radial inflow of gas onto a compact object having central mass M in the equatorial plane. So for equatorial plane $\theta = \frac{\pi}{2}$ and for radial inflow ϕ is constant therefore, the only non-zero components of the four-velocity are $u^0 = \frac{dt}{ds}$ and $u^1 = \frac{dr}{ds} \equiv u(r)$. Since by normalization condition $u_\mu u^\mu = -1$, we have

$$-\Big(1 - \frac{2M}{r}\Big)(u^0)^2 + \frac{1}{\Big(1 - \frac{2M}{r}\Big)}u^2 = -1$$

Simplifying for u^0 we get

$$u^0 = \frac{\Big(1 - \frac{2M}{r} + u^2\Big)^{1/2}}{\Big(1 - \frac{2M}{r}\Big)}. \tag{2.1.3}$$

[1] The number of sub-atomic particles in a system.

So by Eq. (1.3.15) we have

$$\frac{1}{r^2}(r^2 J^{\mu})_{,\mu} = 0.$$

On expanding this, we see all other terms vanish and we are only left with

$$\frac{1}{r^2}\frac{d}{dr}(r^2 nu) = 0. \tag{2.1.4}$$

On integrating Eq. (2.1.4) over the area we get

$$4\pi r^2 nu \;\; = \;\; \dot{M}, \tag{2.1.5}$$

where $\dot{M}$ is the constant of integration which is further used to calculate the mass accretion rate. On the other hand, the relativistic Euler equation for the energy conservation of time-like vector is given by Eq. (1.3.24)

$$(e+p)(\nabla_{\mu}u^{\nu})u^{\mu} \;\; = \;\; -[g^{\mu\nu}\nabla_{\mu}p + u^{\mu}u^{\nu}\nabla_{\mu}p].$$

For $\nu = 1$ we get momentum conservation equation as

$$(e+p)(\nabla_{\mu}u^{1})u^{\mu} \;\; = \;\; -[g^{\mu 1}\nabla_{\mu}p + u^{\mu}u^{1}\nabla_{\mu}p], \tag{2.1.6}$$

which can be further simplified as

$$\begin{aligned}(e+p)[u^{\mu}u^{1}{}_{,\mu} + \Gamma^{1}{}_{\mu\alpha}u^{\alpha}] \;\; &= \;\; -[g^{\mu 1}\nabla_{\mu}p + u^{\mu}u^{1}\nabla_{\mu}p].\\ (e+p)[u^{1}u^{1}{}_{,1} + \Gamma^{1}{}_{00}(u^{0})^2 + \Gamma^{1}{}_{11}(u)^2] \;\; &= \;\; -[g^{\mu 1}\nabla_{\mu}p + u^{\mu}u^{1}\nabla_{\mu}p]. \end{aligned} \tag{2.1.7}$$

The relevant non-vanishing Christoffel symbols are

$$\begin{aligned}\Gamma^{1}{}_{00} \;\; &= \;\; \frac{M}{r^2}\Big(1 - \frac{2M}{r}\Big).\\ \Gamma^{1}{}_{11} \;\; &= \;\; \frac{-M}{r^2\Big(1 - \frac{2M}{r}\Big)}. \end{aligned} \tag{2.1.8}$$

Using these values in Eq. (2.1.7), we get

$$u\frac{du}{dr} \;\; = \;\; -\frac{dp}{dr}\Big(\frac{1 - \frac{2M}{r} + u^2}{e+p}\Big) - \frac{M}{r^2}. \tag{2.1.9}$$

Now Eq. (2.1.5) and (2.1.9) are the main equations which we will use in the further calculations.

2.1.2 Accretion onto a Schwarzschild black hole

The first law of thermodynamics for closed system is given by

$$TdS = dE + pdV. \tag{2.1.10}$$

where S,V and E denote the entropy, volume and total energy of the fluid respectively. As our system is adiabatic, so there will be no change in entropy. If we let N the baryon's number and n the baryonic number density, then by using Eq. (2.1.10) the mass-energy conservation equation becomes

$$d\Big(\frac{e}{n}\Big) + pd\Big(\frac{1}{n}\Big) = 0, \tag{2.1.11}$$

which upon simplification gives

$$\frac{de}{dn} = \frac{e+p}{n}. \tag{2.1.12}$$

By using the chain rule we can define the sound speed a^2 as

$$a^2 \equiv \frac{dp}{de} = \frac{dp}{dn}\frac{n}{e+p}. \tag{2.1.13}$$

Now we solve equations for the particle flux and momentum flux given in (2.1.5) and (2.1.9) respectively, which leads us to the accretion rate. On differentiating Eq. (2.1.5) we get

$$\frac{n'}{n} + \frac{u'}{u} + \frac{2}{r} = 0, \tag{2.1.14}$$

and Eq. (2.1.9) can be re-written in compact form as

$$uu' + \frac{1}{e+p}\frac{dp}{dr}\Big(1 - \frac{2M}{r} + u^2\Big) + \frac{M}{r^2} = 0. \tag{2.1.15}$$

where prime denotes the derivative w.r.t r. Using Eq. (2.1.13) in (2.1.15) we obtain

$$uu' + a^2\Big(1 - \frac{2M}{r} + u^2\Big)\frac{n'}{n} + \frac{M}{r^2} = 0. \tag{2.1.16}$$

We can solve Eqs. (2.1.14) and (2.1.16) to obtain

$$u' = \frac{N_1}{N}, \qquad n' = -\frac{N_2}{N}, \tag{2.1.17}$$

where,

$$N_1 = \frac{1}{n}\Big[\Big(1-\frac{2M}{r}+u^2\Big)\frac{2a^2}{r}-\frac{M}{r^2}\Big], \tag{2.1.18}$$

$$N_2 = \frac{1}{u}\Big(\frac{2u^2}{r}-\frac{M}{r^2}\Big), \tag{2.1.19}$$

and

$$N = \frac{1}{un}\Big[u^2-\Big(1-\frac{2M}{r}+u^2\Big)a^2\Big]. \tag{2.1.20}$$

Now we prove that, for a certain equation of state which obeys the constraint $a^2 < 1$, the flow must pass through the sonic (critical) point outside the event horizon. Whenever r approaches to infinity, the flow satisfies the condition $u^2 \ll 1$ and the flow is subsonic with $u^2 < a^2$, so Eq. (2.1.20) becomes

$$N = \frac{1}{un}(u^2-a^2) < 0. \tag{2.1.21}$$

However, at the event horizon $r = 2M$ we have

$$N = \frac{u}{n}(1-a^2) > 0. \tag{2.1.22}$$

Thus outside the horizon, N must pass through the sonic point, which implies

$$N_1 = N_2 = N = 0 \tag{2.1.23}$$

In figure 2.1 we see six different type of solutions (flows), which are characterized by the radius at the sonic point (r_s) within the limit $r \to \infty$ and $r \to 0$. For type I $u^2(r_s) = a^2(r_s)$ and $r < r_s$ whereas, for type II $u^2(r_s) = a^2(r_s)$ but $r > r_s$. Since in both cases u^2 is doubled-valued (giving two values at the same r) therefore, we can say that these solutions are mathematically possible but physically impossible because velocity must have a unique value at every point. For type III $u^2(r_s) > a^2(r_s)$ i.e. the flow is supersonic and for type IV $u^2(r_s) < a^2(r_s)$ which shows the flow is subsonic everywhere. For type V we see $u^2(r_s) \to 0$ as $r \to 0$ and in type VI we see $u^2(r_s) \to 0$ as $r \to \infty$ but in both cases $u(r_s)^2 = a(r_s)^2$, so these two types show the transonic behaviour of the flow. Further by following the Michel's work [16], we get the velocity at the sonic point as

$$u_s^2 = \frac{M}{2r_s}. \tag{2.1.24}$$

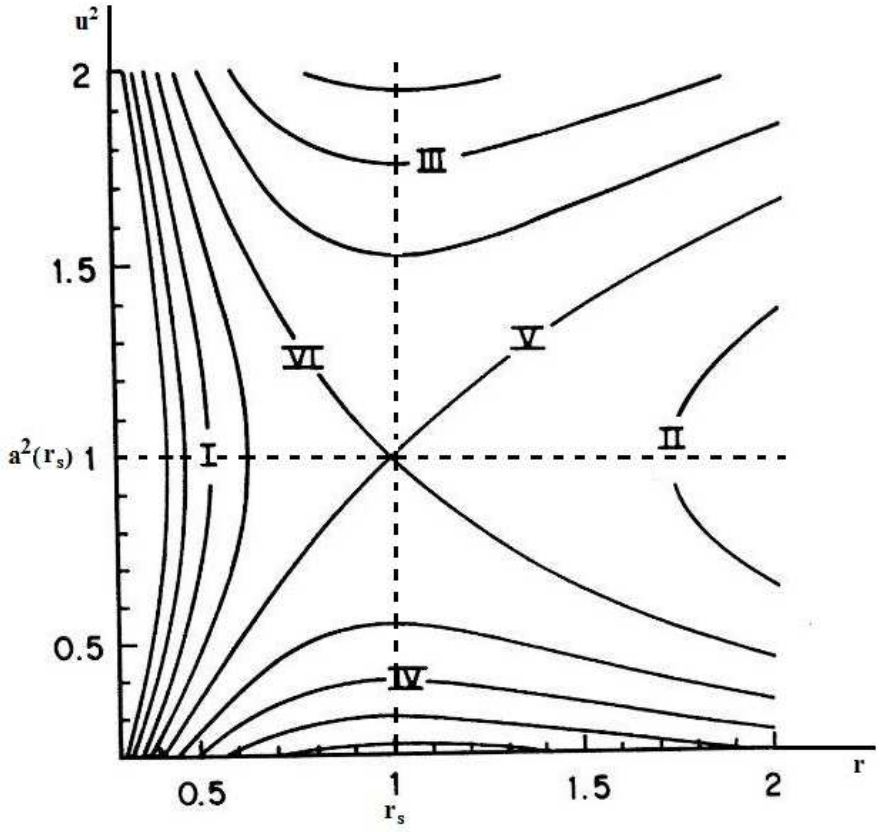

Figure 2.1: Different behaviours of the flow relative to the sonic point.

On the other hand, if we solve the Eq. (2.1.18) and (2.1.19) at the sonic point we obtain

$$u_s^2 = \frac{a_s^2}{1+3a_s^2}. \tag{2.1.25}$$

Hence, on comparing (2.1.24) and (2.1.25) we have

$$u_s^2 = \frac{a_s^2}{1+3a_s^2} = \frac{M}{2r_s}. \tag{2.1.26}$$

For the mass accretion rate at sonic point, we must multiply Eq. (2.1.5) by m_b (mass of each baryon) to obtain

$$\dot{M} = 4\pi r_s^2 m_b n_s u_s. \tag{2.1.27}$$

Further, we solve the energy conservation equation of particles and get the relativistic Bernoulli equation [16]

$$\Big(\frac{e+p}{n}\Big)^2\Big(1-\frac{2M}{r}+u^2\Big)=\Big(\frac{e_\infty+p_\infty}{n_\infty}\Big)^2. \tag{2.1.28}$$

2.1.3 The polytropic solution

To calculate the explicit value of $\dot{M}$, we must assume some equation of state. Here, we assume the polytropic equation of state [15] such that:

$$p=kn^\Gamma, \tag{2.1.29}$$

where k and Γ are constants. Using Eq. (2.1.29) into (2.1.12) we get

$$\frac{de}{dn}-\frac{e}{n}=kn^{\Gamma-1}. \tag{2.1.30}$$

Now this is a linear differential equation, so we solve it by using integrating factor $\frac{1}{n}$ which leads us to

$$e=mn+\frac{kn^\Gamma}{\Gamma-1}, \tag{2.1.31}$$

where m is the mass of the baryons. Similarly, the sound speed becomes

$$a^2 \;=\; \frac{dp}{de}=\frac{\Gamma kn^{\Gamma-1}}{m+\frac{\Gamma kn^{\Gamma-1}}{\Gamma-1}}, \tag{2.1.32}$$

which on further simplification becomes

$$k\Gamma n^{\Gamma-1}=\frac{a^2m}{1-\frac{a^2}{\Gamma-1}}. \tag{2.1.33}$$

Using the value of Eq. (2.1.31) and (2.1.33) we can rewrite the Bernoulli equation (2.1.28) as

$$\Big(1+\frac{a^2}{\Gamma-1-a^2}\Big)^2\Big(1-\frac{2M}{r}+u^2\Big)=\Big(1+\frac{a_\infty^2}{\Gamma-1-a_\infty^2}\Big)^2. \tag{2.1.34}$$

On inverting the above equation and using (2.1.26) we obtain

$$(1+3a_s^2)\Big(1-\frac{a_s^2}{\Gamma-1}\Big)^2=\Big(1-\frac{a_\infty^2}{\Gamma-1}\Big)^2. \tag{2.1.35}$$

We expand the above equation upto the second order as

$$\begin{aligned}(1+3a_s^2)\Big(1-\frac{2a_s^2}{\Gamma-1}+\frac{a_s^4}{(\Gamma-1)^2}\Big) &= 1-\frac{2a_\infty^2}{\Gamma-1},\\ 1+3a_s^2-\frac{2a_s^2}{\Gamma-1}-\frac{6a_s^4}{\Gamma-1}+\frac{a_s^4}{(\Gamma-1)^2} &= 1-\frac{2a_\infty^2}{\Gamma-1}. \end{aligned} \tag{2.1.36}$$

For transonic solutions $1 \leq \Gamma \leq 5/3$. Here, we are making a relationship between the particles at the boundary and the sonic point. Therefore, on comparing the both sides of the above equation, we obtain

$$\begin{aligned} a_s^2 &\approx \Big(\frac{2}{5-3\Gamma}\Big)a_\infty \qquad \text{for} \qquad \Gamma \neq \frac{5}{3},\\ \text{and} \qquad a_s^2 &\approx \frac{2}{3}a_\infty; \qquad\qquad \text{for} \qquad \Gamma = \frac{5}{3}. \end{aligned} \tag{2.1.37}$$

Similarly, from Eq. (2.1.26) we obtain the critical radius in terms of the mass of the black hole M and the boundary conditions at infinity given by

$$\begin{aligned} r_s &\approx \frac{5-3\Gamma}{4}\frac{M}{a_\infty^2} \qquad \text{for} \qquad \Gamma \neq \frac{5}{3},\\ \text{and} \qquad r_s &\approx \frac{3}{4}\frac{M}{a_\infty} \qquad\qquad \text{for} \qquad \Gamma = \frac{5}{3}. \end{aligned} \tag{2.1.38}$$

For $\frac{a^2}{\Gamma-1} \ll 1$ in Eq. (2.1.33) we have

$$\Big(\frac{n}{n_\infty}\Big) \approx \Big(\frac{a}{a_\infty}\Big)^{2/\Gamma-1}. \tag{2.1.39}$$

At sonic point, it becomes

$$\frac{n_s}{n_\infty} \approx \Big(\frac{a_s}{a_\infty}\Big)^{2/\Gamma-1}. \tag{2.1.40}$$

Using these values along with Eq. (2.1.26) in (2.1.27) we obtain

$$\dot{M} = 4\pi\lambda_s M^2 m_b n_\infty a_\infty^{-3}, \tag{2.1.41}$$

where λ_s is the dimensionless parameter and is given as

$$\lambda_s = \Big(\frac{1}{2}\Big)^{(\Gamma+1)/2(\Gamma-1)}\Big(\frac{5-3\Gamma}{4}\Big)^{(3\Gamma-5)/2(\Gamma-1)}. \tag{2.1.42}$$

For instance, the values of λ_s are given in Table 2.1.

$\mathbf{\Gamma}$	$\lambda_{\mathbf{s}}$
1	1.120
4/3	0.707
7/5	0.625
3/2	0.500
5/3	0.250

Table 2.1: Values of dimensionless parameter λ_s

2.2 Homoclinic Accretion in the Schwarzschild Anti-de-Sitter Spacetime

Besides Bondi-type (global) solutions there exists homoclinic solutions for which critical point of the flow forms a trajectory which joins critical point to itself. Recently, homoclinic solutions have been discovered for polytropic equation of state but in this section we show that these solutions also exists for isothermal equation of state. As the global solutions do not exists for the matter models with a non-vanishing rest mass at infinity because of the asymptotic behaviour therefore, we derive an upper bound on the mass of the black hole for which accretion solution is transonic [14].

2.2.1 Notations and equations for accretion

The line element for the Schwarzschild anti-de-Sitter is given by

$$ds^2 = -\Big(1-\frac{2M}{r}-\frac{\Lambda}{3}r^2\Big)dt^2+\frac{dr^2}{\Big(1-\frac{2M}{r}-\frac{\Lambda}{3}r^2\Big)}+r^2(d\theta^2+\sin^2\theta d\phi^2), \quad (2.2.1)$$

where Λ is the cosmological constant (numerically 2.036×10^{-35}) and is negative for anti-de-Sitter spacetime. To remove the singularity at horizon we use the Eddington-Finkelstein coordinates which are regular at the horizon. At the event horizon g_{tt} must vanishes i.e.

$$1-\frac{2M}{r}-\frac{\Lambda}{3}r^2=0,$$

which on further simplification gives

$$r^3+\frac{3}{\mid\Lambda\mid}r-\frac{6M}{\mid\Lambda\mid} = 0.$$

Now this is depressed cubic equation of the form $r^3+pr+q=0$ with $p=\frac{3}{|\Lambda|}$ and $q=-\frac{6M}{|\Lambda|}$. For a real positive root we use Cardano's method for $p>0$ i.e.

$$r = -2\sqrt{\frac{p}{3}}\sinh\Big[\frac{1}{3}\sinh^{-1}\Big(\frac{3q}{2p}\sqrt{\frac{3}{p}}\Big)\Big].$$

Thus, the event horizon is given by

$$r_h = \frac{2}{\sqrt{|\ \Lambda\ |}}\sinh\Big[\frac{1}{3}\sinh^{-1}(3M\sqrt{|\ \Lambda\ |})\Big]. \tag{2.2.2}$$

The conservation laws are given by

$$\nabla_\mu(nu^\mu)=0 \qquad \text{and} \qquad \nabla_\mu(T^{\mu\nu})=0. \tag{2.2.3}$$

For static and spherically symmetric flow in radial direction $u^\theta=u^\Phi=0$ and hence all quanitites in Eq. (2.2.1) are the funtions of radial coordinate r only. Assuming the solution is smooth, we integrate the conservation laws defined in (2.2.3) to obtain

$$nur^2=C_1 \qquad \text{and} \qquad (e+p)u_0ur^2=C_2, \tag{2.2.4}$$

where C_1 and C_2 are the constant of integrations. On dividing them, we get

$$hu_0 = C_3. \tag{2.2.5}$$

By using the normalization condition $u_\mu u^\mu=-1$ we get

$$u_0 = -\sqrt{1-\frac{2M}{r}-\frac{\Lambda}{3}r^2+u^2}. \tag{2.2.6}$$

Using (2.2.6) in (2.2.5) we obtain

$$h\sqrt{1-\frac{2M}{r}-\frac{\Lambda}{3}r^2+u^2} = C_3. \tag{2.2.7}$$

By the first law of thermodynamics defined in Eq. (2.1.10) we have

$$\frac{de}{dn} = \frac{e+p}{n}.$$

(i) Isothermal equation of state

For isothermal equation of state $p = ke$, where $0 < k \leq 1$ Eq. (2.1.12) will become a linear equation of the form

$$\frac{de}{dn} - \frac{(1+k)e}{n} = 0. \tag{2.2.8}$$

We use the integrating factor $\frac{1}{n^{1+k}}$, which leads us to

$$e = C_1 n^{1+k}. \tag{2.2.9}$$

Using this value in enthalpy ($h = \frac{e+p}{n}$) we get

$$h = (1+k)C_1 n^k \tag{2.2.10}$$

(ii) Polytropic equation of state

For polytropic equation of state $p = kn^\Gamma$, where $k > 0$ and $\Gamma > 1$ Eq. (2.1.12) becomes

$$\frac{de}{dn} - \frac{e}{n} = kn^{\Gamma-1}, \tag{2.2.11}$$

which by the use of integrating factor $\frac{1}{n}$ gives

$$e = \frac{kn^\Gamma}{\Gamma - 1} + C_2 n. \tag{2.2.12}$$

Similarly, the expression for enthalpy becomes

$$h = C_2 + \frac{\Gamma}{\Gamma - 1} kn^{\Gamma-1}. \tag{2.2.13}$$

Differentiating the conservation laws defined in (2.2.4) w.r.t. radial coordinate, we obtain

$$\frac{du}{dr} = \frac{2u}{r} \cdot \frac{a^2\Big[1 - \frac{2M}{r} - \frac{\Lambda}{3}r^2 + u^2\Big] - \frac{M}{2r} + \frac{\Lambda}{6}r^2}{u^2 - a^2\Big[1 - \frac{2M}{r} - \frac{\Lambda}{3}r^2 + u^2\Big]}, \tag{2.2.14}$$

where $\frac{dh}{de} = \frac{ha^2}{n}$ and a^2 is the speed of sound such that $a^2 = k$ for isothermal equations of state and for polytropic equation of state $a^2 = (\Gamma - 1)(1 - \frac{1}{h})$. If we let a parameter $l = l(r)$ such that

$$\begin{aligned} \frac{dr}{dl} &= r\Big\{u^2 - a^2\Big[1 - \frac{2M}{r} - \frac{\Lambda}{3}r^2 + u^2\Big]\Big\}. \\ &\equiv f_1(r, u). \end{aligned} \tag{2.2.15}$$

Then by applying chain rule in Eq. (2.2.14)

$$\begin{aligned}\frac{du}{dl} &= 2u\Big\{a^2\Big[1-\frac{2M}{r}-\frac{\Lambda}{3}r^2+u^2\Big]-\frac{M}{2r}+\frac{\Lambda}{6}r^2\Big\}\\ &\equiv f_2(r,u). \end{aligned} \tag{2.2.16}$$

Now Eqns. (2.2.15) and (2.2.16) form a dynamical system whose phase portrait consists of the graphs r vs u. The system defined by these equations has sonic (critical) point (r_s, u_s) when $f_1(r_s, u_s) = f_2(r_s, u_s) = 0$, i.e.

$$u_s^2 - a_s^2\Big[1-\frac{2M}{r_s}-\frac{\Lambda}{3}r_s^2+u_s^2\Big] = 0, \tag{2.2.17}$$

$$a_s^2\Big[1-\frac{2M}{r_s}-\frac{\Lambda}{3}r_s^2+u_s^2\Big]-\frac{M}{2r_s}+\frac{\Lambda}{6}r_s^2 = 0. \tag{2.2.18}$$

Here, the quantities with s denotes the values at the sonic point. On solving these equations we get

$$u_s^2 = \frac{M}{2r_s}-\frac{\Lambda}{6}r_s^2, \tag{2.2.19}$$

$$a_s^2 = \frac{\frac{M}{2r_s}-\frac{\Lambda}{6}r_s^2}{1-\frac{3M}{2r_s}-\frac{\Lambda}{2}r_s^2}. \tag{2.2.20}$$

The radial component of three-velocity at the sonic point is given by

$$(v^r)_s^2 = \Big(\frac{u^r}{u_t}\Big)_s^2 = \frac{u_s^2}{1-\frac{2M}{r_s}-\frac{\Lambda}{3}r_s^2+u_s^2}. \tag{2.2.21}$$

On substituting Eq. (2.2.19) into (2.2.21) we get

$$(v^r)_s^2 = \frac{\frac{M}{2r_s}-\frac{\Lambda}{6}r_s^2}{1-\frac{3M}{2r_s}-\frac{\Lambda}{2}r_s^2}, \tag{2.2.22}$$

i.e. we can say

$$a_s^2 = (g^{rr}v_r v^r)_s = (v^r v^r)_s. \tag{2.2.23}$$

Therefore, we commonly use the word 'sonic point' instead of critical point.

2.2.2 Asymptotic behaviour of isothermal solutions

In this section, we study the asymptotic behaviour of isothermal fluids when $r \to \infty$. For this we use Eq. (2.2.4) and (2.2.7) which yeilds

$$1 - \frac{2M}{r} - \frac{\Lambda}{3}r^2 + u^2 \;=\; Ar^{4k} \mid u \mid^{2k}, \tag{2.2.24}$$

where A is a positive constant such that $A = \frac{e^{2(rk-1)}n^{2(1+k)}}{(1+k)^2}$. Further, if we assume the asymptotic expansion of u such that $u \simeq Br^{\alpha}$, we get

$$1 - \frac{2M}{r} - \frac{\Lambda}{3}r^2 + B^2r^{2\alpha} \;=\; AB^{2k}r^{2k(2+\alpha)}. \tag{2.2.25}$$

Now if we compare both sides of above equation we find that it has two cases. If the order of leading term is $B^2r^{2\alpha}$, then we may have $2k(2+\alpha) = 2\alpha$ and if the order of the leading term is $-\frac{\Lambda}{3}r^2$, then we have $2k(2+\alpha) = 2$. These two possibilities leads us to $\alpha = 2k/(1-k)$ and $\alpha = (1-2k)/k$ respectively. Here, only for $k = 1/3$ both asymptotes coincides by giving $\alpha = 1$ so these two exponents corresponds to the two different branches of the solution which are asymptotically supersonic and subsonic respectively. For $1/3 < k < 1$ we have $(1-2k)/k < 2k/(1-k)$ but at $k = 1/3$ both have the same behaviour. For $k < 1/3$ we cannot have the asymptotic behaviour of the form $u \simeq Br^{\alpha}$ therefore, global solutions do not exists for $k < 1/3$.

2.2.3 Solution for sub-relativistic fluids

For instance, an explicit homoclinic solution can be found for the sub-relativistic fluids whose equation of state can be given as $p = e/4$ (i.e. $k = 1/4$). So Eq. (2.2.24) becomes

$$1 - \frac{2M}{r} - \frac{\Lambda}{3}r^2 + u^2 \;=\; Ar\sqrt{\mid u \mid}. \tag{2.2.26}$$

As we are mainly concerned with the transonic solutions therefore, we determine the value of A by the solution that passes through the sonic point given in Eq. (2.2.20). Putting the value of $k = 1/4$ we get

$$\frac{M}{2r_s} - \frac{\Lambda}{6}r_s^2 \;=\; \frac{1}{4}\Big(1 - \frac{3M}{2r_s} - \frac{\Lambda}{2}r_s^2\Big), \tag{2.2.27}$$

which on further simplification gives

$$\Lambda r_s^3 + 6r_s - 21M = 0. \tag{2.2.28}$$

As $\Lambda < 0$ in anti-de-Sitter spacetime, so the above equation can be written as

$$r_s^3 - \frac{6}{\mid \Lambda \mid} r_s + \frac{21M}{\mid \Lambda \mid} = 0. \tag{2.2.29}$$

Now this is again a depressed cubic equation of the form $r_s^3 + pr_s + q = 0$ with $p = -\frac{6}{\Lambda}$ and $q = \frac{21M}{\Lambda}$, so by using the Cardano's method for $p < 0$

$$r = -2\sqrt{-\frac{p}{3}} \cos\Big[\frac{1}{3}\cos^{-1}\Big(\frac{3q}{2p}\sqrt{-\frac{3}{p}}\Big) - \frac{2k\pi}{3}\Big].$$

Thus, the location of sonic point will be given as

$$r_s = \frac{2\sqrt{2}}{\sqrt{\mid \Lambda \mid}} \cos\Big[\frac{\pi}{3} + \frac{1}{3}\cos^{-1}\Big(\frac{21M\sqrt{\mid \Lambda \mid}}{4\sqrt{2}}\Big)\Big]. \tag{2.2.30}$$

The square of the radial velocity at the sonic point (u_s^2) is given in Eq. (2.2.19) and so the value of A in Eq. (2.2.26) corresponds to the transonic solution can be defined as

$$A = A_s \equiv \frac{4}{r_s}\Big(\frac{M}{2r_s} - \frac{\Lambda}{6}r_s^2\Big)^{3/4}. \tag{2.2.31}$$

Now we see that Eq. (2.2.26) is a depressed quartic polynomial of the form

$$ar^4 + cr^2 + dr + e = 0, \tag{2.2.32}$$

with $a = 1$, $c = 2 - \frac{2\Lambda}{3}r^2 - \frac{4M}{r}$, $d = -Ar^2$ and $e = 1 - \frac{4M}{r} - \frac{2\Lambda}{3}r^2 + \frac{4M\Lambda}{3}r + \frac{4M^2}{r^2} + \frac{\Lambda^2}{9}r^4$. So the discriminant will be given as

$$\Delta = 256a^3e^3 - 128a^2c^2e^2 + 144a^2cd^2e - 27a^2d^4 + 16ac^4e - 4ac^3d^2$$

If we let

$$\Delta = \Big(\frac{Ar}{4}\Big)^4 - \frac{1}{3^3}\Big(1 - \frac{2M}{r} - \frac{\Lambda}{3}r^2\Big)^3. \tag{2.2.33}$$

For the transonic solution $\Delta \geq 0$. The solution of the Eq. (2.2.26) is given by the help of Ferrari's method as

$$X_\pm = \frac{y}{2}\Big(1 \pm \sqrt{\frac{Ar}{\sqrt{2}y^{3/2}} - 1}\Big)^2, \tag{2.2.34}$$

where y is the real root such that

$$y = \left[\left(\frac{Ar}{4}\right)^2 + \sqrt{\Delta}\right]^{3/2} + \left[\left(\frac{Ar}{4}\right)^2 - \sqrt{\Delta}\right]^{3/2}. \qquad (2.2.35)$$

Let R be the largest root of the equation $\Delta = 0$ then the two different behaviours of solutions are given below. The subsonic branch will be

$$\mid u \mid = \begin{cases} X_+ & 0 < r \leq r_s, \\ X_- & r_s \leq r < R, \end{cases}$$

whereas, the branch that is supersonic outside the r_s is given as

$$\mid u \mid = \begin{cases} X_- & r_h < r \leq r_s, \\ X_+ & r_s \leq r < R. \end{cases}$$

For all other values the accretion solution is non-transonic. The solution for $p = e/4$ is also shown in the Figure 2.2.

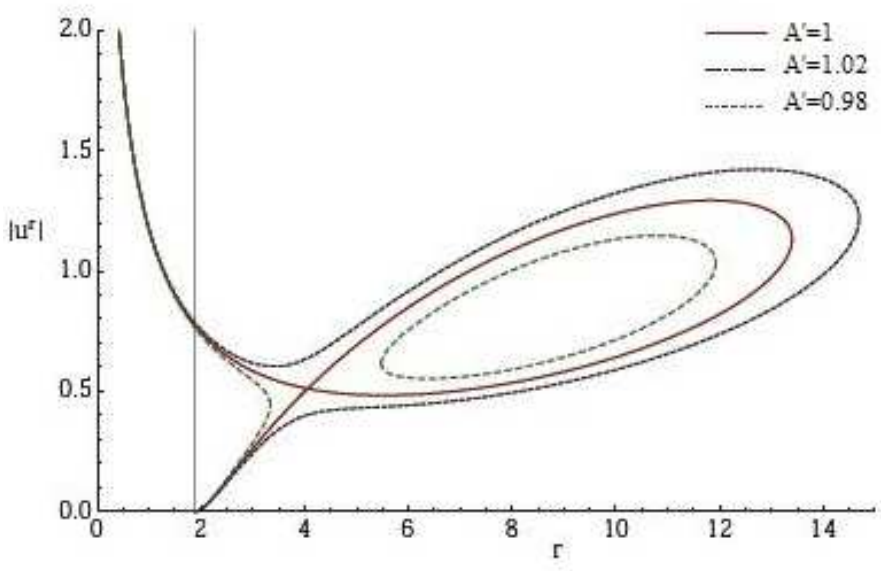

Figure 2.2: Solutions obtained for the sub-relativistic fluids with $M = 1$ and $\Lambda = -0.05$. The vertical line shows the location of horizon and the middle solid line shows the transonic solution.

2.2.4 Critical points in the isothermal case

From the section 2.2.3 we find that isothermal equation of state $p = ke$ is valid for $0 < k < 1/3$. It suggests that there exists two critical points on the phase portrait of (r, u) for the certain values of parameters which should belong to the homoclinic orbit. Furthermore, for transonic accretion we have also a restriction on the mass of the black hole. In case of isothermal fluid, Eq. (2.2.20) gives

$$\frac{M}{2r_s} - \frac{\Lambda}{6}r_s^2 = k\Big(1 - \frac{3M}{2r_s} - \frac{\Lambda}{2}r_s^2\Big), \tag{2.2.36}$$

which on further simplification gives a depressed cubic equation as

$$\frac{\Lambda}{2}\Big(\frac{1}{3} - k\Big)r_s^3 + kr_s - \frac{3}{2}M\Big(k + \frac{1}{3}\Big) = 0. \tag{2.2.37}$$

Dividing by $\frac{\Lambda}{2}\Big(\frac{1}{3} - k\Big)$ on both sides of the above equation, we obtain

$$f(r_s) = r_s^3 + 3pr_s + 2q = 0, \tag{2.2.38}$$

where

$$p = \frac{2k}{\Lambda(1-3k)}, \qquad q = -\frac{3M(3k+1)}{2\Lambda(1-3k)}.$$

For $\Lambda < 0$ and $0 < k < 1/3$ Eq. (2.2.38) has a real negative root. On the other hand, a real positive root exists iff the discriminant $W = p^3 + q^2 < 0$ which further leads to the upper bound of the mass of the black hole for transonic accretion given as $W = p^3 + q^2 \leq 0$ which simplifies to

$$\begin{aligned} &\Rightarrow \qquad \frac{9M^2(3k+1)\Lambda(1-3k) + 32k^3}{4\Lambda^3(1-3k)^3} \leq 0 \\ &\Rightarrow \qquad M^2 \leq \frac{32k^3}{9(1-3k)(1+3k)^2 \mid \Lambda \mid}. \end{aligned} \tag{2.2.39}$$

This statement can also be followed directly by the analysis of complex roots in the Cardano's formula as

$$r_s = [-q + \sqrt{p^3 + q^2}]^{3/2} + [-q - \sqrt{p^3 + q^2}]^{3/2},$$

which on substituting the condition $W = p^3 + q^2 \leq 0$ gives

$$r_s = [-q + \iota\sqrt{\mid W \mid}]^{3/2} + [-q - \iota\sqrt{\mid W \mid}]^{3/2}, \tag{2.2.40}$$

with $0 < k < 1/3$. Furthermore, when $\Lambda < 0$ and $k > 1/3$ the discriminant W is always positive and gives a real root. This mass limit is also illustrated in Fig 2.3.

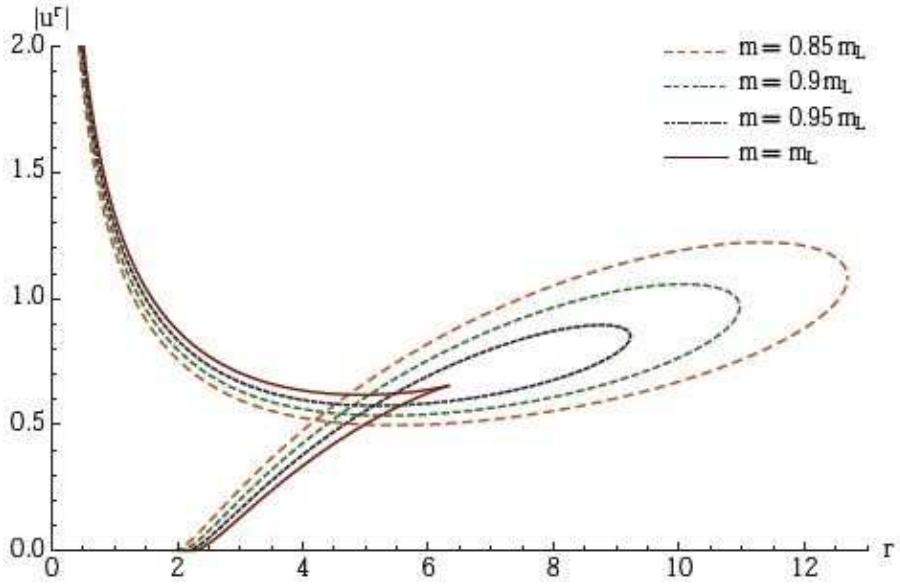

Figure 2.3: Transonic solutions obtained for the sub-relativistic fluids with $\Lambda = -0.05$. The graph shows the different values of the black hole mass where, m_L denotes the maximum limit on mass of the black hole at the sonic point.

To analyse the critical points we should persue our calculation by computing the Jacobians of Eq. (2.2.15) and (2.2.16) i.e.

$$M = \begin{bmatrix} \frac{\partial f_1}{\partial r} & \frac{\partial f_1}{\partial u} \\ \frac{\partial f_2}{\partial r} & \frac{\partial f_1}{\partial u} \end{bmatrix}$$

This is obvious that it has two eigenvalues say μ_1 and μ_2 and we know that stability depends upon the nature of the eigenvalues. We can generally have the following classification [23]:
(i) If $\mu_1 < 0$ and $\mu_2 < 0$, it will be a stable critical point.
(ii) If $\mu_1 > 0$ and $\mu_2 > 0$, it will be unstable critical point.
(iii) If $\mu_1 < 0$ and $\mu_2 > 0$ or $\mu_1 > 0$ and $\mu_2 < 0$, then it will be a saddle critical point.

2.2.5 Polytropic solutions

From section 2.2.2 we know that no global solutions exist for polytropic equation of state. We can further show it by comparing Eq. (2.2.13) to the conservation equation defined in Eq. (2.2.7) which yeilds

$$h\sqrt{1-\frac{2M}{r}-\frac{\Lambda}{3}r^2+u^2} = \left(1+\frac{\Gamma k}{\Gamma-1}n^{\Gamma-1}\right)\sqrt{1-\frac{2M}{r}-\frac{\Lambda}{3}r^2+u^2}=C_4, \tag{2.2.41}$$

where C_4 is an arbitrary constant. Now it depends on the order of r that whether square root behaves asymptotically because of term having Λ. The only way to remove this divergent behaviour is to have h that vanishes very fast which is impossible since $h > 1$ whereas, the unity in the expression of h comes from the pressure and the densities of the rest mass of the particles of gas.

2.3 Conclusion

In this chapter, we have reviewed both the method of accretion for polytropic fluids and homoclinic solutions of isothermal as well as polytropic fluids to the Schwarzschild and Schwarzschild anti-de-Sitter black holes respectively. In case of accretion, we have analysed the different behaviours of fluid and found that for transonic solutions the accretion rate is maximum whereas, by homoclinic solutions we have found the maximum limit on the mass of the black hole for which the accretion is transonic.

Chapter 3

Accretion by the Reissner-Nordström Anti-de-Sitter Black Hole

This chapter is the review of the accretion of fluids onto RN black hole in the presence of a cosmological constant which was done by F. Ficek [22]. We show that for isothermal equations of state, it is possible to get the analytical solutions of the flowing fluid. Further, the relations between location of horizons and sonic (critical) points are derived. However, for polytropic equation of state it is not easy to find the analytical solutions of the fluid, so we calculate the general expressions for the behaviour of the fluid. The basic motivation behind this work, comes from the fact that the structure of RN black hole resembles somehow to the Kerr black hole which could influence accretion. As they share the similar structure of horizons, so we can assume that the accretion solutions in both spacetimes may also be same.

In this chapter, first we consider the general equations and conservation laws of the flow which are required for the accretion and find the analytical solution at the sonic point. Then by Hamiltonian system we show that the equations are autonomous (independent of parameter t) and in the end the solutions for isothermal and polytropic equations of state are found.

3.1 Metric of the RN Anti-de-Sitter Spacetime

The metric for RN anti-de-Sitter black hole is given by [10, 11]

$$ds^2 = -f(r)dt^2 + \frac{dr^2}{f(r)} + r^2(d\theta^2 + \sin^2\theta d\phi^2), \tag{3.1.1}$$

where $f(r) \equiv 1 - \frac{2M}{r} + \frac{Q^2}{r^2} - \frac{\Lambda r^2}{3}$ such that $\Lambda < 0$ (anti-de-Sitter). The metric defined in Eq. (3.1.1) is singular at $f(r) = 0$ which gives at maximum three real, positive roots which corresponds to the inner (Cauchy horizon), middle (event horizon) and the outer (cosmological horizon). The cauchy and event horizons exists for $\Lambda \leq 0$ whereas, the cosmological horizon exists only when $\Lambda > 0$. To get rid of the singularity which arises at horizon, we introduce the advanced Eddington-Finkelstein (EF) coordinates because in the case of black holes, these coordinates are regular at the event horizon [23] given by

$$dt' = dt - \frac{\frac{2M}{r} - \frac{Q^2}{r^2} + \frac{\Lambda r^2}{3}}{1 - \frac{2M}{r} + \frac{Q^2}{r^2} - \frac{\Lambda r^2}{3}} dr. \tag{3.1.2}$$

This leads (3.1.1) to the following form:

$$\begin{aligned} ds^2 = & -\Big(1 - \frac{2M}{r} + \frac{Q^2}{r^2} - \frac{\Lambda r^2}{3}\Big)dt'^2 - 2\Big(\frac{2M}{r} - \frac{Q^2}{r^2} + \frac{\Lambda r^2}{3}\Big)dt'dr \\ & + \Big(1 + \frac{2M}{r} - \frac{Q^2}{r^2} + \frac{\Lambda r^2}{3}\Big)dr^2 + r^2(d\theta^2 + \sin^2\theta d\phi^2), \end{aligned} \tag{3.1.3}$$

while the determinant of the metric defined in (3.1.3) is $g = -r^4 \sin^2\theta$ and $\sqrt{\mid g \mid} = r^2 \sin\theta$.

3.2 Flows in the RN Anti-de-Sitter Spacetime

Now we consider the perfect fluid flowing in the spacetime given by

$$T^{\mu\nu} = (e + p)u^\mu u^\nu + pg^{\mu\nu}, \tag{3.2.1}$$

where e and p denotes the energy density and pressure respectively. As the accretion is steady state, spherically symmetric so in both coordinate systems

(t and t') all quantities are the function of radial coordinate only. As the fluid is moving radially in equatorial plane therefore $u^\theta = u^\phi = 0$ and for simplicity if we let $u^r = u$, then by using the normalization condition we get

$$u^{t'} = \frac{\left(\frac{2M}{r} - \frac{Q^2}{r^2} + \frac{\Lambda r^2}{3}\right)u + \sqrt{1 - \frac{2M}{r} + \frac{Q^2}{r^2} - \frac{\Lambda r^2}{3} + u^2}}{1 - \frac{2M}{r} + \frac{Q^2}{r^2} - \frac{\Lambda r^2}{3}}, \tag{3.2.2}$$

$$u_{t'} = -\sqrt{1 - \frac{2M}{r} + \frac{Q^2}{r^2} - \frac{\Lambda r^2}{3} + u^2}. \tag{3.2.3}$$

So it is clear that in both coordinate system u_t and $u_{t'}$ has exactly the same form. Furthermore, the motion of fluid is described by the conservation laws given by

$$\nabla_\mu J^\mu = \nabla_\mu(nu^\mu) = 0, \tag{3.2.4}$$

$$\nabla_\mu T^{\mu\nu} = \nabla_\mu((e+p)u^\mu u^\nu + pg^{\mu\nu}) = 0. \tag{3.2.5}$$

Now we simplify the above equations. Eq. (3.2.4) gives

$$\frac{1}{r^2}\partial_r(r^2 nu) = 0. \tag{3.2.6}$$

As enthalpy defines the total heat content of a system, so if we let enthalpy as $h = \frac{e+p}{n}$ and expand the Eq. (3.2.5), we get

$$\begin{aligned} \nabla_\mu T^{\mu\nu} &= \nabla_\mu(hnu^\mu u^\nu) + g^{\mu\nu}\partial_\mu p \\ &= nu^\mu \nabla_\mu(hu^\nu) + g^{\mu\nu}\partial_\mu p = 0. \end{aligned} \tag{3.2.7}$$

For isentropic flow ($dh = \frac{dp}{n}$), the above expression becomes

$$u^\mu \nabla_\mu(hu_\nu) + g^{\mu\nu}\partial_\mu h = 0. \tag{3.2.8}$$

Using the definition of covariant derivative in Eq. (3.2.8), we have

$$u^\mu \nabla_\mu(hu_\nu) + \partial_\nu h = u^\mu \partial_\mu(hu_\nu) - h\Gamma^\lambda{}_{\mu\nu} u_\lambda u^\mu + \partial_\nu h = 0. \tag{3.2.9}$$

As the flow is isentropic therefore $\partial_\nu h = 0$ and the zeroth component of the above equation ($\nu = t$) reads

$$u^t \partial_r(hu_t) - [hu^t u_t \Gamma^t{}_{tt} + u^t u_r \Gamma^r{}_{tt} + u^r u_t \Gamma^t{}_{rt} + u^r u_r \Gamma^r{}_{rt}] = 0. \tag{3.2.10}$$

On putting the values of Christoffel symbols in the above expression, we find that the expression in square bracket becomes zero and we are left only with

$$\partial_r(hu_t) = 0. \tag{3.2.11}$$

We note that the function u is same for both coordinates (u_t and $u_{t'}$), so whenever we approach to the point of singularity in any of these coordinates, we can switch to other coordinate in order to avoid it. This is the reason that why we are not differentiating u_t and $u_{t'}$. Further, on integrating Eq. (3.2.6) and (3.2.11) we obtain the mass conservation and energy-momentum conservation equations respectively given by

$$r^2nu = C_1, \tag{3.2.12}$$

$$h\sqrt{1-\frac{2M}{r}+\frac{Q^2}{r^2}-\frac{\Lambda r^2}{3}+u^2} = C_2. \tag{3.2.13}$$

Now, these are the main equations which we will use further to analyse the flow of a perfect fluid in the background of the Reissner-Nordström anti-de-Sitter spacetime.

3.3 Sonic point in the RN Anti-de-Sitter Spacetime

Let a be the local speed of sound (the speed of sound at any point inside the flow). The location where the four-velocity of the fluid satisfies the relation $a^2 = (u/u_t)^2$ is called a sonic point. In case of barotropic equation of state ($h = h(n)$), we have

$$\frac{dh}{h} = a^2\frac{dn}{n}. \tag{3.3.1}$$

Now differentiating Eq. (3.2.12) and (3.2.13) and using (3.3.1), we obtain

$$\left[\left(\frac{u}{u_t}\right)^2 - a^2\right]\partial_r \ln u = \frac{1}{r(u_t)^2}\left[2a^2(u_t)^2 - \frac{M}{r}+\frac{Q^2}{r^2}+\frac{\Lambda r^2}{3}\right]. \tag{3.3.2}$$

For sonic point, both sides of the above equation must vanish, so if $\mid u \mid < \infty$ we have

$$a_s^2 = \left(\frac{u_s}{u_{t_s}}\right)^2, \tag{3.3.3}$$

$$2a^2(u_{t_s})^2 - \frac{M}{r_s} + \frac{Q^2}{r_s^2} + \frac{\Lambda r_s^2}{3} = 0, \tag{3.3.4}$$

where the quantities with s denotes the values at sonic point. Using (3.3.3) into (3.3.4), we get

$$(u_s)^2 = \frac{M}{2r_s} - \frac{Q^2}{2r_s^2} - \frac{\Lambda r_s^2}{6}. \tag{3.3.5}$$

Further, if we differentiate Eq. (3.2.12) and (3.2.13) and evaluate them at the sonic point, we obtain the expression for radial velocity [14] at the sonic point as

$$(u_s)^2 = a_s^2\left[1 - \frac{3M}{2r_s} + \frac{Q^2}{2r_s^2} - \frac{\Lambda}{2}r_s^2\right]. \tag{3.3.6}$$

On combining Eqs. (3.3.5) and (3.3.6), we get

$$\begin{aligned}(u_s)^2 &= \frac{M}{2r_s} - \frac{Q^2}{2r_s^2} - \frac{\Lambda r_s^2}{6} \\ &= a_s^2\left[1 - \frac{3M}{2r_s} + \frac{Q^2}{2r_s^2} - \frac{\Lambda}{2}r_s^2\right].\end{aligned} \tag{3.3.7}$$

To further solve the Eqs. (3.2.12), (3.2.13) and (3.3.3), we need suitable boundary conditions. For this we denote r_∞, ρ_∞ and a_∞ as the radius, density and speed of sound respectively at the boundary. They can either be finite or infinite.

3.4 Hamiltonian System for the RN Anti-de-Sitter Spacetime

Hamiltonian system is a tool which preserves the total energy of a system. For energy conservation, the Hamiltonian system must be autonomous (i.e. it does not depends explicitly on the time parameter). So on differentiating Eq. (3.2.12) and (3.2.13), and using the value of (3.3.1) we obtain

$$\frac{du}{dr} = \frac{2u}{r}\,\frac{a^2\left(1 - \frac{2M}{r} + \frac{Q^2}{r^2} - \frac{\Lambda r^2}{3} + u^2\right) - \left(\frac{M}{2r} - \frac{Q^2}{r^2} - \frac{\Lambda r^2}{6}\right)}{u^2 - a^2\left(1 - \frac{2M}{r} + \frac{Q^2}{r^2} - \frac{\Lambda r^2}{3} + u^2\right)}. \tag{3.4.1}$$

If we introduce a parameter l, such that

$$\frac{dr}{dl} = r\left[u^2 - a^2\left(1 - \frac{2M}{r} + \frac{Q^2}{r^2} - \frac{\Lambda r^2}{3} + u^2\right)\right], \tag{3.4.2}$$

$$\frac{du}{dl} = 2u\left[a^2\left(1 - \frac{2M}{r} + \frac{Q^2}{r^2} - \frac{\Lambda r^2}{3} + u^2\right) - \left(\frac{M}{2r} - \frac{Q^2}{2r^2} - \frac{\Lambda r^2}{6}\right)\right]. \tag{3.4.3}$$

Thus, it is clear from the above equations that the system is autonomous (i.e. it does not explicitly depends on the independent parameter l), so it remains invariant under reparametrization. Hence, if we define another parameter such that $l = \tilde{l}(l)$, we can define our Hamiltonian system as:

$$\begin{aligned} \frac{dr}{d\tilde{l}} &= \frac{\partial \mathcal{H}}{\partial u}, \\ \frac{du}{d\tilde{l}} &= -\frac{\partial \mathcal{H}}{\partial r}, \end{aligned} \tag{3.4.4}$$

We can consider the above Hamiltonian system in u/u_t variable. If we square both side of Eq. (3.2.3) we have

$$(u_t)^2 = 1 - \frac{2M}{r} + \frac{Q^2}{r^2} - \frac{\Lambda r^2}{3} + u^2. \tag{3.4.5}$$

On dividing both sides by $(u_t)^2$ Eq. (3.4.5) becomes

$$\left(\frac{u}{u_t}\right)^2 = 1 - \frac{1 - \frac{2M}{r} + \frac{Q^2}{r^2} - \frac{\Lambda r^2}{3}}{(u_t)^2}. \tag{3.4.6}$$

As the LHS of Eq. (3.2.13) is the Hamiltonian with r vs u variables, so by using the above expression we can rewrite it as

$$\begin{aligned} \mathcal{H} &= h u_t. \\ &= h\sqrt{\frac{1 - \frac{2M}{r} + \frac{Q^2}{r^2} - \frac{\Lambda r^2}{3}}{1 - \left(\frac{u}{u_t}\right)^2}}. \end{aligned} \tag{3.4.7}$$

If we differentiate the Hamiltonian given in Eq. (3.4.7) w.r.t r and u, we get

$$\frac{\partial \mathcal{H}}{\partial r} = \frac{\frac{M}{r^2}-\frac{Q^2}{r^3}-\frac{\Lambda}{3}r}{\sqrt{\left[1-\left(\frac{u}{u_t}\right)^2\right]\left(1-\frac{2M}{r}+\frac{Q^2}{r^2}-\frac{\Lambda}{3}r^2\right)}}h+\sqrt{\frac{1-\frac{2M}{r}+\frac{Q^2}{r^2}-\frac{\Lambda}{3}r^2}{1-\left(\frac{u}{u_t}\right)^2}}\frac{\partial h}{\partial r}, \tag{3.4.8}$$

$$\frac{\partial \mathcal{H}}{\partial\left(\frac{u}{u_t}\right)} = \frac{\left(\frac{u}{u_t}\right)\sqrt{1-\frac{2M}{r}+\frac{Q^2}{r^2}-\frac{\Lambda}{3}r^2}}{\left[1-\left(\frac{u}{u_t}\right)^2\right]^{3/2}}h+\sqrt{\frac{1-\frac{2M}{r}+\frac{Q^2}{r^2}-\frac{\Lambda}{3}r^2}{1-\left(\frac{u}{u_t}\right)^2}}\frac{\partial h}{\partial\left(\frac{u}{u_t}\right)}. \tag{3.4.9}$$

Using Eq. (3.4.6) in (3.2.12) we can write

$$nr^2\sqrt{\frac{1-\frac{2M}{r}+\frac{Q^2}{r^2}-\frac{\Lambda}{3}r^2}{\left(\frac{u_t}{u}\right)^2}} = C_3, \tag{3.4.10}$$

where C_3 is an arbitray constant. Using Eq. (3.4.10) in (3.4.7) and then differentiating it w.r.t r and u we get

$$\frac{\partial h}{\partial r} = -\frac{2a^2h}{r}\frac{1-\frac{3M}{2r}+\frac{Q^2}{2r^2}-\frac{\Lambda}{2}r^2}{1-\frac{2M}{r}+\frac{Q^2}{r^2}-\frac{\Lambda}{3}r^2}, \tag{3.4.11}$$

$$\frac{\partial h}{\partial\left(\frac{u}{u_t}\right)} = -\frac{ha^2}{\frac{u}{u_t}\left[1-\left(\frac{u}{u_t}\right)^2\right]}. \tag{3.4.12}$$

Using these values in Eq. (3.4.8) and (3.4.9) we get the equation analogous to the system defined in (3.4.4) as

$$\frac{d}{dr}\left(\frac{u}{u_t}\right) = \frac{\left(\frac{u}{u_t}\right)\left[1-\left(\frac{u}{u_t}\right)^2\right]}{r\left[\left(\frac{u}{u_t}\right)^2-a^2\right]}\cdot\frac{2a^2\left(1-\frac{3M}{2r}+\frac{Q^2}{2r^2}-\frac{\Lambda r^2}{2}\right)-\frac{M}{r}+\frac{Q^2}{r^2}+\frac{\Lambda r^2}{3}}{1-\frac{2M}{r}+\frac{Q^2}{r^2}-\frac{\Lambda r^2}{3}}. \tag{3.4.13}$$

3.5 Accretion of Isothermal Test Fluids

In this section we consider the isothermal equation of state ($p = ke$). In general, the adiabatic sound speed is defined as $a^2 = dp/de$. So by comparing

the adiabatic sound speed to the equation of state, we find $a^2 = k$. By the first law of thermodynamics

$$\frac{de}{dn} = \frac{e+p}{n}(= h). \tag{3.5.1}$$

On integrating this term from the r_∞ to any point inside the fluid, we obtain

$$\exp \int_{e_\infty}^{e} \frac{de'}{e' + p\,(e')} \;\; = \;\; \frac{n}{n_\infty}, \tag{3.5.2}$$

where e' is any arbitray point inside the fluid different from e. So Eq. (3.5.2) can further be written as:

$$n \;\; = \;\; n_\infty \exp\left(\int_{e_\infty}^{e} \frac{de'}{e' + p\,(e')}\right) \tag{3.5.3}$$

In case of isothermal equation of state $p = ke$, it gives

$$n_\infty \left(\frac{e}{e_\infty}\right)^{\frac{1}{(k+1)}}. \tag{3.5.4}$$

Comparing Eq. (3.5.3) and (3.5.1), we get

$$h \;\; = \;\; \frac{(k+1)e_\infty}{n_\infty}\Big(\frac{n}{n_\infty}\Big)^k. \tag{3.5.5}$$

Thus, Eq. (3.2.13) can be re-written as

$$n^k \sqrt{1 - \frac{2M}{r} + \frac{Q^2}{r^2} - \frac{\Lambda r^2}{3} + u^2} = const. \tag{3.5.6}$$

Further, comparison of Eq. (3.2.12) and (3.2.13) gives

$$\sqrt{1 - \frac{2M}{r} + \frac{Q^2}{r^2} - \frac{\Lambda r^2}{3} + u^2} = C r^{2k} u^k. \tag{3.5.7}$$

As we are mainly concerned with the flows that passes through the sonic (critical) point. So transonic flows are interesting in this context as they maximize the accretion rate. On the other hand, for $a^2 = k$, Eq. (3.3.7) is given by

$$(u_s)^2 = \frac{M}{2r_s} - \frac{Q^2}{2r_s^2} - \frac{\Lambda r_s^2}{6} = k\Big(1 - \frac{3M}{2r_s} + \frac{Q^2}{2r_s^2} - \frac{\Lambda}{2} r_s^2\Big). \tag{3.5.8}$$

Now by taking the different values of k we solve Eq. (3.5.7) and (3.5.8) and find the solutions $u(r)$. For instance, we consider $k = 1$ (ultra-stiff fluid), $k = 1/2$ (ultra-relativistic fluid), $k = 1/3$ (radiation fluid) and $k = 1/4$ (sub-relativistic fluid).

3.5.1 Ultra-stiff fluid

Ultra-stiff fluids are those fluids in which isotropic pressure and energy density are equal. For instance, the equation of state for the ultra-stiff fluids is $p = e$ i.e. the value of state parameter is defined as $k = 1$. So Eq. (3.5.7) implies

$$u^2 = \frac{1 - \frac{2M}{r} + \frac{Q^2}{r^2} - \frac{\Lambda r^2}{3}}{Cr^4 - 1}, \tag{3.5.9}$$

which shows there exists a double root (same solution but with different signs) and the value of r_s will be similar to the value of event horizon. On putting the value of r_s into (3.5.8) we can compute u_s so that we get the critical points as $(r_s, \pm u_s)$ and then we can solve them simultaneously to obtain the value of C in Eq. (3.5.9), which gives us the explicit form of the solution.

3.5.2 Ultra-relativistic fluid

Ultra-relativistic fluids are the fluids where isotropic pressure is less than the energy density. In this case, the equation of state is defined as $p = \frac{e}{2}$. From Eq. (3.5.8) we have

$$\frac{\Lambda r_s^4}{6} - r_s^2 + \frac{5Mr_s}{2} - \frac{3Q^2}{2} = 0. \tag{3.5.10}$$

On the other hand Eq. (3.5.7) implies

$$u = -\frac{1}{2}Cr^2 \pm \frac{1}{2}\sqrt{C^2r^4 - 4\Big(1 - \frac{2M}{r} + \frac{Q^2}{r^2} - \frac{\Lambda r^2}{3}\Big)}. \tag{3.5.11}$$

Again we can obtain the value of r_s and u_s from the above equations by repeating the same procedure as defined for ultra-stiff fluids.

3.5.3 Radiation fluid

The fluid which obeys the equation of state $p = \frac{e}{3}$ is called the radiation fluid. So for $k = 1/3$ Eq. (3.5.8) leads us to

$$r_s^2 - 3Mr_s + 2Q^2 = 0, \tag{3.5.12}$$

which can be solved easily and the critical points are given by

$$r_{s_\pm} = \frac{3M \pm \sqrt{9M^2 - 8Q^2}}{2}, \tag{3.5.13}$$

where $9M^2 - 8q^2 \geq 0$. By using Eq. (3.5.7) the relationship between four-velocity and radial component is given by

$$\left(1 - \frac{2M}{r} + \frac{Q^2}{r^2} - \frac{\Lambda r^2}{3} + u^2\right)^3 = Cr^4u^2, \tag{3.5.14}$$

which shows there exists a correlation between the locations of critical points and horizons and is shown in figure 3.1.

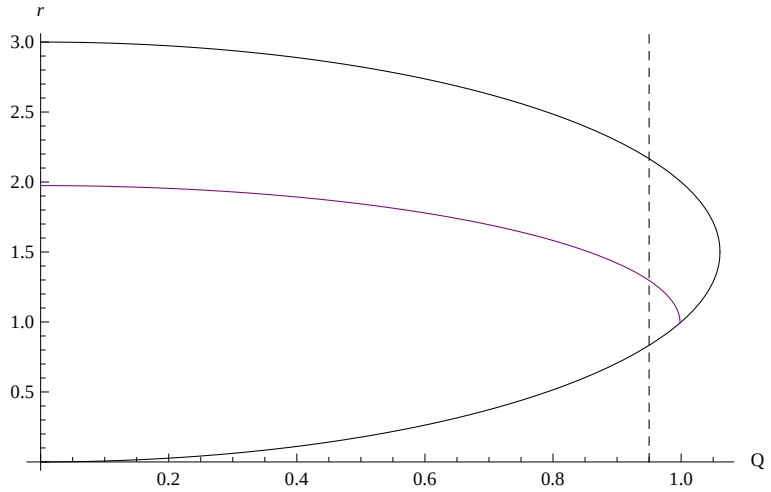

Figure 3.1: Plot showing the location of critical points r and horizons depending on $\Lambda = -1/100$ and $Q = 95/100$ for the equation of state $p = e/3$. The black line shows the critical point and the coloured line shows the event horizon.

3.5.4 Sub-relativistic fluid

Using value $k = 1/4$ in Eq. (3.5.7) and (3.5.8) we get

$$\frac{\Lambda r_s^4}{6} + r_s^2 - \frac{7Mr_s}{2} + \frac{5Q^2}{2} = 0, \tag{3.5.15}$$

$$\left(1 - \frac{2M}{r} + \frac{Q^2}{r^2} - \frac{\Lambda r^2}{3} + u^2\right)^2 = C^2r^2u. \tag{3.5.16}$$

By repeating the above procedure we can obtain the value for the function $(u/u_t)^2$ and then by assuming different values of C we obtain the solutions u_s to get the critical points $(r_s, \pm u_s)$.

In figure 3.2 we plot the transonic solutions obtained for the isothermal equation of state with different state parameters i.e. $k = 1, 1/2, 1/3, 1/4$.

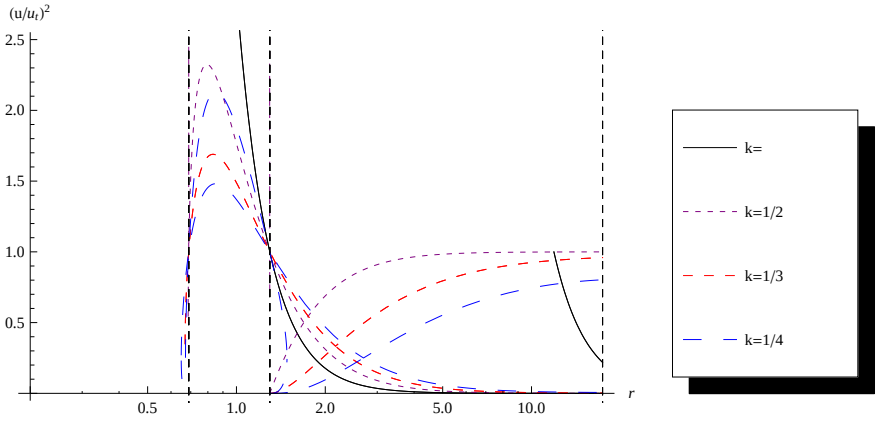

Figure 3.2: Transonic solutions obtained for the isothermal equation of state with $M = 1$, $Q = 0.95$ and $\Lambda = -0.01$. The vertical lines show the location of horizons.

3.6 Accretion of Polytropic Test Fluids

In this section we assume a polytropic equation of state i.e. $p = kn^{\Gamma}$. Using this, we can express enthalpy as [21]

$$h = 1 + \frac{a^2}{\Gamma - 1 - a^2}, \tag{3.6.1}$$

or

$$h = \frac{\Gamma - 1}{\Gamma - 1 - a^2}. \tag{3.6.2}$$

Using Eq. (3.6.2) in (3.2.13) we obtain

$$\frac{\sqrt{1 - \frac{2M}{r} + \frac{Q^2}{r^2} - \frac{\Lambda r^2}{3} + u^2}}{\Gamma - 1 - a^2} = C_3. \tag{3.6.3}$$

When r is sufficiently large (say infinite), then the above equation will be

$$\frac{\sqrt{1-\frac{2M}{r_\infty}+\frac{Q^2}{r_\infty^2}-\frac{\Lambda r_\infty^2}{3}+u_\infty^2}}{\Gamma-1-a_\infty^2} = C_4, \tag{3.6.4}$$

where C_3 and C_4 are the constants. If we compare Eq. (3.6.3) and (3.6.4) we find that

$$\frac{\sqrt{1-\frac{2M}{r}+\frac{Q^2}{r^2}-\frac{\Lambda r^2}{3}+u^2}}{\Gamma-1-a^2} = \frac{\sqrt{1-\frac{2M}{r_\infty}+\frac{Q^2}{r_\infty^2}-\frac{\Lambda r_\infty^2}{3}+u_\infty^2}}{\Gamma-1-a_\infty^2}. \tag{3.6.5}$$

Alternatively,

$$\begin{aligned}&(\Gamma-1-a_\infty^2)\sqrt{1-\frac{2M}{r}+\frac{Q^2}{r^2}-\frac{\Lambda r^2}{3}+u^2}\\ =\ &(\Gamma-1-a^2)\sqrt{1-\frac{2M}{r_\infty}+\frac{Q^2}{r_\infty^2}-\frac{\Lambda r_\infty^2}{3}+u_\infty^2}.\end{aligned} \tag{3.6.6}$$

Now at sonic point, enthalpy becomes

$$\frac{h}{h_\infty}=\left(\frac{n}{n_\infty}\frac{a_\infty^2}{a^2}\right)^{\Gamma-1}. \tag{3.6.7}$$

Using the value from Eq. (3.6.2), we can write

$$n = n_\infty\left(\frac{a^2}{a_\infty^2}\frac{\Gamma-1-a^2}{\Gamma-1-a_\infty^2}\right)^{\frac{1}{\Gamma-1}}. \tag{3.6.8}$$

Futhermore, as $r^2nu=C_1$. When r is sufficiently large, it will be $r_\infty^2 n_\infty u_\infty = C_5$. So, on combining Eq. (3.6.7) and Eq. (3.6.8) we get

$$u=u_\infty.\frac{r_\infty^2}{r^2}\left(\frac{a_\infty^2}{a^2}.\frac{\Gamma-1-a^2}{\Gamma-1-a_\infty^2}\right)^{\frac{1}{\Gamma-1}}. \tag{3.6.9}$$

At the crtitical point r_s Eq. (3.6.6) becomes

$$\begin{aligned}&(\Gamma-1-a_s^2)^2\left(1-\frac{2M}{r_\infty}+\frac{Q^2}{r_\infty^2}-\frac{\Lambda r_\infty^2}{3}+B\right)\\ =\ &(\Gamma-1-a_\infty^2)^2\left(1-\frac{3M}{2r_s}+\frac{Q^2}{2r_s^2}-\frac{\Lambda r_s^2}{2}\right),\end{aligned} \tag{3.6.10}$$

where,

$$B \equiv u_s^2 \frac{r_s^4}{r_\infty^4} \left(\frac{a_s^2}{a_\infty^2} \frac{\Gamma - 1 - a_\infty^2}{\Gamma - 1 - a_s^2} \right)^{\frac{2}{\Gamma - 1}} . \tag{3.6.11}$$

We note that Eq. (3.6.11) has only one unknown r_s. So, if we solve this equation with boundary values of r_∞ and a_∞, we obtain the critical values of r_s, a_s^2 and u_s. Same like isothermal case we can compute two critical points in polytropic case also i.e. $(r_s, \pm u_s)$. Further, Eq. (3.6.10) can also be solved numerically to obtain the function $u(r)$.

3.7 Conclusion

In this chapter, we have reviewed the accretion on the Reissner-Nordström anti-de-Sitter black hole. We have considered the isothermal as well as polytropic test fluids. For isothermal test fluids the specific cases of so called ultra-stiff fluid, ultra-relativistic fluid, radiation fluid and sub-relativistic fluid are discussed. We have derived the analytical solutions at the sonic point and also discussed that how this issue can be treated via Hamiltonian dynamical system.

Chapter 4

Accretion by the Static Spherically Symmetric Black Hole

In this chapter, we extend our previous work and make a general formulism of accretion without specifying the metric coefficient f. The results are valid for all spacetimes that are static spherically symmetric of the form

$$ds^2 = f(r)dt^2 + \frac{1}{f(r)}dr^2 + r^2(d\theta^2 + \sin^2\theta d\phi^2). \tag{4.0.1}$$

4.1 General Equations for Spherical Accretion

In this section, we define the governing equations for spherical accretion. Here, we are considering the gas as a perfect fluid. For this, we define the two basic laws of accretion i.e. particle conservation and energy conservation. We assume that the fluid is simple containing a single particle species; the fluid could be made of different particle species with low reactions rates or no reactions at all. Let n be the baryon number density in the fluid rest frame and

$$u^\mu = dx^\mu/d\tau, \tag{4.1.1}$$

be the intrinsic four velocity of the fluid where τ is the proper time. We define the particle flux or current density by $J^\mu = nu^\mu$. From the law of particle conservation, there will be no change in the number of particles i.e.

neither particles are created nor destroyed. In other words, we say that for this system, the divergence of current density is conserved

$$\nabla_\mu J^\mu = \nabla_\mu (nu^\mu) = 0, \tag{4.1.2}$$

where ∇_μ is the covariant derivative. On the other hand, the stress-energy (SET) for a perfect fluid is given by

$$T^{\mu\nu} = (e+p)u^\mu u^\nu + pg^{\mu\nu}, \tag{4.1.3}$$

where e denotes the energy density and p is the pressure. The Michel-type accretion is steady state and spherically symmetric [16], so all the physical quantities (n, e, p, u^μ) and others that will be introduced later are functions of the radial coordinate r only. Furthermore, we assume that the fluid is radially flowing in the equatorial plane ($\theta = \pi/2$), therefore $u^\theta = 0$ and $u^\phi = 0$. For ease of notation we set $u^r = u$. Using the normalization condition $u^\mu u_\mu = -1$, we obtain,

$$u_t = \pm\sqrt{f + u^2}. \tag{4.1.4}$$

On the equatorial plane ($\theta = \pi/2$), the continuity equation (4.1.2) yields

$$\begin{aligned} \nabla_\mu (nu^\mu) &= \frac{1}{\sqrt{-g}}\partial_\mu(\sqrt{-g}nu^\mu) \\ &= \frac{1}{r^2}\partial_r(r^2 nu) = 0. \end{aligned} \tag{4.1.5}$$

or, upon integrating,

$$r^2 nu = C_1, \tag{4.1.6}$$

where C_1 is a constant of integration. This shows that, in a unit of proper time, the particle flux $\pi r^2 nu$ through a sphere a radius r remains constant for all r.

The thermodynamics of simple fluids is described by the two equations [1]

$$dp = n(dh - Tds), \quad de = hdn + nTds, \tag{4.1.7}$$

where T is the temperature, s is the specific entropy (entropy per particle), and

$$h = \frac{e+p}{n}, \tag{4.1.8}$$

is the specific enthalpy (enthalpy per particle)[1].

A theorem in relativistic hydrodynamics [1] states that the scalar $hu_\mu\xi^\mu$ is conserved along the trajectories of the fluid:

$$u^\nu\nabla_\nu(hu_\mu\xi^\mu) = 0, \tag{4.1.9}$$

where ξ^μ is a Killing vector of spacetime generator of symmetry. In the special case we are considering in this work $\xi^\mu = (1, 0, 0, 0)$ is timelike yielding

$$\partial_r(hu_t) = 0 \quad \text{or} \quad h\sqrt{f + u^2} = C_2, \tag{4.1.10}$$

where C_2 is a constant of integration. This equation can be derived directly upon evaluating

$$\nabla_\mu T^\mu{}_t = nu^\mu\nabla_\mu(hu_t) + \nabla_t(nh - e) = 0, \tag{4.1.11}$$

where we have used $T^\mu{}_\nu = nhu^\mu u_\nu + (nh - e)\delta^\mu{}_\nu$. Since, the flow is stationary, any time derivative vanishes ($\nabla_t(nh - e) \equiv 0$), hence the result.

If the fluid had a uniform pressure, that is, if the fluid were not subject to acceleration, the specific enthalpy h reduces to the particle mass m and Eq. (4.1.9) reduces to $mu_\mu\xi^\mu = cst$ along the fluidlines. This is the well know energy conservation law which stems from the fact that the fluid flow is in this case geodesic. Now, if the pressure throughout the fluid is not uniform, acceleration develops through the fluid and the fluid flow becomes non-geodesic; the energy conservation equation $mu_\mu\xi^\mu = cst$, which is no longer valid, generalizes to its inertial equivalent [1] $hu_\mu\xi^\mu = cst$ as expressed in Eqs. (4.1.9) and (4.1.10).

It is well known that a perfect fluid (4.1.3) is adiabatic; that is, the specific entropy is conserved along the evolution lines of the fluid ($u^\mu\nabla_\mu s = 0$). This is easily established using the conservation of the SET, Eq. (4.1.2), and the second equation in (4.1.7). First, rewrite $T^{\mu\nu}$ as $nhu^\mu u^\nu + (nh - e)g^{\mu\nu}$, then project the conservation formula of the stress energy-momentum tensor onto u^μ

$$\begin{aligned} u_\nu\nabla_\mu T^{\mu\nu} &= u_\nu\nabla_\mu[nhu^\mu u^\nu + (nh - e)g^{\mu\nu}] \\ &= u^\mu(h\nabla_\mu n - \nabla_\mu e) = -nTu^\mu\nabla_\mu s = 0. \end{aligned} \tag{4.1.12}$$

[1]If m is the baryonic mass, then $\rho = mn$ is the mass density. Now, if $\mathfrak{h} = h/m$ and $\mathfrak{s} = s/m$ denote the enthalpy and entropy per unit mass, respectively, then $\rho\mathfrak{h} = nh$ and $\rho\mathfrak{s} = ns$. In terms of $(\mathfrak{h}, \mathfrak{s}, \rho)$, Eqs. (4.1.7) and (4.1.8) take the forms $dp = n(d\mathfrak{h} - Td\mathfrak{s})$, $de = \mathfrak{h}d\rho + \rho Td\mathfrak{s}$, and $\mathfrak{h} = (e + p)/\rho$.

In the special case we are considering in this work where the fluid motion is radial, stationary (no dependence on time), and it conserves the spherical symmetry of the black hole, the latter equation reduces to $\partial_r s = 0$ everywhere, that is, $s \equiv$ const.. Thus, the motion of the fluid is isentropic and equations (4.1.7) reduce to

$$dp = ndh, \quad de = hdn. \tag{4.1.13}$$

Equations (4.1.6) and (4.1.10) are the main equations that we will use to analyze the flow of a perfect fluid in the background of f(R) black hole.

Another formula that will turn useful in the subsequent sections is the barotropic equation. Notice that the canonical form of the equation of state (EOS) of a simple fluid is $e = e(n, s)$ [24]. Since s is constant, this reduces to the barotropic form

$$e = F(n). \tag{4.1.14}$$

From the second equation (4.1.13) we have $h = de/dn$ yielding

$$h = F'(n), \tag{4.1.15}$$

where the prime denotes differentiation with respect to n. Now, the first equation (4.1.13) yields $p' = nh'$ with $h = F'$ we obtain

$$p' = nF'', \tag{4.1.16}$$

which we integrate by parts to derive

$$p = nF' - F. \tag{4.1.17}$$

Here we identify, up to a sign, the Legendre transform of the energy density F. This conclusion is purely thermodynamic and it does not depend on the symmetric properties of the flow (presence of a timelike Killing vector and spherical symmetric flow); rather, it is valid for any isentropic flow (s constant everywhere). The conclusion states that the pressure is the negative of the Legendre transform of the energy density and that an EOS of the form $p = G(n)$ is not independent of an EOS $e = F(n)$. The relationship between F and G can be derived upon integrating the first differential equation

$$nF'(n) - F(n) = G(n). \tag{4.1.18}$$

In a locally inertial frame, the three-dimensional speed of sound a is given by $a^2 = (\partial p/\partial e)_s$ [25]. Since the entropy s is constant, this reduces to $a^2 = dp/de$. Using (4.1.13), we derive a useful formula needed for the remaining sections

$$a^2 = \frac{dp}{de} = \frac{ndh}{hdn} \Rightarrow \frac{dh}{h} = a^2 \frac{dn}{n}. \tag{4.1.19}$$

Using (4.1.15), this reduces to

$$a^2 = \frac{ndh}{hdn} = \frac{n}{F'} F'' = n(\ln F')'. \tag{4.1.20}$$

Another useful formula is the three-velocity of a fluid element v as measured by a locally static observer. Since the motion is radial in the plane $\tau = \pi/2$, we have $d\tau = d\phi = 0$ and the metric (4.0.1) implies the decomposition

$$ds^2 = -(\sqrt{f}dt)^2 + (dr/\sqrt{f})^2$$

in the standard special relativistic way [26] as seen by a locally static observer. The latter measures proper distances and proper times by $d\ell = dr/\sqrt{f}$ and $d\tau_0 = \sqrt{f}dt$ corresponding to radial dr and time dt changes, respectively, and measures the three-velocity v of the fluid element by

$$v \equiv \frac{d\ell}{d\tau_0} = \frac{dr/\sqrt{f}}{\sqrt{f}dt}. \tag{4.1.21}$$

This yields

$$v^2 = \Big(\frac{u}{fu^t}\Big)^2 = \frac{u^2}{u_t^2} = \frac{u^2}{f + u^2}, \tag{4.1.22}$$

where we have used $u^r = u = dr/d\tau$, $u^t = dt/d\tau$, $u_t = -fu^t$, and (4.1.4). This implies

$$u^2 = \frac{fv^2}{1 - v^2} \quad \text{and} \quad u_t^2 = \frac{f}{1 - v^2}, \tag{4.1.23}$$

and (4.1.6) becomes

$$\frac{r^4 n^2 f v^2}{1 - v^2} = C_1^2. \tag{4.1.24}$$

In relativistic hydrodynamics one usually derives the above formulas on considering the woldlines of a fluid element and that of a locally static observer.

4.2 Hamiltonian System for a General Static Spherically Symmetric Spacetime

We have derived two integrals of motion (C_1, C_2) given in (4.1.6) and (4.1.10). Either of these integrals, or any combination of them, can be used as a Hamiltonian for the fluid flow. The simplest Hamiltonian system has one degree of freedom, in which case the Hamiltonian $\mathcal{H}$ is a two-variable function (x, y). Let $\mathcal{H}$ be the square of the lhs of (4.1.10):

$$\mathcal{H} = h^2(f + u^2). \tag{4.2.1}$$

Now, we need to fix the two dynamical variables (x, y) on which $\mathcal{H}$ depends and the time variable $\bar{t}$ of the Hamiltonian dynamical system. There are different ways to fix the dynamical variables; one may choose (x, y) to be (r, u), (r, v^2), (r, n), (r, h), or even (r, p). The time variable $\bar{t}$ for the dynamical system is any variable on which $\mathcal{H}$ (4.2.1) does not depend explicitly so that the dynamical system is autonomous.

In the above section we have seen that, under the symmetry requirements of the problem, h is an explicit function of the baryon number density n only; this applies to the pressure p too. So, if (x, y) are chosen to be (r, h) (resp. (r, p)), the Hamiltonian (4.2.1) takes the form

$$\mathcal{H} = h(n)^2\Big[f(r) + \frac{C_1^2}{r^4 n^2}\Big] \qquad (C_1^2 > 0), \tag{4.2.2}$$

where we have used (4.1.6) (resp. $\mathcal{H} = h(p)^2\big[f(r) + \frac{C_1^2}{r^4 n(p)^2}\big]$).

This conclusion does not extend to other dynamical variables, that is, if one chooses (x, y) to be, say, (r, v), it is not true to assume $h = h(r)$ or $h = h(v)$, for, by (4.1.6) and (4.1.23), n is a function of (r, v) and so is h. With $h = h(r, v)$, the Hamiltonian (4.2.1) of the dynamical system reads

$$\mathcal{H}(r, v) = \frac{h(r, v)^2 f(r)}{1 - v^2}, \tag{4.2.3}$$

where we have used (4.1.23) to eliminate u^2 from (4.2.1). We have thus fixed the dynamical variable to be (r, v). No use has been made of (4.1.6) to derive (4.2.3); use of it will be made in the derivation of the critical points (CPs), particularly, of the sonic points.

From now on, partial derivatives will be denoted as $\partial f/\partial x = f_{,x}$.

4.3 Sonic Points for a General Static Spherically Symmetric Spacetime

In the remaining part of this section, we assume that the parametric Hamiltonian of the dynamical system is given by (4.2.3). In this section we use (4.2.3) to derive the CPs of the dynamical system..

With $\mathcal{H}$ given by (4.2.3), the dynamical system reads

$$\dot{r} = \mathcal{H}_{,v}\,, \qquad \dot{v} = -\mathcal{H}_{,r}. \tag{4.3.1}$$

(here the dot denotes the $\bar{t}$ derivative). In (4.3.1) it is understood that r is kept constant when performing the partial differentiation with respect to v in $\mathcal{H}_{,v}$ and that v is kept constant when performing the partial differentiation with respect to r in $\mathcal{H}_{,r}$. We will keep using this simple notation in the subsequent steps of this section. The CPs of the dynamical system are the points (r_c, v_c) where the rhs's in (4.3.1) are zero. Evaluating the rhs's we find

$$\mathcal{H}_{,v} = \frac{2fh^2v}{(1-v^2)^2}\Big[1 + \frac{1-v^2}{v}\,(\ln h)_{,v}\Big], \tag{4.3.2}$$

$$\mathcal{H}_{,r} = \frac{h^2}{1-v^2}\big[f_{,r} + 2f\,(\ln h)_{,r}\big]. \tag{4.3.3}$$

The rightmost formula in (4.1.19) yields

$$(\ln h)_{,v} = a^2(\ln n)_{,v} \quad \text{ and } \quad (\ln h)_{,r} = a^2(\ln n)_{,r}. \tag{4.3.4}$$

Now, using (4.1.24) we see that if r is kept constant we have the equation $nv/\sqrt{1-v^2} = \text{const.}$ which upon differentiating with respect to v we obtain

$$(\ln n)_{,v} = -\frac{1}{v(1-v^2)} \Rightarrow (\ln h)_{,v} = -\frac{a^2}{v(1-v^2)}; \tag{4.3.5}$$

and if v is kept constant we have the equation $r^2 n\sqrt{f} = \text{const.}$ which upon differentiating with respect to r we obtain

$$(\ln n)_{,r} = -\frac{4 + r(\ln f)_{,r}}{2r} \Rightarrow (\ln h)_{,r} = -\frac{a^2[4 + r(\ln f)_{,r}]}{2r}. \tag{4.3.6}$$

Finally, the system (4.3.1) reads

$$\dot{r} = \frac{2fh^2}{v(1-v^2)^2}\,(v^2 - a^2), \tag{4.3.7}$$

$$\dot{v} = -\frac{h^2}{r(1-v^2)}[rf_{,r}(1-a^2) - 4fa^2]. \tag{4.3.8}$$

Let us assume that h is never zero and finite (the same applies to n). The rhs's vanish if

$$v_c^2 = a_c^2 \quad \text{and} \quad r_c(1-a_c^2)f_{c,r_c} = 4f_c a_c^2, \tag{4.3.9}$$

where $f_c = f(r)|_{r=c}$ and $f_{c,r_c} = f_{,r}|_{r=c}$. The second equation expresses the speed of sound at the CP, a_c^2, in terms of r_c

$$a_c^2 = \frac{r_c f_{c,r_c}}{r_c f_{c,r_c} + 4f_c}, \tag{4.3.10}$$

which will allow to determine r_c once the EOS $a^2 = dp/de$ [or $e = F(n)$] is known. The remaining needed ingredient is a simplified expression for n/n_c. If we write the constant C_1^2 in (4.1.24) as

$$C_1^2 = r_c^4 n_c^2 v_c^2 \, \frac{f_c}{1-v_c^2} = r_c^4 n_c^2 v_c^2 \, \frac{r_c f_{c,r_c}}{4v_c^2} = \frac{r_c^5 n_c^2 f_{c,r_c}}{4}, \tag{4.3.11}$$

where we have used (4.3.9). Using this in (4.1.24) we obtain

$$\left(\frac{n}{n_c}\right)^2 = \frac{r_c^5 f_{c,r_c}}{4} \, \frac{1-v^2}{r^4 f v^2}. \tag{4.3.12}$$

As we shall see in the subsequent sections, there will be two types of fluid flow approaching the horizon, in the one type the speed v vanishes and in the other one the speed approaches that of light in such a way that the ratio $(1-v^2)/f$ may remain finite. In the former type of motion, the number density n diverges on the horizon independently of the expression of f.

An expression for u_c^2 is derived upon substituting (4.3.9) into (4.1.23), then making use of (4.3.10)

$$u_c^2 = \frac{f a_c^2}{1-a_c^2} = \frac{r_c f_{c,r_c}}{4}. \tag{4.3.13}$$

Another sonic CP is the point corresponding to $f_c = 0$ and $a_c^2 = 1$. But the roots of $f_c = 0$ may coincide with the horizons r_h of the black hole. This implies that the fluid becomes ultra-stiff as it approaches the horizon where $r_c = r_h$ (the fluid is not necessarily ultra-stiff for all r). Now, by (4.1.24), since $f_c = 0$ we must necessarily have $v_c^2 = 1$. This point, however, may fail to behave as a critical point in the mathematical sense, for the rhs's of (4.3.7) and (4.3.8) may become undetermined or may have nonzero values there. For further calculations, first we assume some equation of state.

4.4 Isothermal test fluids

Isothermal flow is often referred to the fluid flowing at a constant temperature. In other words, we can say that the sound speed of the accretion flow remains constant throughout the accretion process. This ensures that the sound speed of accretion flow at any radii is always equivalent to the sound speed at sonic point [27]. Here our system is adiabatic, so it is more likely that the flow of our fluid is isothermal in nature. Therefore, in this section we find the general solution to the isothermal equation of state of the form $p = ke$, that is of the form $p = kF(n)$ (4.1.14) with $G(n) = kF(n)$ (4.1.18). Here k is the state parameter constrained by $(0 < k \leq 1)$ [23]. Generally, the adiabatic sound speed is defined as $a^2 = dp/de$. So by comparing the adiabatic sound speed to the equation of state, we find $a^2 = k$.

The differential equation (4.1.18) reads

$$nF'(n) - F(n) = kF(n), \tag{4.4.1}$$

yielding

$$e = F = \frac{e_c}{n_c^{k+1}}\, n^{k+1}, \tag{4.4.2}$$

where we have chosen the constant of integration[2] so that (4.1.8) and (4.1.15) lead to the same expression for h

$$h = \frac{(k+1)e_c}{n_c^{k+1}}\, n^k = \frac{(k+1)e_c}{n_c}\Big(\frac{n}{n_c}\Big)^k. \tag{4.4.3}$$

Now, setting

$$K = \Big(\frac{r_c^5 f_{c,r_c}}{4}\Big)^k \Big(\frac{(k+1)e_c}{n_c}\Big)^2 = \text{const.},$$

and using (4.3.12) we simplify $h(r,v)^2$ by

$$h^2 = K\Big(\frac{1-v^2}{v^2 r^4 f}\Big)^k. \tag{4.4.4}$$

Upon performing the transformation $\bar{t} \to K\bar{t}$ and $\mathcal{H} \to \mathcal{H}/K$, the constant K gets absorbed in a redefinition of the time $\bar{t}$. Using (4.4.4), the new Hamiltonian $\mathcal{H}$ and the dynamical system (4.3.7), (4.3.8) read

$$\mathcal{H}(r,v) = \frac{f}{1-v^2}\Big(\frac{1-v^2}{v^2 r^4 f}\Big)^k = \frac{f^{1-k}}{(1-v^2)^{1-k} v^{2k} r^{4k}}. \tag{4.4.5}$$

[2]This constant, e_c/n_c^{k+1}, in (4.4.2) could have been chosen e_∞/n_∞^{k+1} or e_0/n_0^{k+1} where (e_0, n_0) are any reference (energy density, number density).

4.5 Conclusion

In this chapter, we have developed a general formulism for the static spherically symmetric accretion. We can find the further solutions for accretion by assuming the isothermal as well as polytropic equation of state. In case of isothermal we can analysed the accretion process for the ultra-stiff, ultra-relativistic, radiation and sub-relativistic fluids. In the similar way, we can also find the transonic solutions which leads us to the maximum accretion rate.

Conclusion

The main purpose of this thesis was to study the astrophysical flows near black holes. The motivation behind this work is the ability of a black hole to capture matter around it due to gravity, which tends to increase its mass and the process is called accretion. We have studied the phenomenon of spherical accretion of the perfect fluid (gas) onto the static spherically symmetric black hole. We considered the Schwarzschild, Schwarzschild anti-de-Sitter and Reissner-Nordström anti-de-Sitter black holes.

For Schwarzschild black hole, we found that the mass of the black hole increases when gas accretes onto it. For Schwarzschild anti-de-Sitter black hole, we have found the interesting results that besides Bondi-type solutions there exists homoclinic solutions which further leads us to the transonic behaviour of the flow. As for transonic flow, the velocity of fluid is close to the speed of sound. Therefore, we get the maximum accretion rate. For this we have considered the isothermal as well as the polytropic equation of state.

For Reissner-Nordström anti-de-Sitter black hole, we have studied the hamiltonian approach to find the solutions. For isothermal equation of state, we have discussed the particular type of fluids such as ultra-stiff fluids, ultra-relativistic fluids, radiation fluids and sub-relativistic fluids. We have found the solutions at the sonic (critical) points where velocity of the fluid becomes equal to the speed of sound.

Further, we have developed a general formulism for spherical accretion of all the static spherically symmetric black holes at the sonic point. This work can be used to find the solutions for the fluid's velocity by considering the different equations of state. Hence, it is concluded that the mass of such black holes increases when a perfect fluid accretes on them.

Bibliography

[1] L. Rezzolla and O. Zanotti, *"Relativistic Hydrodynamics"*(Oxford University Press, 2013).

[2] J.D. Walecka, *"Introduction to General Relativity"*(World Scientific Publishing Company, 2007).

[3] G.E. Romero and G.S. Vila, *"Introduction to Black Hole Astrophysics"*(Springer, 2014).

[4] E. Poisson, *"A Relativist's Toolkit: The Mathematics of Black Hole Mechanics"*(Cambridge University Press, 2004).

[5] M.P. Hobson, G. Efstathiou and A.N. Lasenby, *"General Relativity: An Introduction for Physicists"*(Cambridge University Press, 2006).

[6] H. Stephani, D. Kramer, M. Maccallum, C. Hoenselaers and H. Herlt, *"Exact Solutions to Einstein's Field Equations"*(Cambridge University Press, 2003).

[7] K. Schwarzschild, B. Sitzungsbesichte, Phys. Math Klasse. 189-198 (1916).

[8] R. Ruffini and J.A. Wheeler, Phys. Today **24**, 30 (1971).

[9] P.S. Joshi, *"Gravitational Collapse and Spacetime Singularities"*(Cambridge University Press, 2007).

[10] H. Reissner, Ann. Phys. **50**, 106 (1916).

[11] G. Nordström, Proc. Koninkl. Ned. Akad. Weten. **20**, 1238 (1918).

[12] S.L. Shapiro and S.A. Teukolsky, *"Black Holes, White Dwarfs and Neutron Stars: The Physics of Compact Objects"* (Wiley, New York, 1983).

[13] C. Clarke and B. Carswell, *"Principles of Astrophysical Fluid Dynamics"*(Cambridge University Press, 2007).

[14] P. Mach, Phys. Rev. D **91**, 084016 (2015).

[15] H. Bondi, Mon. Not. Roy. Astron. Soc. **112**, 195 (1952).

[16] F.C. Michel, Astrophys. Space Sci. **15**, 153 (1972).

[17] E.O. Babichev, V. I. Dokuchaev and Yu. N. Eroshenko, arXiv: 1406.0841v1.

[18] M. Jamil and M. Akbar, Gen. Rel. Grav. **43**, 1061 (2011).

[19] A.R. Amani and H. Farahani, Int. J. Theor. Phys. **51**, 2943 (2012).

[20] P. Mach, E. Malec and J. Karkowski, Phys. Rev. D **88**, 084056 (2013).

[21] A. Ganguly, S. G. Ghosh and S. D. Maharaj, Phys. Rev. D **90**, 064037 (2014).

[22] F. Ficek, Class. Quantum Grav. **32**, 235008 (2015).

[23] P. Mach, E. Malec and J. Karkowski, Phys. Rev. D **88**, 084056 (2013).

[24] E. Gourgoulhon, *"An introduction to relativistic hydrodynamics"* (EAS Publications Series, France, 2006).

[25] S. Weinberg, *"Gravitation and Cosmology: Principles and Applications of the General Theory of Relativity"* (Wiley, New York, 1972).

[26] G.F.R. Ellis, R. Maartens, and M.A.H. MacCallum, *"Relativistic Cosmology"* (Cambridge University Press, 2012).

[27] S. Ghosh and P. Banik, Int. J. Mod. Phys. D **24**, 1550084 (2015).

Eur. Phys. J. C (2016) 76:280
DOI 10.1140/epjc/s10052-016-4112-y

THE EUROPEAN PHYSICAL JOURNAL C

Regular Article - Theoretical Physics

Cyclic and heteroclinic flows near general static spherically symmetric black holes

Ayyesha K. Ahmed[1,a], **Mustapha Azreg-Aïnou**[2,b], **Mir Faizal**[3,4,c], **Mubasher Jamil**[1,d]

[1] Department of Mathematics, School of Natural Sciences (SNS), National University of Sciences and Technology(NUST), Islamabad H-12, Pakistan
[2] Engineering Faculty, Başkent University, Bağlıca Campus, Ankara, Turkey
[3] Department of Physics and Astronomy, University of Lethbridge, Alberta T1K 3M4, Canada
[4] Department of Physics and Astronomy, University of Waterloo, Waterloo, ON N2L 3G1, Canada

Received: 5 January 2016 / Accepted: 26 April 2016 / Published online: 19 May 2016

Abstract We investigate the Michel-type accretion onto a static spherically symmetric black hole. Using a Hamiltonian dynamical approach, we show that the standard method employed for tackling the accretion problem has masked some properties of the fluid flow. We determine new analytical solutions that are neither transonic nor supersonic as the fluid approaches the horizon(s); rather, they remain subsonic for all values of the radial coordinate. Moreover, the three-velocity vanishes and the pressure diverges on the horizon(s), resulting in a flow-out of the fluid under the effect of its own pressure. This is in favor of the earlier prediction that pressure-dominant regions form near the horizon. This result does not depend on the form of the metric and it applies to a neighborhood of any horizon where the time coordinate is timelike. For anti-de Sitter-like f(R) black holes we discuss the stability of the critical flow and determine separatrix heteroclinic orbits. For de Sitter-like f(R) black holes, we construct polytropic cyclic, non-homoclinic, physical flows connecting the two horizons. These flows become non-relativistic for Hamiltonian values higher than the critical value, allowing for a good estimate of the proper period of the flow.

1 Introduction

General relativity is one of the best-tested theories in physics, however, there seem to be indications that it might be modified at sufficiently large scales (as well as small scales). The most important indication of the modification of general relativity comes from the observations made on the Supernova type Ia (SN Ia) and Cosmic Microwave Background (CMB) radiation [1–3]. These observations indicate that our universe is undergoing accelerated expansion. This could be explained by dark energy, and the vacuum energy in quantum field theories could have been used as a proposal for dark energy [4,5]. However, the problem with this proposal is that the vacuum energy in quantum field theory is much more than the dark energy required to explain the present rate of expansion of the universe. There seem to be serious limitations on modifying quantum field theories such that the vacuum energy is reduced to fit the amount of dark energy in the universe. In fact, it has been argued that such modifications will lead to a violation of the weak equivalence principle [6,7].

The action for general relativity has also been modified to explain the accelerated expansion of the universe, and currently f(R) gravity is one of the best-studied modifications of general relativity [8–12]. This is because the f(R) gravity theories are known to produce an accelerated expansion of the universe [13–15]. Furthermore, if a cosmological constant exists, it will not have any measurable effect for most astrophysical phenomena [16,17]. However, the f(R) gravity theories can have astrophysical consequences. In fact, astrophysical consequences have also been used to constrain a certain type of f(R) gravity models [18,19]. So, it becomes both interesting and important to study astrophysical phenomena using f(R) gravity. Several methods for the static spherically symmetric solutions in f(R) gravity are studied in Refs. [20,21]. Regular black holes in f(R) gravity are studied in Refs. [22–24]. Myung discussed the stability of f(R) black holes [25]. Further, there are many applications of f(R) gravity, e.g. gravity waves, brane models, effective equation approach, LHC test etc., [26–28]

[a] e-mail: ayyesha.kanwal@sns.nust.edu.pk
[b] e-mail: research1938@yahoo.com
[c] e-mail: mirfaizalmir@googlemail.com
[d] e-mail: mjamil@sns.nust.edu.pk

An important astrophysical effect of black holes is that they tend to accrete matter, and such accretion on a black hole have been thoroughly studied [29–32]. The first studies of the accretion around a black hole were done by Bondi in the Newtonian framework [33]; this effect is now known by the name of Michel-type accretion. In his work, Bondi studied the hydrodynamics of polytropic flow, and demonstrated that settling and transonic solutions exist for the gas accreting onto compact objects. The relativistic versions of Michel-type accretion have also been studied using the steady state spherically symmetric flow of a test gas around a black hole [34,35]. It may be noted that the luminosity spectra and the effect of an interstellar magnetic field in ionized gases [36], the effect of radiative processes [36–38], and the effect of rotation [39] on accreting processes have also been studied. Recently, the Michel-type accretion of perfect fluids for a black hole in the presence of a cosmological constant has also been studied [40–42]. Jamil and collaborators studied the effects of phantom energy accretion onto static spherically symmetric black holes and the primordial black holes and found the masses of black holes to decrease and vanishing near the Big Rip [43–46]. The accretion on topologically charged black holes of the f(R) theories and the Einstein–Maxwell–Gauss–Bonnet black hole has also been investigated by focusing on both inward and outward flows from the accretion disk [47,48]. Using the fact that data from the high-mass X-ray binary Cygnus X-1 has been used to constrain the values of the parameters for the f(R) gravity theories [49], in this paper, we will rather analyze some other aspects of the Michel-type accretion for a black hole in a theory of f(R) gravity.

The order of the paper is as follows. In Sect. 2 we discuss the general equations for spherical accretion including conservation laws for any static metric. We particularly show that the pressure of the perfect fluid for such spherically symmetric flows is, up to a sign, the Legendre transform of the energy density. This leads to a nice differential equation allowing the determination of the energy density, enthalpy, or pressure knowing one of the equations of state. In Sect. 3, without restricting ourselves to a specific static black hole, we study the accretion phenomenon using the Hamiltonian dynamical system in the plane (r, v) where r is the radial coordinate and v is the three-dimensional speed of the fluid. We discuss sonic and non-sonic critical points for ordinary fluids as well as for non-ordinary matter. In Sect. 4 we write down the metric for static spherically symmetric black hole in a particular model of f(R) gravity [50] and discuss some of its properties. In Sect. 5 we study the isothermal fluid and various subcases. There we provide examples of new solutions among which critical flows and purely subsonic flows with vanishing speed and divergent pressure on the horizon as well as separatrix heteroclinic orbits by restricting the analysis to an f(R) anti-de Sitter-like black hole. We also determine solutions that are purely supersonic and solution with transonic flows. We discuss the stability of some of these flows. In Sect. 6 we apply the results of our Hamiltonian dynamical analysis to polytropic fluids. In Sect. 7 we again consider the accretion of a polytropic fluid onto an f(R) black hole solution where the function f(R) is modeled by (a) Hu–Sawicki [51] and (b) Starobinsky [8] formulas. The last section contains the conclusion and discussions of the above derivations.

Throughout the paper we have used the common relativistic notation. The chosen metric signature is $(-, +, +, +)$ and we have the geometric units $G = c = 1$.

2 General equations for spherical accretion

In this section, in Sect. 3, and in the first part of each of Sects. 5 and 6 we consider any static spherically symmetric metric of the form

$$\mathrm{d}s^2 = -f\mathrm{d}t^2 + \frac{\mathrm{d}r^2}{f} + r^2(\mathrm{d}\theta^2 + \sin^2\theta\mathrm{d}\phi^2), \tag{1}$$

without specifying the form of the metric coefficient f. Our results will apply to any black hole of that form and to any horizon in a neighborhood of which the time coordinate is timelike. In the second part of each of Sects. 5 and 6 we consider some applications to an f(R) anti-de Sitter-like, to Schwarzschild, and to an f(R) de Sitter-like black hole.

In this section, we define the governing equations for spherical accretion. Here, we are considering the gas as a perfect fluid. We analyze the accretion rate and flow of a perfect fluid in f(R) gravity. For this purpose, we define the two basic laws of accretion i.e. particle conservation and energy conservation. We assume that the fluid is simple containing a single particle species; the fluid could be made of different particle species with low reactions rates or no reactions at all. Let n be the baryon number density in the fluid rest frame and

$$u^\mu = \mathrm{d}x^\mu/\mathrm{d}\tau \tag{2}$$

be the intrinsic four-velocity of the fluid where τ is the proper time. We define the particle flux or current density by $J^\mu = nu^\mu$. From the law of particle conservation, there will be no change in the number of particles i.e. particles neither are created nor destroyed. In other words, we say that for this system, the divergence of the current density is conserved,

$$\nabla_\mu J^\mu = \nabla_\mu(nu^\mu) = 0, \tag{3}$$

where ∇_μ is the covariant derivative. On the other hand, the stress-energy tensor (SET) for a perfect fluid is given by

$$T^{\mu\nu} = (e + p)u^\mu u^\nu + pg^{\mu\nu}, \tag{4}$$

where e denotes the energy density and p is the pressure. The Michel-type accretion is steady state and spherically symmetric [40–42], so all the physical quantities (n, e, p, u^μ) and others that will be introduced later are functions of the radial coordinate r only. Furthermore, we assume that the fluid is radially flowing in the equatorial plane ($\theta = \pi/2$); therefore $u^\theta = 0$ and $u^\phi = 0$. For convenience of notation we set $u^r = u$. Using the normalization condition $u^\mu u_\mu = -1$ and (1), we obtain

$$u_t = \pm\sqrt{f + u^2}. \tag{5}$$

On the equatorial plane ($\theta = \pi/2$), the continuity equation (3) yields

$$\nabla_\mu(nu^\mu) = \frac{1}{\sqrt{-g}}\partial_\mu(\sqrt{-g}nu^\mu) = \frac{1}{r^2}\partial_r(r^2 nu) = 0, \tag{6}$$

or, upon integrating,

$$r^2 nu = C_1, \tag{7}$$

where C_1 is a constant of integration. This shows that, in the units of proper time, the particle flux $\pi r^2 nu$ through a sphere with radius r remains constant for all r.

The thermodynamics of simple fluids is described by the two equations [59]

$$\mathrm{d}p = n(\mathrm{d}h - T\mathrm{d}s), \quad \mathrm{d}e = h\mathrm{d}n + nT\mathrm{d}s, \tag{8}$$

where T is the temperature, s is the specific entropy (entropy per particle), and

$$h = \frac{e + p}{n}, \tag{9}$$

is the specific enthalpy (enthalpy per particle).[1]

A theorem in relativistic hydrodynamics [59,60] states that the scalar $hu_\mu\xi^\mu$ is conserved along the trajectories of the fluid:

$$u^\nu\nabla_\nu(hu_\mu\xi^\mu) = 0, \tag{10}$$

where ξ^μ is a Killing vector of the spacetime generator of the symmetry. In the special case we are considering in this work $\xi^\mu = (1, 0, 0, 0)$ is timelike, yielding

$$\partial_r(hu_t) = 0 \quad \text{or} \quad h\sqrt{f + u^2} = C_2, \tag{11}$$

where C_2 is a constant of integration. This equation can be derived directly upon evaluating

$$\nabla_\mu T^\mu{}_t = nu^\mu\nabla_\mu(hu_t) + \nabla_t(nh - e) = 0, \tag{12}$$

where we have used $T^\mu{}_\nu = nhu^\mu u_\nu + (nh - e)\delta^\mu{}_\nu$. Since the flow is stationary, any time derivative vanishes ($\nabla_t(nh - e) \equiv 0$), hence the result.

If the fluid had a uniform pressure, that is, if the fluid were not subject to acceleration, the specific enthalpy h reduces to the particle mass m and Eq. (10) reduces to $mu_\mu\xi^\mu = cst$ along the fluid lines. This is the well-known energy conservation law which stems from the fact that the fluid flow is in this case geodesic. Now, if the pressure throughout the fluid is not uniform, acceleration develops through the fluid and the fluid flow becomes non-geodesic; the energy conservation equation $mu_\mu\xi^\mu = cst$, which is no longer valid, generalizes to its inertial equivalent [59] $hu_\mu\xi^\mu = cst$ as expressed in Eqs. (10) and (11).

It is well known that a perfect fluid (4) is adiabatic; that is, the specific entropy is conserved along the evolution lines of the fluid ($u^\mu\nabla_\mu s = 0$). This is easily established using the conservation of the SET, Eq. (3), and the second equation in (8). First, rewrite $T^{\mu\nu}$ as $nhu^\mu u^\nu + (nh - e)g^{\mu\nu}$, then project the conservation formula of the SET onto u^μ

$$\begin{aligned} u_\nu\nabla_\mu T^{\mu\nu} &= u_\nu\nabla_\mu\left[nhu^\mu u^\nu + (nh - e)g^{\mu\nu}\right] \\ &= u^\mu\left(h\nabla_\mu n - \nabla_\mu e\right) = -nTu^\mu\nabla_\mu s = 0. \end{aligned} \tag{13}$$

In the special case we are considering in this work where the fluid motion is radial, stationary (no dependence on time), and it conserves the spherical symmetry of the black hole, the latter equation reduces to $\partial_r s = 0$ everywhere, that is, $s \equiv$ const.. Thus, the motion of the fluid is isentropic and Eq. (8) reduce to

$$\mathrm{d}p = n\mathrm{d}h, \quad \mathrm{d}e = h\mathrm{d}n. \tag{14}$$

Equations (7) and (11) are the main equations that we will use to analyze the flow of a perfect fluid in the background of f(R) black hole.

Another formula that will turn out to be useful in the subsequent sections is the barotropic equation. Notice that the canonical form of the equation of state (EOS) of a simple fluid is $e = e(n, s)$ [60]. Since s is constant, this reduces to the barotropic form

$$e = F(n). \tag{15}$$

From the second of Eq. (14) we have $h = \mathrm{d}e/\mathrm{d}n$, yielding

$$h = F'(n), \tag{16}$$

[1] If m is the baryonic mass, then $\rho = mn$ is the mass density. Now, if $\mathfrak{h} = h/m$ and $\mathfrak{s} = s/m$ denote the enthalpy and entropy per unit mass, respectively, then $\rho\mathfrak{h} = nh$ and $\rho\mathfrak{s} = ns$. In terms of $(\mathfrak{h}, \mathfrak{s}, \rho)$, Eqs. (8) and (9) take the forms $dp = n(d\mathfrak{h} - Td\mathfrak{s})$, $de = \mathfrak{h}d\rho + \rho Td\mathfrak{s}$, and $\mathfrak{h} = (e + p)/\rho$.

where the prime denotes differentiation with respect to n. Now, the first of Eq. (14) yields $p' = nh'$; with $h = F'$ we obtain

$$p' = nF'', \tag{17}$$

which we integrate by parts to derive

$$p = nF' - F. \tag{18}$$

Here we identify, up to a sign, the Legendre transform of the energy density F. This conclusion is purely thermodynamic and it does not depend on the symmetric properties of the flow (presence of a timelike Killing vector and spherical symmetric flow); rather, it is valid for any isentropic flow (s constant everywhere). The conclusion states that the pressure is the negative of the Legendre transform of the energy density and that an EOS of the form $p = G(n)$ is not independent of an EOS $e = F(n)$. The relationship between F and G can be derived upon integrating the first differential equation,

$$nF'(n) - F(n) = G(n). \tag{19}$$

In a locally inertial frame, the three-dimensional speed of sound a is given by $a^2 = (\partial p/\partial e)_s$ [61]. Since the entropy s is constant, this reduces to $a^2 = \mathrm{d}p/\mathrm{d}e$. Using (14), we derive a useful formula needed for the remaining sections

$$a^2 = \frac{\mathrm{d}p}{\mathrm{d}e} = \frac{n\mathrm{d}h}{h\mathrm{d}n} \Rightarrow \frac{\mathrm{d}h}{h} = a^2\frac{\mathrm{d}n}{n}. \tag{20}$$

Using (16), this reduces to

$$a^2 = \frac{n\mathrm{d}h}{h\mathrm{d}n} = \frac{n}{F'}F'' = n(\ln F')'. \tag{21}$$

Another useful formula is the three-velocity of a fluid element v as measured by a locally static observer. Since the motion is radial in the plane $\theta = \pi/2$, we have $\mathrm{d}\theta = \mathrm{d}\phi = 0$ and the metric (1) implies the decomposition

$$\mathrm{d}s^2 = -(\sqrt{f}\mathrm{d}t)^2 + (\mathrm{d}r/\sqrt{f})^2$$

in the standard special relativistic way [62,63] as seen by a locally static observer. The latter measures proper distances and proper times by $\mathrm{d}\ell = \mathrm{d}r/\sqrt{f}$ and $\mathrm{d}\tau_0 = \sqrt{f}\mathrm{d}t$ corresponding to radial $\mathrm{d}r$ and time $\mathrm{d}t$ changes, respectively, and measures the three-velocity v of the fluid element by

$$v \equiv \frac{\mathrm{d}\ell}{\mathrm{d}\tau_0} = \frac{\mathrm{d}r/\sqrt{f}}{\sqrt{f}\mathrm{d}t}. \tag{22}$$

This yields

$$v^2 = \left(\frac{u}{fu^t}\right)^2 = \frac{u^2}{u_t^2} = \frac{u^2}{f+u^2}, \tag{23}$$

where we have used $u^r = u = \mathrm{d}r/\mathrm{d}\tau$, $u^t = \mathrm{d}t/\mathrm{d}\tau$, $u_t = -fu^t$, and (5). This implies

$$u^2 = \frac{fv^2}{1-v^2} \quad \text{and} \quad u_t^2 = \frac{f}{1-v^2}, \tag{24}$$

and (7) becomes

$$\frac{r^4n^2fv^2}{1-v^2} = C_1^2. \tag{25}$$

In relativistic hydrodynamics one usually derives the above formulas on considering the world lines of a fluid element and that of a locally static observer. If $\mathbf{u}$ and $\mathbf{u_0}$ are the respective four-velocities, we have [60,64]

$$\mathbf{u} = \Gamma(\mathbf{u_0} + \mathbf{U}) \quad (\text{with } \mathbf{u_0}\cdot\mathbf{U} = 0), \tag{26}$$

where $\mathbf{U}$ is the relative four-velocity, that is, the velocity of the observer attached to the fluid element relative to the locally static observer with the property $\mathbf{u_0}\cdot\mathbf{U} = 0$, where the dot represents the scalar product with respect to the metric (1). Γ is the Lorentz factor $\Gamma \equiv -\mathbf{u_0}\cdot\mathbf{u} = d\tau_0/d\tau$ [60,64]. In the case of radial motion in the $\theta = \pi/2$ plane, we have

$$\begin{aligned}\mathbf{u} &= (u^t, u, 0, 0) = u^t\partial_t + u\partial_r,\\ \mathbf{u_0} &= (1/\sqrt{f}, 0, 0, 0) = \partial_t/\sqrt{f},\\ \mathbf{U} &= (0, V^r, 0, 0) = V^r\partial_r.\end{aligned} \tag{27}$$

Here u^t and $u = u^r$ are as defined in (2) and $V^r = dr/d\tau_0 = \sqrt{f}v$. Since ∂_r is not a unit four-vector, rather it is v, and not V^r, the three-velocity that the locally static physical observer, who uses the orthonormal basis $(\partial_t/\sqrt{f}, \sqrt{f}\partial_r, \partial_\theta/r, \partial_\phi/r)$, measures. Squaring (26) we obtain

$$\Gamma = \frac{1}{\sqrt{1-\mathbf{U}\cdot\mathbf{U}}} = \frac{1}{\sqrt{1-v^2}}, \tag{28}$$

where we have used $\mathbf{U}\cdot\mathbf{U} = g_{rr}V^rV^r = v^2$ in the last expression. Equations (24) are rederived from (26), (27), and (28).

All the above expressions remain valid for an observer outside the horizon, more precisely, for an observer where the time coordinate is timelike. We define the value v_h of v on the horizon(s) r_h as the limit of the continuous three-velocity field $v(r)$ as r approaches r_h from within the region where the time coordinate is timelike ($f > 0$):

$$v_h = \lim_{r \underset{(f>0)}{\to} r_h} v(r). \tag{29}$$

3 Hamiltonian systems

We have derived two integrals of motion (C_1, C_2) given in (7) and (11). Either of these integrals, or any combination of them, can be used as a Hamiltonian for the fluid flow. The simplest Hamiltonian system has one degree of freedom, in which case the Hamiltonian $\mathcal{H}$ is a two-variable function (x, y). Let $\mathcal{H}$ be the square of the lhs of (11):

$$\mathcal{H} = h^2(f + u^2). \tag{30}$$

Now, we need to fix the two dynamical variables (x, y) on which $\mathcal{H}$ depends and the time variable $\bar{t}$ of the Hamiltonian dynamical system. There are different ways to fix the dynamical variables; one may choose (x, y) to be (r, u) [42], (r, v^2) [42], (r, n) [65], (r, h), or even (r, p). The time variable $\bar{t}$ for the dynamical system is any variable on which $\mathcal{H}$ (30) does not depend explicitly so that the dynamical system is autonomous.

In Sect. 2 we have seen that, under the symmetry requirements of the problem, h is an explicit function of the baryon number density n only; this applies to the pressure p too. So, if (x, y) are chosen to be (r, h) (resp. (r, p)), the Hamiltonian (30) takes the form

$$\mathcal{H} = h(n)^2 \left[f(r) + \frac{C_1^2}{r^4 n^2} \right] \quad (C_1^2 > 0), \tag{31}$$

where we have used (7) (resp. $\mathcal{H} = h(p)^2[f(r) + \frac{C_1^2}{r^4 n(p)^2}]$).

This conclusion does not extend to other dynamical variables, that is, if one chooses (x, y) to be, say, (r, v), it is not correct to assume $h = h(r)$ or $h = h(v)$, for, by (7) and (24), n is a function of (r, v), and so is h. With $h = h(r, v)$, the Hamiltonian (30) of the dynamical system reads

$$\mathcal{H}(r, v) = \frac{h(r, v)^2 f(r)}{1 - v^2}, \tag{32}$$

where we have used (24) to eliminate u^2 from (30). We have thus fixed the dynamical variable to be (r, v). No use has been made of (7) to derive (32); use of it will be made in the derivation of the critical points (CPs), particularly, of the sonic points.

From now on, partial derivatives will be denoted as $\partial f/\partial x = f_{,x}$.

3.1 Sonic points

In the remaining part of this section, we assume that the parametric Hamiltonian of the dynamical system is given by (32). In this section we use (32) to derive the CPs of the dynamical system and derive them in Appendix B VIIIC using (31).

With $\mathcal{H}$ given by (32), the dynamical system reads

$$\dot{r} = \mathcal{H}_{,v}, \quad \dot{v} = -\mathcal{H}_{,r} \tag{33}$$

(here the dot denotes the $\bar{t}$ derivative). In (33) it is understood that r is kept constant when performing the partial differentiation with respect to v in $\mathcal{H}_{,v}$ and that v is kept constant when performing the partial differentiation with respect to r in $\mathcal{H}_{,r}$. We will keep using this simple notation in the subsequent steps of this section. The CPs of the dynamical system are the points (r_c, v_c) where the rhs in (33) are zero. Evaluating the rhs we find

$$\mathcal{H}_{,v} = \frac{2fh^2 v}{(1 - v^2)^2} \left[1 + \frac{1 - v^2}{v} (\ln h)_{,v} \right], \tag{34}$$

$$\mathcal{H}_{,r} = \frac{h^2}{1 - v^2} \left[f_{,r} + 2f (\ln h)_{,r} \right]. \tag{35}$$

The rightmost formula in (20) yields

$$(\ln h)_{,v} = a^2 (\ln n)_{,v} \quad \text{and} \quad (\ln h)_{,r} = a^2 (\ln n)_{,r}. \tag{36}$$

Now, using (25) we see that if r is kept constant we have the equation $nv/\sqrt{1 - v^2} = \text{const.}$, by which upon differentiating with respect to v we obtain

$$(\ln n)_{,v} = -\frac{1}{v(1 - v^2)} \Rightarrow (\ln h)_{,v} = -\frac{a^2}{v(1 - v^2)}; \tag{37}$$

and if v is kept constant we have the equation $r^2 n \sqrt{f} = \text{const.}$, by which upon differentiating with respect to r we obtain

$$(\ln n)_{,r} = -\frac{4 + r(\ln f)_{,r}}{2r} \Rightarrow (\ln h)_{,r} = -\frac{a^2[4 + r(\ln f)_{,r}]}{2r}. \tag{38}$$

Finally, the system (33) reads

$$\dot{r} = \frac{2fh^2}{v(1 - v^2)^2} \left(v^2 - a^2 \right), \tag{39}$$

$$\dot{v} = -\frac{h^2}{r(1 - v^2)} \left[r f_{,r} (1 - a^2) - 4 f a^2 \right]. \tag{40}$$

Let us assume that h is never zero and finite (the same applies to n). The rhs vanish if

$$v_c^2 = a_c^2 \quad \text{and} \quad r_c (1 - a_c^2) f_{c,r_c} = 4 f_c a_c^2, \tag{41}$$

where $f_c = f(r)|_{r=c}$ and $f_{c,r_c} = f_{,r}|_{r=c}$. The second equation expresses the speed of sound at the CP, a_c^2, in terms of r_c

$$a_c^2 = \frac{r_c f_{c,r_c}}{r_c f_{c,r_c} + 4 f_c}, \tag{42}$$

which will allow one to determine r_c once the EOS $a^2 = dp/de$ [or $e = F(n)$] is known. The remaining needed ingredient is a simplified expression for n/n_c. If we write the constant C_1^2 in (25) as

$$C_1^2 = r_c^4 n_c^2 v_c^2 \frac{f_c}{1 - v_c^2} = r_c^4 n_c^2 v_c^2 \frac{r_c f_{c,r_c}}{4 v_c^2} = \frac{r_c^5 n_c^2 f_{c,r_c}}{4}, \tag{43}$$

where we have used (41). Using this in (25) we obtain

$$\left(\frac{n}{n_c}\right)^2 = \frac{r_c^5 f_{c,r_c}}{4} \frac{1 - v^2}{r^4 f v^2}. \tag{44}$$

As we shall see in the subsequent sections, there will be two types of fluid flow approaching the horizon, in the one type the speed v vanishes and in the other one the speed approaches that of light in such a way that the ratio $(1 - v^2)/f$ may remain finite. In the former type of motion, the number density n diverges on the horizon independently of the expression of f.

An expression for u_c^2 is derived upon substituting (41) into (24), then making use of (42)

$$u_c^2 = \frac{f a_c^2}{1 - a_c^2} = \frac{r_c f_{c,r_c}}{4}. \tag{45}$$

Another sonic CP is the point corresponding to $f_c = 0$ and $a_c^2 = 1$. But the roots of $f_c = 0$ may coincide with the horizons r_h of the black hole. This implies that the fluid becomes ultra-stiff as it approaches the horizon where $r_c = r_h$ (the fluid is not necessarily ultra-stiff for all r). This conclusion does not apply to f(R) gravity only; rather, to any static spherically symmetric metric of the form (1). To the best of our knowledge, this result has not been announced elsewhere. Now, by (25), since $f_c = 0$ we must necessarily have $v_c^2 = 1$. This point, however, may fail to behave as a CP in the mathematical sense, for the rhs of (39) and (40) may become undetermined or may have nonzero values there. This point $(r = r_h, v = 1)$ may behave as a focus point as we shall see in the next section.

3.2 Non-sonic critical points

From (39), we see that $f_c = 0$ and $f_{c,r_c} = 0$ may lead to a non-sonic CP. However, this CP would be a double root of $f = 0$, which is out of the scope of this paper where we only consider non-extremal black holes.

Another obvious CP, which lies within the scope of f(R) gravity, corresponds to $h(r_c) = 0$ (39) and (40). This is not possible for ordinary matter but is the case for non-ordinary matter with negative pressure. When this is the case, h may vanish at some point with no special constraint on v^2 and a^2. This means that for non-ordinary fluids, the flow may not become transonic at all. We will not pursue this discussion here, for it is out of the scope of this work. In the next section, however, we will pursue this discussion for ordinary matter where it is generally admitted that "`the flow must be supersonic at the horizon, though it is necessarily subsonic at a large distance`" [66]. We will explicitly show, through physical solutions, the existence of subsonic flow for all values of the radial coordinate. Moreover, the speed of the flow vanishes as the fluid approaches the horizon, so the flow does not necessary become supersonic nor transonic near the horizon [67,68]. Our conclusion remains true even for the Schwarzschild black hole. We believe that the use of standard methods for tackling the accretion problems has masked many features of them.

The conclusions made in this section, concerning the sonic CP [from (39) to (45)], do not apply to f(R) gravity only, for we have not fixed the form of the metric coefficient f yet; they apply to any static metric with $g_{tt} = -1/g_{rr}$ and $g_{\theta\theta} = r^2$.

Applications are given in the following sections where we consider three models of f(R) gravity.

4 Black hole in f(R) gravity

Recently, an interesting model of f(R) gravity has been proposed [50], and the motion of test particles around a black hole in this theory has been investigated. The Lagrangian for this model of f(R) theory is given by [50]

$$\mathrm{f}(R) = R + \Lambda + \frac{R + \Lambda}{d^2 (6\alpha^2)^{-1} R + 2\alpha^{-1}} \ln \frac{R + \Lambda}{R_c}, \tag{46}$$

where Λ is the cosmological constant, R_c is a constant of integration,[2] and α, d are free parameters of this theory. The limit that is relevant for astrophysical scale corresponds to $R \gg \Lambda$ and $\mathrm{d}^2(6\alpha^2)^{-1} R \gg 2\alpha$. In this limit, we obtain $\mathrm{f}(R) = R + \Lambda + \mathrm{d}^2(6\alpha^2)^{-1} R \ln \frac{R}{R_c}$. The limit that is relevant to the cosmological scale is $R \sim R d^2 (6\alpha^2)^{-1} \sim \Lambda$ yielding $\mathrm{f}(R) = R + \Lambda$. This limit constrains the accelerating expansion [52]. It is useful to introduce a parameter $\beta = \alpha/d$ in terms of which both limits of the theory can be studied [50]. In this theory, the metric for a spherically symmetric black hole with mass M takes the form

[2] R_c is merely a constant of integration which is used to balance the dimensions of R. Its value, which "`is not sensitive to the SNIa data`" [52], is not known by any physical theory and can only be determined using astronomical constraints as suggested by Safari and Rahvar [52].

$$ds^2 = -f\,dt^2 + \frac{dr^2}{f} + r^2\left(d\theta^2 + \sin^2\theta d\phi^2\right)$$
$$\text{with} \quad f \equiv 1 - \frac{2M}{r} + \beta r - \frac{\Lambda r^2}{3}. \tag{47}$$

If $\Lambda = 0$, (47) reduces to the special case of a Kiselev black hole [55,56] and if $\beta = 0$, (47) reduces to a Schwarzschild–de-Sitter or Schwarzschild–anti-de-Sitter black hole.

The present model of f(R) can explain the flat rotation curve of galaxies, consistent with solar system tests and also explains the pioneer anomaly/acceleration. For details concerning the motivation for this particular model of f(R) theory, we refer the reader to the original work by Saffari and Rahvar [52]. Of course the present analysis can also be done for other f(R) black holes such as (32) of Ref. [53] and will be reported elsewhere. However, due to the generality of our work, further analysis will be trivial as was the case with f(T) gravity black holes [54].

It is well known that f(R) theory has a representation equivalent to a particular class of scalar-tensor (ST) theories namely, the Brans–Dicke (BD) theory i.e. a scalar field being non-minimally coupled to gravity or curvature with a vanishing kinetic term of the scalar field. This description holds for both metric and Palatini f(R) theories [69,70]. Furthermore, the no-hair theorem for black holes in a general ST theory suggests that the Schwarzschild solution is the only asymptotically flat, exterior, vacuum, static and spherically symmetric solution to ST theory [71]. However, it does not rule out the existence of non-asymptotically flat ST black holes without hair. For instance, the Reissner–Nordström anti-de Sitter kind of topological black holes are derived in BD-Maxwell ST theory [72]. In the same context, we study a non-asymptotically flat f(R) black hole.

The roots of $f = 0$, or equivalently, the roots of $P = 0$, where $P \equiv 3rf = -\Lambda r^3 + 3\beta r^2 + 3r - 6M$ is a polynomial of degree 3, determine all possible horizons of (47). If $\Lambda > 0$, the equation $P = 0$ has always some negative root, which we ignore because of the physical singularity at $r = 0$, and it may have two positive roots or a double positive root depending on the values of its coefficients. These two positive roots, if any, determine the event and cosmological horizons. In this case, the fluid flow would be confined in the space region enclosed by the two horizons. If there are no positive roots, the metric coefficient g_{tt} is positive for all $r > 0$; this case is not interesting.

We will be interested in the cases where the positive roots of $P = 0$ are single. Assuming $\Lambda < 0$ (anti-de Sitter-like black hole) and $\beta \geq 0$, then if $\beta^2 > -\Lambda$, $P = 0$ has either two negative roots and one positive root or one double negative root and one positive root; if $0 \leq \beta^2 \leq -\Lambda$, $P = 0$ has one single positive root. On converting the polynomial $P(r)$ into the Weierstrass polynomial $w(z) \equiv 4z^3 - g_2 z - g_3$ by the transformation $r = z + \beta/\Lambda$, we can parameterize the roots of $P = 0$ based on the parametrization of the roots of $w(z)$ as given in the Appendix A VIII [58]. The horizon is given by

$$r_h = \frac{\beta}{\Lambda} + \sqrt{\frac{g_2}{3}}\cos\left(\frac{\eta}{3}\right), \tag{48}$$

if $P = 0$ has at least two real roots;

$$r_h = \frac{\beta}{\Lambda} + \frac{1}{2\cdot 9^{1/3}}\left[\left(9g_3 + \sqrt{3}\sqrt{-\Delta}\right)^{1/3} + \left(9g_3 - \sqrt{3}\sqrt{-\Delta}\right)^{1/3}\right], \tag{49}$$

if $P = 0$ has only one real root. Here g_2 and g_3 are defined by

$$g_2 = \frac{12(\beta^2 + \Lambda)}{\Lambda^2}, \quad g_3 = \frac{4(2\beta^3 + 3\beta\Lambda - 6M\Lambda^2)}{\Lambda^3}, \tag{50}$$

and Δ and the angle $0 \leq \eta \leq \pi$ are defined as in Eqs. (A.2) and (A.4), respectively.

Now, assuming $\Lambda > 0$ (de Sitter-like black hole) and $\beta \geq 0$, $P = 0$ has always one negative root and will have two positive roots, corresponding to an event horizon $r_{\rm eh}$ and a cosmological horizon $r_{\rm ch} > r_{\rm eh}$ if $2(\beta^2+\Lambda)r_+ > 6M\Lambda - \beta$ where r_+ is the positive root of $P'(r) = 0$. When this is the case, the roots are given

$$r_{\rm ch} = \frac{\beta}{\Lambda} + \sqrt{\frac{g_2}{3}}\cos\left(\frac{\eta}{3}\right),$$
$$r_{\rm eh} = \frac{\beta}{\Lambda} - \sqrt{\frac{g_2}{3}}\cos\left(\frac{\pi + \eta}{3}\right), \tag{51}$$

where g_2 and g_3 are defined by (50). Δ and the angle $0 \leq \eta \leq \pi$ are defined as in Eqs. (A.2) and (A.4), respectively. To have a common notation with the case $\Lambda < 0$, we will for short denote $r_{\rm eh}$ and $r_{\rm ch}$ by r_h.

The scalar invariants R, $R^{\mu\nu}R_{\mu\nu}$, and $R^{\mu\nu\sigma\rho}R_{\mu\nu\sigma\rho}$ are given by

$$I_1 = R = \frac{6\beta}{r} - 4\Lambda, \tag{52}$$

$$I_2 = R^{\mu\nu}R_{\mu\nu} = \frac{2\left(5\beta^2 - 6r\beta\Lambda + 2r^2\Lambda^2\right)}{r^2}, \tag{53}$$

$$I_3 = R^{\mu\nu\sigma\rho}R_{\mu\nu\sigma\rho} = \frac{48M^2}{r^6} + \frac{8\beta^2}{r^2} - \frac{8\beta\Lambda}{r} + \frac{8\Lambda^2}{3}, \tag{54}$$

which reduce to the Schwarzschild values $I_1 = I_2 = 0$ and $I_3 = 48M^2/r^6$ if $\beta = \Lambda = 0$. Clearly $r = 0$ is the curvature singularity, which is not removable.

5 Isothermal test fluids

Isothermal flow is often referred to the fluid flowing at a constant temperature. In other words, we can say that the sound speed of the accretion flow remains constant throughout the accretion process. This ensures that the sound speed of accretion flow at any radii is always equivalent to the sound speed at sonic point [73]. Here our system is adiabatic, so it is more likely that the flow of our fluid is isothermal in nature. Therefore, in this section we find the general solution to the isothermal equation of state of the form $p = ke$, which is of the form $p = kF(n)$, see (15), with $G(n) = kF(n)$, see (19). Here k is the state parameter constrained by $(0 < k \leq 1)$ [41]. Generally, the adiabatic sound speed is defined as $a^2 = dp/de$. So by comparing the adiabatic sound speed to the equation of state, we find $a^2 = k$.

The differential equation (19) reads

$$nF'(n) - F(n) = kF(n), \tag{55}$$

yielding

$$e = F = \frac{e_c}{n_c^{k+1}} n^{k+1}, \tag{56}$$

where we have chosen the constant of integration[3] so that (9) and (16) lead to the same expression for h

$$h = \frac{(k+1)e_c}{n_c^{k+1}} n^k = \frac{(k+1)e_c}{n_c} \left(\frac{n}{n_c}\right)^k. \tag{57}$$

Now, setting

$$K = \left(\frac{r_c^5 f_{,r_c}}{4}\right)^k \left(\frac{(k+1)e_c}{n_c}\right)^2 = \text{const.},$$

and using (44) we simplify $h(r, v)^2$ by

$$h^2 = K\left(\frac{1-v^2}{v^2 r^4 f}\right)^k. \tag{58}$$

Upon performing the transformation $\bar{t} \to K\bar{t}$ and $\mathcal{H} \to \mathcal{H}/K$, the constant K gets absorbed in a re-definition of the time $\bar{t}$. Using (58), the new Hamiltonian $\mathcal{H}$ and the dynamical system (39), (40) read

$$\begin{aligned}
\mathcal{H}(r, v) &= \frac{f}{1-v^2}\left(\frac{1-v^2}{v^2 r^4 f}\right)^k = \frac{f^{1-k}}{(1-v^2)^{1-k} v^{2k} r^{4k}}, \\
\dot{r} &= \frac{2(v^2-a^2)f}{v(1-v^2)^2}\left(\frac{1-v^2}{v^2 r^4 f}\right)^k, \\
\dot{v} &= -\frac{1}{r(1-v^2)}\left(\frac{1-v^2}{v^2 r^4 f}\right)^k \left[r f_{,r}\left(1-a^2\right) - 4 f a^2\right],
\end{aligned} \tag{59}$$

where the dot denotes differentiation with respect to the new time $\bar{t}$.

For a subsequent physical discussion we need an expression for the pressure. With $p = ke$, we obtain upon substituting (44) into (56)

$$p \propto \left(\frac{1-v^2}{v^2 r^4 f}\right)^{\frac{k+1}{2}}. \tag{60}$$

Since the Hamiltonian (59) remains constant on a solution curve, if the latter approaches the horizon (any horizon) from within the region where t is timelike, f approaches 0, and so the speed v must either approach 1 or 0 so that the Hamiltonian retains the same constant value (otherwise, the Hamiltonian would always assume a 0 value on the horizon regardless its constant value elsewhere). In former case $(v \to 1)$, the pressure (60) may remain finite in a neighborhood of the horizon. In the latter case $(v \to 0)$, the pressure diverges as the solution curve approaches the horizon. This is a very general conclusion which holds for any metric coefficient f and any horizon of the black hole. If the latter is of de Sitter type $(\Lambda > 0)$, a pressure-dominant region may form near both the event and the cosmological horizons. This is in favor of a proposal that a pressure-dominant region would form near the horizon [74].

If $f(r) = 0$ has a single root as r approaches r_h (corresponding to an event, a cosmological, or any horizon in a neighborhood of which t is timelike), which is our case, then, in the latter case $(v \to 0)$, as the curve approaches the horizon $f \sim (r - r_h)$ and $v^{2k} \sim f^{1-k}$, thus $v^2 \sim (r - r_h)^{(1-k)/k}$. Using this in (60) we see that the pressure diverges, as the curve approaches the horizon, as

$$p \sim (r - r_h)^{-\frac{k+1}{2k}}. \tag{61}$$

If r_h is a double root of $f = 0$, we obtain

$$p \sim (r - r_h)^{-\frac{k+1}{k}}.$$

Before we proceed, let us see what the constraints on k to have a physical flow are. Along a solution curve, the Hamiltonian of the dynamical system (59) is constant [where the constant is proportional to C_2 (11)]. A global flow solution that extends to spatial infinity corresponds to

[3] This constant, e_c/n_c^{k+1}, in (56) could have been chosen e_∞/n_∞^{k+1} or e_0/n_0^{k+1} where (e_0, n_0) are any reference (energy density, number density).

$$v \simeq v_1 r^{-\alpha} + v_\infty \quad \text{as} \quad r \to \infty, \tag{62}$$

where ($\alpha > 0$, v_1, $|v_\infty| \leq 1$) are constants. Inserting this in the Hamiltonian (59) it reduces to

$$\mathcal{H} \simeq \begin{cases} \text{(a):} & \frac{f^{1-k}}{r^{4k}}, \quad (\text{if } 0 < |v_\infty| < 1); \\ \text{(b):} & \frac{f^{1-k}}{r^{(4-2\alpha)k}}, \quad (\text{if } v_\infty = 0); \\ \text{(c):} & \frac{f^{1-k}}{r^{(4+\alpha)k-\alpha}}, \quad (\text{if } |v_\infty| = 1). \end{cases} \tag{63}$$

Using the metric (47), each case splits into two subcases as follows.

$$\text{(a)} \Rightarrow \begin{cases} \text{(a1):} & \mathcal{H} \simeq r^{2-6k}, \quad (\text{if } \Lambda \neq 0); \\ \text{(a2):} & \mathcal{H} \simeq r^{1-5k}, \quad (\text{if } \Lambda = 0, \beta \neq 0). \end{cases} \tag{64}$$

Since $\mathcal{H}$ is constant along a solution curve we must have $k = 1/3$ ($\Lambda \neq 0$) and $k = 1/5$ ($\Lambda = 0, \beta \neq 0$), respectively. These are the only possibilities allowing for a fluid flow with a non-vanishing, non-relativistic three-dimensional speed.

$$\text{(b)} \Rightarrow \begin{cases} \text{(b1):} & \mathcal{H} \simeq r^{2-6k+2\alpha k}, \quad (\text{if } \Lambda \neq 0); \\ \text{(b2):} & \mathcal{H} \simeq r^{1-5k+2\alpha k}, \quad (\text{if } \Lambda = 0, \beta \neq 0). \end{cases} \tag{65}$$

Thus, for ordinary fluids we deduce

$$\text{(b1):} \quad \tfrac{1}{3} < k < 1 \quad \text{and} \quad 0 < \alpha \leq 2, \tag{66}$$

$$\text{(b2):} \quad \tfrac{1}{5} < k < 1 \quad \text{and} \quad 0 < \alpha \leq 2, \tag{67}$$

and for non-ordinary fluids ($-1 \leq k < 0$) we deduce

$$\text{(b1):} \quad -1 \leq k < 0 \quad \text{and} \quad \alpha \geq 4, \tag{68}$$

$$\text{(b2):} \quad -1 \leq k < 0 \quad \text{and} \quad \alpha \geq 3. \tag{69}$$

On comparing the leading terms in the expansion (62), we see that the fluid flow for ordinary matter is faster at spatial infinity than it is for non-ordinary matter,

$$\text{(c)} \Rightarrow \begin{cases} \text{(c1):} & \mathcal{H} \simeq r^{2-6k+\alpha-\alpha k}, \quad (\text{if } \Lambda \neq 0); \\ \text{(c2):} & \mathcal{H} \simeq r^{1-5k+\alpha-\alpha k}, \quad (\text{if } \Lambda = 0, \beta \neq 0). \end{cases} \tag{70}$$

Thus, for ordinary fluids we deduce

$$\text{(c1):} \quad \tfrac{1}{3} < k < 1 \quad \text{and} \quad \alpha = \tfrac{2(3k-1)}{1-k} > 0, \tag{71}$$

$$\text{(c2):} \quad \tfrac{1}{5} < k < 1 \quad \text{and} \quad \alpha = \tfrac{5k-1}{1-k} > 0, \tag{72}$$

while for non-ordinary matter ($-1 \leq k < 0$) the subcases (c1, c2) are impossible to hold. Thus, non-ordinary fluids cannot have a relativistic flow at spatial infinity.

In the following we will analyze the behavior of the fluid by taking different cases for the state parameter k. For instance, we have $k = 1$ (ultra-stiff fluid), $k = 1/2$ (ultra-relativistic fluid), $k = 1/3$ (radiation fluid), and $k = 1/4$ (sub-relativistic fluid). For the case of the metric (47), Eq. (42) reduces to

$$k = \frac{(3\beta - 2\Lambda r_c) r_c^2 + 6M}{3[(4 + 5\beta r_c - 2\Lambda r_c^2) r_c - 6M]}, \tag{73}$$

and we keep in mind that $a^2 = k$ in (59). The system (59) and (73) form our basic equations for the remaining part of this section, which is devoted to applications. We mainly focus on anti-de Sitter-like f(R) black holes with an application to Schwarzschild black hole. Further applications to anti-de Sitter-like and de Sitter-like f(R) black holes with polytropic EOS for the test fluids are given in Sect. 6.

5.1 Solution for ultra-stiff fluid ($k = 1$)

Ultra-stiff fluids are those fluids in which isotropic pressure and energy density are equal. For instance, the usual equation of state for the ultra-stiff fluids is $p = \text{ke}$ i.e. the value of state parameter is defined as $k = 1$. This reduces (42) or (73) to $f_c = 0$, thus $r_c = r_h$ (48, 49). The Hamiltonian (59) reduces to

$$\mathcal{H} = \frac{1}{v^2 r^4}. \tag{74}$$

Since the Hamiltonian in Eq. (74) is a constant, one immediately obtains[4]

$$v \sim 1/r^2. \tag{75}$$

It is clear from (74) that the point $(r, v^2) = (r_h, 1)$ is not a CP of the dynamical system, as was noticed in the previous section. Notice that $\mathcal{H}$ no longer depends on f; thus, this expression and the following conclusions are valid for any metric of the form (1).

From (74) we see that, for physical flows ($|v| < 1$), the lower value of $\mathcal{H}$ is $\mathcal{H}_{\text{min}} = 1/r_h^4$: $\mathcal{H} > \mathcal{H}_{\text{min}}$. As shown in Fig. 1, physical flows are represented by the curves sandwiched by the two black curves, which are contour plots of $\mathcal{H}(r, v) = \mathcal{H}_{\text{min}}$. The upper curves where $v > 0$ correspond to fluid outflow or particle emission and the lower curves where $v < 0$ correspond to fluid accretion.

If $\mathcal{H}_0 > \mathcal{H}_{\text{min}}$ is the value of the Hamiltonian on a solution curve, then in the (r, v) plane the curve is the plot

[4] For the cases $k = 1$ and $k = 1/2$ we have expressed explicitly v as a function of r as in Eqs. (75) and (83); it is possible to do the same for the other cases $k = 1/3$ and $k = 1/4$ [see Eqs. (89) and (92)] but the expressions of $v(r)$ would be cumbersome. That is why we preferred a numerical analysis in this section. It is worth mentioning that Eqs. (75) and (83) may be derived from the metric and the conservation laws using the classical approach for accretion [34].

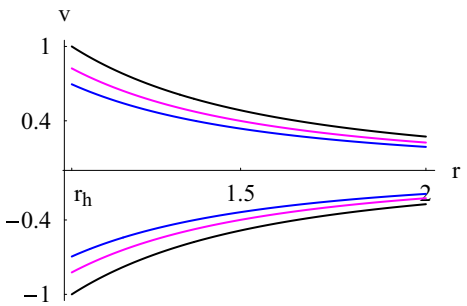

Fig. 1 Contour plot of $\mathcal{H}$ (74), which is the simplified expression of $\mathcal{H}$ (59), for an anti-de Sitter-like f(R) black hole $k = 1$, $M = 1$, $\beta = 0.85$, $\Lambda = -0.075$. The parameters are $r_h \simeq 1.04439$. *Black plot* the solution curve through the CP for which $\mathcal{H} = \mathcal{H}_{\min} = r_h^{-4} \simeq 0.84053$. *Magenta plot* the solution curve for which $\mathcal{H} = \mathcal{H}_{\min} + 0.4$. *Blue plot* the solution curve for which $\mathcal{H} = \mathcal{H}_{\min} + 0.9$

Table 1 Types of flow on a solution curve for $k = 1$ (Fig. 1)

Types	Flow behavior
I	$\mathcal{H} > \mathcal{H}_{\min} = r_h^{-4}$: Subsonic flow for $v < 0$ and $v > 0$
II	$\mathcal{H} < \mathcal{H}_{\min} = r_h^{-4}$: Unphysical flow

$v = \pm 1/(\sqrt{\mathcal{H}_0} r^2)$. Using this we can evaluate all the other quantities, for instance (44) becomes

$$\left(\frac{n}{n_c}\right)^2 = \frac{r_h^5 f_{,r}|_{r=r_h}}{4} \frac{\mathcal{H}_0 r^4 - 1}{r^4 f}, \tag{76}$$

for any solution curve $\mathcal{H}_0 > \mathcal{H}_{\min} = r_h^{-4}$, and

$$\left(\frac{n}{n_c}\right)^2 = \frac{r_c f_{,r_c}}{4} \frac{1 - v^2}{f} = \frac{r_h f_{,r}|_{r=r_h}}{4} \frac{r^4 - r_h^4}{r^4 f}, \tag{77}$$

for the solution curve through $(r, v^2) = (r_h, 1)$ $(\mathcal{H}_0 = \mathcal{H}_{\min})$, which all depend on f.

A contour plot of $\mathcal{H}$ (74), depicted in Fig. 1, shows two type of motion: (a) purely subsonic accretion (black, magenta, or blue curves where $v < 0$) or subsonic flow-out (black, magenta, or blue curves where $v > 0$) for $\mathcal{H} > \mathcal{H}_{\min} = r_h^{-4}$, and (b) purely supersonic accretion or flow-out (along the red and green curves) for $\mathcal{H} < \mathcal{H}_{\min} = r_h^{-4}$. The flow in (b), along the green and red curves, however, is unphysical, for the speed of the flow exceeds that of light on some portions of the curves. A brief elaboration is given in Table 1.

5.2 Solution for ultra-relativistic fluid ($k = 1/2$)

Ultra-relativistic fluids are those fluids whose isotropic pressure is less than the energy density. In this case, the equation of state is defined as $p = \frac{e}{2}$ yielding $k = 1/2$. Using this expression in (73) reduces to

$$Q(r_c) = \frac{\Lambda}{6} r_c^3 - \frac{3\beta}{4} r_c^2 - r_c + \frac{5}{2} M = 0. \tag{78}$$

This polynomial has always one and only one positive root if $\Lambda < 0$ and $\beta \geq 0$. Converting this polynomial into the Weierstrass one $w(z)$ by the transformation $r_c = z + 3\beta/(2\Lambda)$, the CP r_c is given either by (see Appendix A)

$$r_c = \frac{3\beta}{2\Lambda} + \sqrt{\frac{g_2}{3}} \cos\left(\frac{\eta}{3}\right), \tag{79}$$

if $Q = 0$ has at least two real roots, or by

$$r_c = \frac{3\beta}{2\Lambda} + \frac{1}{2 \cdot 9^{1/3}} \left[\left(9g_3 + \sqrt{3}\sqrt{-\Delta}\right)^{1/3} + \left(9g_3 - \sqrt{3}\sqrt{-\Delta}\right)^{1/3} \right], \tag{80}$$

if $Q = 0$ has only one real root. Here g_2 and g_3 are defined by

$$g_2 = \frac{3(9\beta^2 + 8\Lambda)}{\Lambda^2}, \quad g_3 = \frac{27\beta^3 + 36\beta\Lambda - 60M\Lambda^2}{\Lambda^3},$$

and Δ and the angle $0 \leq \eta \leq \pi$ are defined as in Eqs. (A.2) and (A.4), respectively.

In the limit $\beta \to 0$, we recover the Schwarzschild anti-de Sitter spacetime and Eq. (79) reduces to

$$r_c = \sqrt{\frac{g_2}{3}} \cos\left(\frac{\eta}{3}\right). \tag{81}$$

The Hamiltonian (59) takes the simple form

$$\mathcal{H} = \frac{\sqrt{f}}{r^2 |v| \sqrt{1 - v^2}}. \tag{82}$$

It is clear from this expression that the point $(r, v^2) = (r_h, 1)$ is not a CP of the dynamical system. For some given value of $\mathcal{H} = \mathcal{H}_0$, Eq. (82) can be solved for v^2. We find

$$v^2 = \frac{1 \pm \sqrt{1 - 4g(r)}}{2}, \tag{83}$$

where $g(r) \equiv f/(\mathcal{H}_0 r^4)$. The plot in Fig. 2 depicts, instead, v versus r for $M = 1$, $\beta = 0.85$, and $\Lambda = -0.075$ resulting in $r_c \simeq 1.33467$ and $\mathcal{H}_c \simeq 0.926185$. The five solution curves, shown in Fig. 2, correspond to $\mathcal{H}_0 = \{\mathcal{H}_c, \mathcal{H}_c \pm 0.04, \mathcal{H}_c \pm 0.09\}$. The upper plot for $v > 0$ corresponds to fluid outflow or particle emission and that for $v > 0$ corresponds to fluid accretion. The plot shows four types of fluid motion. (1) We have purely supersonic accretion ($v < -v_c$), which ends inside the horizon, or purely supersonic outflow ($v > v_c$); (2) we have purely subsonic accretion followed by subsonic flow-out, this is the case of the branches of the blue and magenta solution curves corresponding to $-v_c < v < v_c$. Notice that for this motion the fluid reaches the horizon,

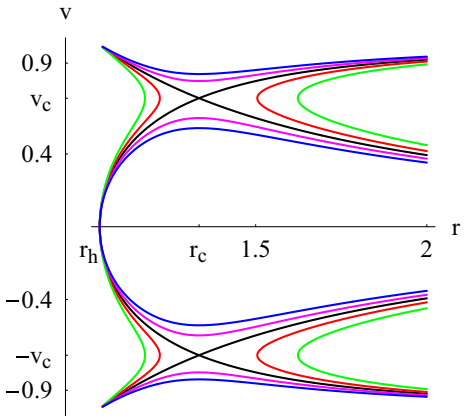

Fig. 2 Contour plot of $\mathcal{H}$ (59) for an anti-de Sitter-like f(R) black hole $k = 1/2$, $M = 1$, $\beta = 0.85$, $\Lambda = -0.075$. The parameters are $r_h \simeq 1.04439$, $r_c \simeq 1.33467$, $v_c = 1/\sqrt{2} \simeq 0.707107$. *Black plot* the solution curve through the saddle CPs (r_c, v_c) and $(r_c, -v_c)$ for which $\mathcal{H} = \mathcal{H}_c \simeq 0.926185$. *Red plot* the solution curve for which $\mathcal{H} = \mathcal{H}_c - 0.04$. *Green plot* the solution curve for which $\mathcal{H} = \mathcal{H}_c - 0.09$. *Magenta plot* the solution curve for which $\mathcal{H} = \mathcal{H}_c + 0.04$. *Blue plot*: the solution curve for which $\mathcal{H} = \mathcal{H}_c + 0.09$

Table 2 Different behaviors of the fluid flow for $k = 1/2$ (Fig. 2)

Types	Flow behavior
I	Supersonic for $-1 < v < v_c$ and $1 > v > v_c$
II	Subsonic for $-v_c < v < v_c$
III	Critical supersonic accretion until $(r_c, -v_c)$, subsonic flow from $(r_c, -v_c)$ until (r_c, v_c), suppersonic flow-out
IV	Subsonic accretion until $(r_c, -v_c)$ then supersonic
V	Supersonic flow-out until (r_c, v_c) then subsonic

$f(r_h) = 0$, with vanishing speed ensuring that the Hamiltonian (82) remains constant. The critical black solution curve reveals two types of motions: if we assume that dv/dr is continuous at the CPs, then (3) we have a supersonic accretion until $(r_c, -v_c)$, followed by a subsonic accretion until $(r_h, 0)$, where the speed vanishes, then a subsonic flow-out until (r_c, v_c), followed by a supersonic flow-out, or (4) (lower plot) a subsonic accretion followed by a supersonic accretion which ends inside the horizon. In the upper plot, we have a supersonic outflow followed by a subsonic motion. The summary of this is given in Table 2.

The fluid flow in Type (3) from $(r_c, -v_c)$ to (r_c, v_c) describes a heteroclinic orbit that passes through two different saddle CPs: $(r_c, -v_c)$ and (r_c, v_c). It is easy to show that the solution curve from $(r_c, -v_c)$ to (r_c, v_c) reaches (r_c, v_c) as $\bar{t} \to -\infty$, and the curve from (r_c, v_c) to $(r_c, -v_c)$ reaches $(r_c, -v_c)$ as $\bar{t} \to +\infty$; we can change the signs of these two limits upon performing the transformation $\bar{t} \to -\bar{t}$ and $\mathcal{H} \to -\mathcal{H}$.

The flow-out of the fluid, which starts at the horizon, is caused by the high pressure of the fluid, which diverges there (61): The fluid under effects of its own pressure flows back to spatial infinity.

It is clear from Fig. 2 that, after watching the subsonic branches of the blue and magenta solution curves, there is no way to support the claim, recalled at the end of Sect. 3, that "`the flow must be supersonic at the horizon`" [66]. For these new solutions the speed of the fluid increases during the accretion from 0, according to the analysis made from (62) to (72), to some value below v_c where $dv/dr = 0$, then decreases to 0 at the horizon, and the process is reversed during the flow-out. It is easy to show, using (83), that the point where the speed is maximum is r_c, as shown in Fig. 2. Thus, the flow does not necessary become supersonic nor transonic near the horizon [67,68]. This conclusion does not depend on the presence of a negative cosmological or a non-vanishing constant β: such solutions exist even for a Schwarzschild black hole, as the subsonic branches of the blue and magenta solution curves in Fig. 3 show.

Curiously enough, such solutions were never discussed in the literature. This is probably due to the fact that the pioneering work on this subject did not employ the Hamiltonian dynamical system approach to tackle the problem. These new solutions are related to the instability and fine tuning problems in dynamical systems. To see that consider the asymptotic behavior of (82). Since $f \sim -(\Lambda/3)r^2$ as $r \to \infty$ and since $\mathcal{H}$ remains constant on a solution curve, we must have $v \sim v_1 r^{-1}$ ($v_1 < 0$ during accretion), which agrees with (62) and (66). Asymptotically, Eq. (82) reads

$$\mathcal{H} \sim \mathcal{H}_\infty \equiv \frac{\sqrt{-\Lambda/3}}{|v_1|}, \tag{84}$$

which is used to determine the value of $|v_1|$ by

$$|v_1| = \frac{\sqrt{-\Lambda/3}}{\mathcal{H}_\infty}. \tag{85}$$

Notice that as $|v_1|$ increases, $\mathcal{H}_\infty$ decreases. Now consider the lower plot of Fig. 2 and the branch of the black critical curve where first the speed is subsonic until the CP then it becomes supersonic. On this curve $\mathcal{H} \sim \mathcal{H}_\infty = \mathcal{H}_c$, it follows that

$$|v_{1\mathrm{b}}| = \frac{\sqrt{-\Lambda/3}}{\mathcal{H}_c}, \tag{86}$$

where the subscript "b" is for black. If one decreases the value of the asymptotic speed, that is, the value of $|v_1|$ by ϵ: $|v_1| \to |v_{1\mathrm{b}}| - \epsilon$, as is the case of the subsonic magenta curve of Fig. 2, then $\mathcal{H}_\infty$ increases by a corresponding amount: $\mathcal{H}_\infty \to \mathcal{H}_c + \epsilon\sqrt{-\Lambda/3}/|v_{1\mathrm{b}}|^2$. This small perturbation in the value of $|v_1|$ leads the flow to completely change course, by deviating from the black critical curve, and to undergo a

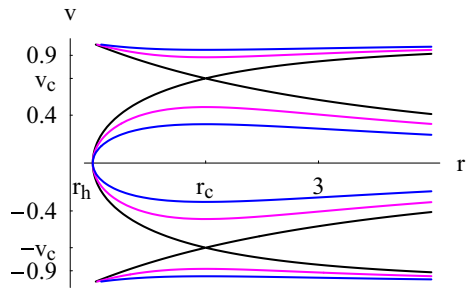

Fig. 3 Contour plot of $\mathcal{H}$ (59) for a Schwarzschild black hole with $k = 1/2$, $M = 1$, $\beta = 0$, $\Lambda = 0$. The parameters are $r_h \simeq 2$, $r_c \simeq 2.5$, $v_c = 1/\sqrt{2} \simeq 0.707107$. *Black plot* the solution curve through the saddle CPs (r_c, v_c) and $(r_c, -v_c)$ for which $\mathcal{H} = \mathcal{H}_c \simeq 0.143108$. *Magenta plot* the solution curve for which $\mathcal{H} = \mathcal{H}_c + 0.03$. *Blue plot*: the solution curve for which $\mathcal{H} = \mathcal{H}_c + 0.09$

purely subsonic motion along the subsonic magenta curve. Conversely, a small increase in the value of the asymptotic speed (of the coefficient $|v_1|$) would lead the flow to follow the red curve adjacent to the black critical curve. Thus, the black critical curve is certainly unstable and in practical situations it would not be easy to fix the value of $|v_1|$, which is an average value for the pressure is not zero, by fine tuning it to have a critical motion, that is, a motion that becomes supersonic beyond the CP and reaches the speed of light as the fluid approaches the horizon.

This stability issue is related to the character of the CPs $(r_c, -v_c)$ and (r_c, v_c) that are saddle points of the Hamiltonian function. As is well known, saddle points of the Hamiltonian function are also saddle points of the Hamiltonian dynamical system. Further analysis of stability requires linearization of the dynamical system and/or use of Lyapunov's theorems [75–77] and their variants [78].

Another type of instability is the flow-out that starts in the vicinity of the horizon ($r = r_h + 0^+, v = 0^+$) under the effect of a divergent pressure. This flow-out is unstable, for it may follow a subsonic path (the magenta or blue curves) or a critical path (the black curve) through the CP (r_c, v_c) and becomes supersonic with a speed approaching that of light. From a cosmological point of view, this point ($r = r_h, v = 0$) looks like an attractor where solution curves converge and a repeller from where the curves diverge [78].

The motion along the rightmost branches of the green and red curves is unphysical. Along the leftmost branches of these curves, we have an accretion starting from the leftmost point of the branch until the horizon where the speed vanishes and the pressure diverges, followed by a flow-out back to the same starting point. To realize such a flow one needs to have a sink and source at the leftmost point of these branches.

5.3 Solution for radiation fluid ($k = 1/3$)

A radiation fluid is the fluid which absorbs the radiation emitted by the black hole. It is the most interesting case in astrophysics. Here, the value of state parameter $k = 1/3$. Equation (73) leads to

$$\beta r_c^2 + 2r - 6M = 0, \tag{87}$$

which is solved by

$$r_c = \frac{\sqrt{1 + 6\beta M} - 1}{\beta}. \tag{88}$$

The Hamiltonian (59) takes the simple form

$$\mathcal{H} = \frac{f^{2/3}}{r^{4/3}|v|^{2/3}(1 - v^2)^{2/3}}. \tag{89}$$

It is clear from this expression that the point $(r, v^2) = (r_h, 1)$ is not a CP of the dynamical system. Equation (89) can be solved for v^2, and a contour plot of it can be depicted, which reveals the same characteristics of the plot shown in Fig. 2; We observe the same types of motion as in the case $k = 1/2$.

5.4 Solution for sub-relativistic fluid ($k = 1/4$): Separatrix heteroclinic flows

Sub-relativistic fluids are those fluids whose energy density exceeds their isotropic pressure. Taking the value of the state parameter $k = 1/4$, Eq. (73) leads to

$$N(r_c) = \Lambda r_c^3 + \frac{3\beta}{2} r_c^2 + 6r_c - 21M = 0. \tag{90}$$

This polynomial has either two distinct positive roots or a double positive root if $\Lambda < 0$ and $\beta \geq 0$. Converting this polynomial into the Weierstrass one $w(z)$ by the transformation $r_c = z - \beta/(2\Lambda)$, the two CPs $r_{c1} < r_{c2}$ are given by (see Appendix A)

$$\begin{aligned} r_{c2} &= \sqrt{\frac{g_2}{3}} \cos\left(\frac{\eta}{3}\right) - \frac{\beta}{2\Lambda}, \\ r_{c1} &= -\sqrt{\frac{g_2}{3}} \cos\left(\frac{\pi + \eta}{3}\right) - \frac{\beta}{2\Lambda}, \end{aligned} \tag{91}$$

where g_2 and g_3 are defined by

$$g_2 = \frac{3(\beta^2 - 8\Lambda)}{\Lambda^2}, \quad g_3 = \frac{-\beta^3 + 12\beta\Lambda + 84M\Lambda^2}{\Lambda^3},$$

and Δ and the angle $0 \leq \eta \leq \pi$ are defined as in Eqs. (A.2) and (A.4), respectively.

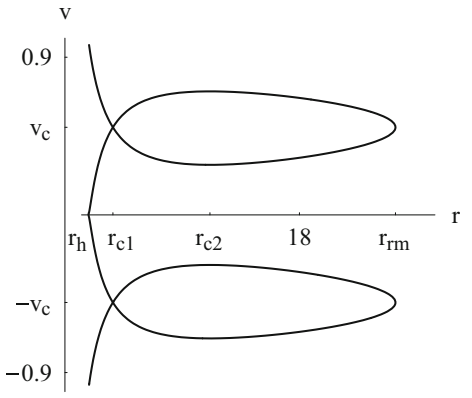

Fig. 4 Contour plot of $\mathcal{H}$ (59) for an anti-de Sitter-like f(R) black hole with $k = 1/4$, $M = 1$, $\beta = 0.05$, $\Lambda = -0.04$. The parameters are $r_h \simeq 1.76955, r_{c1} \simeq 3.65928, r_{c2} \simeq 11.119, v_c = 1/2, r_{\rm rm} \simeq 25.3831$. The plot shows the heteroclinic solution curve through the saddle CPs (r_{c1}, v_c) and $(r_{c1}, -v_c)$ for which $\mathcal{H} = \mathcal{H}(r_{c1}, v_c) = \mathcal{H}(r_{c1}, -v_c) \simeq 0.411311$. The two other CPs, (r_{c2}, v_c) and $(r_{c2}, -v_c)$, are centers where $\mathcal{H} = \mathcal{H}(r_{c2}, v_c) = \mathcal{H}(r_{c2}, -v_c) \simeq 0.411311$

The Hamiltonian (59) takes the simple for

$$\mathcal{H} = \frac{f^{3/4}}{r\sqrt{|v|}(1-v^2)^{3/4}}. \tag{92}$$

It is clear from this expression that the point $(r, v^2) = (r_h, 1)$ is not a CP of the dynamical system. A contour plot of $\mathcal{H}$ (92) is depicted in Fig. 4 in the (r, v) plane. There are two saddle points (r_{c1}, v_c) and $(r_{c1}, -v_c)$ and two centers (r_{c2}, v_c) and $(r_{c2}, -v_c)$. Let $(r_{\rm rm}, v_c)$ and $(r_{\rm rm}, -v_c)$ be the rightmost points of the upper and lower plots, respectively. If we assume that $\mathrm{d}v/\mathrm{d}r$ remains continuous as the fluid crosses the saddle CPs, the accretion motion starts from the rightmost point $(r_{\rm rm}, -v_c)$ on the black curve in the lower plot. If the motion is subsonic it proceeds along the upper branch in the lower plot, goes through the CP $(r_{c1}, -v_c)$, then crosses the horizon.

Otherwise, if the motion is supersonic it proceeds along the lower branch in the lower plot, goes again through the CP $(r_{c1}, -v_c)$ until v vanishes as the fluid approaches the horizon [this is obvious from (92) where v vanishes whenever f does too], then the fluid goes again through the CP (r_{c1}, v_c) and follows the upper branch of the upper plot undergoing a supersonic motion until the rightmost point of the upper plot $(r_{\rm rm}, v_c)$. First, by similar arguments as those given in the case $k = 1/2$, it can be shown that such motion is unstable. Second, the motion may become periodic but it is too hard to achieve that by (a) fine tuning the speed of the fluid at $(r_{\rm rm}, -v_c)$ and (b) realizing a source at $(r_{\rm rm}, -v_c)$ and a sink at $(r_{\rm rm}, v_c)$.

The fluid flow along the branch of the curve from $(r_c, -v_c)$ to (r_c, v_c) describes a heteroclinic orbit that passes through two different saddle CPs: $(r_c, -v_c)$ and (r_c, v_c). It is easy to show that as the flow approaches, from within the heteroclinic orbit, one or the other saddle CP the dynamical-system's time $\bar{t}$ goes to $\pm\infty$.

Here again the flow-out of the fluid, which starts at the horizon, is caused by the high pressure of the fluid, which diverges there (61).

As we have done in the case $k = 1/2$, we consider the fluid flow where r decreases but $v > 0$ or r increases but $v < 0$ as unphysical since the fluid is taken as a test matter and we have neglected its backreaction on the metric of the black hole. As far as a fluid element is taken as a test particle, such a motion is not possible in the background of the black hole metric. This is why a flow along a closed path in Fig. 4, or "homoclinic" as some authors call it, is unphysical. We do not know if homoclinic orbits exist in a more realistic model where the backreaction of the fluid is taken into consideration.

For the clarity of the plot, Fig. 4 has been plotted for unphysical parameters $M = 1$, $\beta = 0.5$, and $\Lambda = -0.075$; for astrophysical values of the parameters $(\Lambda \to 0^-)$, the difference $r_{c2} - r_{c1}$ becomes so large to be represented on a sheet of paper. The constraint that two CPs exist is to have two positive roots for the polynomial in (90): $N(r) = \Lambda r^3 + \frac{3\beta}{2} r^2 + 6r - 21M$. With $\Lambda < 0$ and $\beta > 0$, the polynomial has a local minimum (at some negative value of r) and a local maximum at

$$r_s = -\frac{\sqrt{\beta^2 - 8\Lambda} + \beta}{2\Lambda}. \tag{93}$$

The heteroclinic orbit exists if $N(r_c) = 0$ has two positive CPs; that is, if $N(r_s) > 0$ yielding

$$M < \frac{(\beta^2 - 8\Lambda)^{3/2} + \beta^3 - 12\beta\Lambda}{84\Lambda^2}, \tag{94}$$

generalizing the expression derived in Ref. [79]. This should be read as a constraint on β. In the limit $\Lambda \to 0^-$, this reduces to

$$\beta^3 > 42M\Lambda^2, \tag{95}$$

and the expressions of the two positive CPs and the horizon read

$$r_{c1} \simeq \frac{\sqrt{4 + 14M\beta} - 2}{\beta}, \quad r_{c2} \simeq -\frac{3\beta}{2\Lambda},$$
$$r_h \simeq \frac{\sqrt{1 + 8M\beta} - 1}{2\beta}. \tag{96}$$

It is easy to show that $r_{c1} > r_h$.

In the astrophysical limit $\Lambda \to 0^-$ we find, for general values of k, the following constraints on β:

$$\begin{cases} \beta > \frac{42M\Lambda^2(1-3k)^3}{(1-5k)^2(5-19k)} & \frac{1}{5} < k < \frac{5}{19}; \\ \beta > \frac{2\sqrt{-\Lambda}}{3}\,(21M\sqrt{-\Lambda}-5) & k = \frac{1}{5}. \end{cases} \tag{97}$$

In this limit, the CPs are expressed as

$$r_{c1} \simeq \begin{cases} \frac{\sqrt{k^2(4+30M\beta)+4kM\beta-2M\beta}-2k}{(5k-1)\beta} & \frac{1}{5} < k < \frac{5}{19}; \\ 4M(1-16M^2\Lambda/3) & k = \frac{1}{5}, \end{cases} \tag{98}$$

$$r_{c2} \simeq \begin{cases} \frac{3(1-5k)\beta}{2(1-3k)\Lambda} & \frac{1}{5} < k < \frac{5}{19}; \\ \frac{\sqrt{3}}{\sqrt{-\Lambda}} & k = \frac{1}{5}, \end{cases} \tag{99}$$

while the expression of r_h (96) is independent of k.

6 Polytropic test fluids

A very interesting approach to describe the motion of the fluid is by constructing its models. The prototype of such model is Chaplygin gas. The Chaplygin gas model leads to very interesting results. Some of them are discussed in Ref [80–84]. There are many variations of the Chaplygin gas model that have been proposed in the literature. One of them is the modified Chaplygin gas model [85,86]. In astrophysics, the modified Chaplygin gas is the most general exotic fluid. Its equation of state is

$$p = An - \frac{B}{n^\alpha}, \tag{100}$$

where A and B are constants and $(0 < \alpha < 1)$. If we put $A = 0, B = -k$ and $\alpha = -\gamma$, we get the polytropic equation of state i.e. $p = G(n) = \mathcal{K}n^\gamma$, where $\mathcal{K}$ and γ are constants. For ordinary matter, one generally works with the constraint $\gamma > 1$. In this work, we only observe the constraint $\gamma \neq 1$.

Inserting $p = G(n) = \mathcal{K}n^\gamma$ in the differential equation (19) yields

$$nF' - F = \mathcal{K}n^\gamma.$$

The solution provides the energy density $e = F$ by

$$e = F(n) = mn + \frac{\mathcal{K}n^\gamma}{\gamma - 1}, \tag{101}$$

where a constant of integration has been identified with the baryonic mass m. This yields, see (16),

$$h = m + \frac{\mathcal{K}\gamma n^{\gamma-1}}{\gamma - 1}. \tag{102}$$

The three-dimensional speed of sound is found from (21) by

$$a^2 = \frac{(\gamma-1)X}{m(\gamma-1)+X} \quad (X \equiv \mathcal{K}\gamma n^{\gamma-1}). \tag{103}$$

On comparing (102) and (103) we see that

$$h = m\,\frac{\gamma-1}{\gamma-1-a^2}, \tag{104}$$

similar to the expression for h derived for the accretion onto a black hole in a string cloud background [57].

Using (44) in (102), we obtain

$$h = m\left[1 + Y\left(\frac{1-v^2}{r^4 f v^2}\right)^{(\gamma-1)/2}\right], \tag{105}$$

where

$$Y \equiv \frac{\mathcal{K}\gamma n_c^{\gamma-1}}{m(\gamma-1)}\left(\frac{r_c^5 f_{c,r_c}}{4}\right)^{(\gamma-1)/2} = \text{const.} \tag{106}$$

Inserting (105) into (32) we evaluate the Hamiltonian by

$$\mathcal{H} = \frac{f}{1-v^2}\left[1 + Y\left(\frac{1-v^2}{r^4 f v^2}\right)^{(\gamma-1)/2}\right]^2, \tag{107}$$

where m^2 has been absorbed into a re-definition of $(\bar{t}, \mathcal{H})$.

A couple of remarks concerning the fluid flow onto an anti-de Sitter-like f(R) black hole are in order. For ordinary matter $\mathcal{K} > 0$ and $f_{c,r_c} > 0$ (since we are interested in the cases where $r_c > r_h$), this implies (a) $\Upsilon > 0$ if $\gamma > 1$ or (b) $\Upsilon < 0$ if $\gamma < 1$ $(\gamma \neq 0)$.

For the case (a) the sum of the terms inside the square parentheses in (107) is positive, while the coefficient $f/(1-v^2)$ diverges as $r \to \infty$ $(0 \leq 1 - v^2 < 1)$. So, the Hamiltonian too diverges. Since the latter has to remain constant on a solution curve, we conclude that there are no global solutions in this case (solutions that extend to spatial infinity). This conclusion remains true even if $\Lambda = 0$ provided $\beta \neq 0$. If $\Lambda = 0$ and $\beta = 0$ (the Schwarzschild metric), the global solutions do not exist if $|v_\infty| = 1$ (62) and exist otherwise provided $0 < \alpha \leq 2$ if $|v_\infty| = 0$ or $0 < \alpha$ if $0 < |v_\infty| < 1$.

For the case (b), since $\Upsilon < 0$, we can make it such that

$$1 + Y\left(\frac{1-v^2}{r^4 f v^2}\right)^{(\gamma-1)/2} \propto r^{-1} \quad \text{as} \quad r \to \infty, \tag{108}$$

in order to have global solutions. For instance, if we restrict ourselves to v having an expansion in powers of $1/r$ with a vanishing three-dimensional speed at spatial infinity (62)

$$v \simeq v_1 r^{-\alpha} + v_2 r^{-\delta} \text{ as } r \to \infty \quad (\delta > \alpha > 0), \tag{109}$$

then, on observing (108), we find $\alpha = 3$, $\delta \geq 4$, and

$$v_1^2 = (-3/\Lambda)(Y^2)^{1/(\gamma-1)}. \tag{110}$$

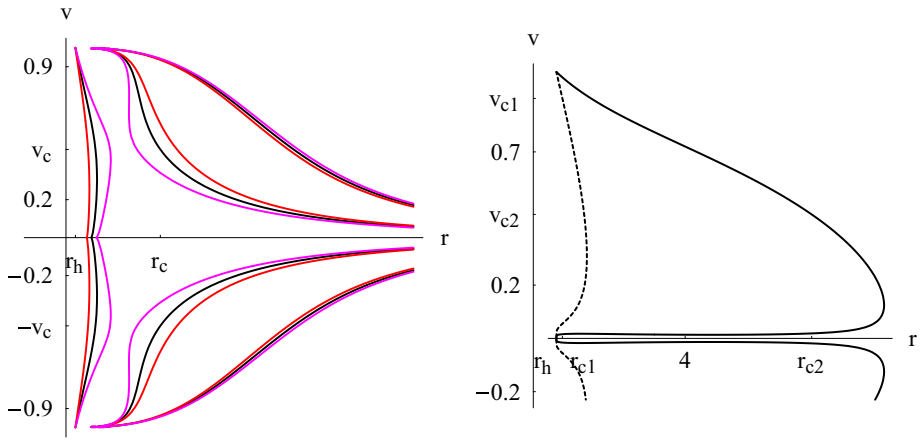

Fig. 5 *Left panel* is a contour plot of $\mathcal{H}$ (107) for an anti-de Sitter-like f(R) black hole with $M = 1$, $\beta = 0.05$, $\Lambda = -0.04$, $\gamma = 1/2$, $Y = -1/8$, $n_c = 0.1$. The parameters are $r_h \simeq 1.76955$, $r_c \simeq 5.37849$, $v_c \simeq 0.464567$. *Black plot* the solution curve through the CPs (r_c, v_c) and $(r_c, -v_c)$ for which $\mathcal{H} = \mathcal{H}_c \simeq 0.379668$. *Red plot* the solution curve for which $\mathcal{H} = \mathcal{H}_c - 0.09$. *Magenta plot* the solution curve for which $\mathcal{H} = \mathcal{H}_c + 0.09$. The *right panel* is a contour plot of $\mathcal{H}$ (107) for an anti-de Sitter-like f(R) black hole with $M = 1$, $\beta = 0.05$, $\Lambda = -0.04$, $\gamma = 5.5/3$, $Y = 1/8$, $n_c = 0.001$. The parameters are $r_h \simeq 1.76955$, $r_{c1} \simeq 1.87377$, $v_{c1} \simeq 0.900512$, $r_{c2} \simeq 6.19113$, $v_{c2} \simeq 0.465236$. *Continuous black plot* the solution curve through the CPs (r_{c2}, v_{c2}) and $(r_{c2}, -v_{c2})$ for which $\mathcal{H} = \mathcal{H}_{c2} \simeq 1.94447$. *Dashed black plot* the solution curve through the CPs (r_{c1}, v_{c1}) and $(r_{c1}, -v_{c1})$ for which $\mathcal{H} = \mathcal{H}_{c1} \simeq 0.443809$. For the clarity of the plot, we have partially removed the branches $v < 0$

This is another, rather much harder, fine tuning problem. Here Y depends on n_c, so is v_1: unless v_1^2 is the rhs of (110), there will be no global solutions to this case too.

For non-ordinary matter, since $\mathcal{K} < 0$, the above two cases are reversed, that is, for $\gamma > 1$ it is possible to have global solutions, again with a fine tuning problem, while for $\gamma < 1$ ($\gamma \neq 0$) there are non-global solutions.

In the following we provide two curve solutions for an anti-de Sitter-like f(R) black hole in the cases $\gamma > 1$ (non-global solution) and $\gamma < 1$ (global solution) and a curve solution for a de Sitter-like f(R) black hole in the case $\gamma > 1$. First, using (44) we rewrite (103) as

$$\left[\frac{n_c}{Y}\left(\frac{r_c^5 f_{c,r_c}}{4}\right)^{1/2} + \left(\frac{1-v^2}{r^4 f v^2}\right)^{(\gamma-1)/2}\right] a^2 = (\gamma-1)\left(\frac{1-v^2}{r^4 f v^2}\right)^{(\gamma-1)/2}. \tag{111}$$

Since at the CPs we have $a_c^2 = v_c^2$ (41), we replace a^2 in (111) and in (42) by v_c^2 and solve the system (111) and (42) to find the CPs (r_c, v_c). We rewrite the latter equations after making the substitution $a_c^2 = v_c^2$ as

$$\left(\gamma - 1 - v_c^2\right)\left(\frac{1-v_c^2}{r_c^4 f_c v_c^2}\right)^{(\gamma-1)/2} = \frac{n_c}{Y}\left(\frac{r_c^5 f_{c,r_c}}{4}\right)^{1/2} v_c^2, \tag{112}$$

$$v_c^2 = \frac{r_c f_{c,r_c}}{r_c f_{c,r_c} + 4 f_c} = \frac{(3\beta - 2\Lambda r_c) r_c^2 + 6M}{3\left[\left(4 + 5\beta r_c - 2\Lambda r_c^2\right) r_c - 6M\right]}. \tag{113}$$

Here we keep using f to show the general character of these equations. Inserting (113) into (112) we can first solve numerically for r_c; then we get v_c from (113). Since the signs of both sides of (112) must be the same, we conclude that, for $\gamma < 1$, $v_c^2 > \gamma - 1$ (which is always satisfied) and that, for $\gamma > 1$, $v_c^2 < \gamma - 1$.

Notice that the solution curves do not cross the r axis at points where $v = 0$ and $r \neq r_h$, for otherwise the Hamiltonian (107) would diverge there. We recall that r_h is the unique horizon of an anti-de Sitter-like f(R) black hole or it represents either the event horizon $r_{\rm eh}$ or the cosmological horizon $r_{\rm ch}$ of a de Sitter-like f(R) black hole. The curves may cross the r axis at the unique point $r = r_h$ in the vicinity of which v behaves as

$$|v| \simeq |v_0||r - r_h|^{\frac{2-\gamma}{2(\gamma-1)}} \quad \text{with} \quad v_0^{2(\gamma-1)} = \frac{Y^2 f'(r_h)^{2-\gamma}}{r_h^{4(\gamma-1)}\mathcal{H}(r_h, 0)}, \tag{114}$$

if $f = 0$ has a single root at r_h. We see that only solutions with $1 < \gamma < 2$ may cross the r axis. Here $\mathcal{H}(r_h, 0)$ is the value of the Hamiltonian on the solution curve, which is the limit of $\mathcal{H}(r, v)$ as $(r, v) \to (r_h, 0)$. This can be evaluated at any other point on the curve. The pressure $p = \mathcal{K} n^\gamma$ diverges at the horizon as

$$p \propto |r - r_h|^{\frac{-\gamma}{2(\gamma-1)}} \quad (1 < \gamma < 2). \tag{115}$$

For both plots of Fig. 5 we took $M = 1$, $\beta = 0.05$, and $\Lambda = -0.04$.

Table 3 Behavior of flow for the polytropic equation of state in Fig. 5

Types	Flow behavior
I	Leftmost branches: Unphysical
II	Left panel: Critical transonic accretion and flow-out
III	Left panel: Non-critical sub-super sonic accretion and flow-out
IV	Right panel: Non-relativistic subsonic accretion and flow-out
	(with source-sink at the rightmost point of the graph)
V	Right panel: Critical transonic accretion and flow-out
	(with source-sink at the rightmost point of the graph)

In the left panel of Fig. 5, we took $\gamma = 1/2$, $Y = -1/8$, and $n_c = 0.1$, yielding one CP ($r_c \simeq 5.37849$, $v_c \simeq 0.464567$). We see from the graph that there are two types of fluid flow, an accretion which starts subsonic at spatial infinity and ends supersonic into the horizon (passing through the non-saddle CP or avoiding it), and a supersonic flow-out from a neighborhood of the horizon which ends subsonic with gradually vanishing speed at spatial infinity according to (109,110) (passing through the non-saddle CP or avoiding it). Along the leftmost branches we have an accretion starting from the leftmost point of the branch until the horizon where the speed vanishes and the pressure diverges, followed by a flow-out back to the same starting point. Had we taken a lower number density $n_c = 0.001$ we would still get the same types of flow, but the uppermost, lowermost, and leftmost branches of the plot would disappear.

In the right panel of Fig. 5, we took $\gamma = 5.5/3$, $Y = 1/8$, and $n_c = 0.001$, yielding four CPs, but none of them is a saddle point: ($r_{c1} \simeq 1.87377$, $v_{c1} \simeq 0.900512$), ($r_{c1}, -v_{c1}$), ($r_{c2} \simeq 6.19113$, $v_{c2} \simeq 0.465236$), and ($r_{c2}, -v_{c2}$). The right panel of Fig. 5 shows a typical flow for this range of parameters ($\gamma = 5.5/3$, $Y = 1/8$). There are three types of flow: subsonic non-global, non-relativistic (resp. more or less relativistic), and non-heteroclinic (for it does not pass through the CPs) accretion starting from the leftmost point of the continuous (resp. dashed) branch until the horizon where the speed vanishes and the pressure diverges, followed by a non-relativistic (resp. more or less relativistic) flow-out. This flow could be made periodic by realizing a source-sink at the rightmost point of the graph, as we have seen earlier. There are two other types of flow: partly subsonic and partly supersonic accretion and flow-out along the continuous and dashed branches. The summary of this is given in Table 3. We emphasize that, since the fluid is seen as a test matter in the geometry of the black hole, there is no homoclinic flow, that is, a flow following a closed curve in the right panel of Fig. 5.

In our next application we rather consider a de Sitter-like f(R) black hole taking $M = 1$, $\beta = 0.05$, $\Lambda = 0.04$, $\gamma = 1.7$, $Y = 1/8$, $n_c = 0.001$ as in Fig. 6. For these values of the parameters, the dynamical system has two non-saddle CPs: ($r_c \simeq 2.13406$, $v_c \simeq 0.824282$) and ($r_c, -v_c$). The flow for $\mathcal{H} \leq \mathcal{H}_c \simeq 0.390248$ shows no difference than that of the right panel of Fig. 5 corresponding to an anti-de Sitter-like f(R) black hole. For $\mathcal{H} > \mathcal{H}_c$, we observe two types of flow connecting the two horizons, one of which is supersonic, relativistic, near the horizons and becomes subsonic midway of the horizons (uppermost and lowermost branches of the magenta curve). The other flow connecting the two horizons is, rather, cyclic physical flow with vanishing speed at both the event $r_{\rm eh} \simeq 1.91048$ and the cosmological $r_{\rm ch} \simeq 9.8282$ horizons, as shown in the right plot of Fig. 6. There is no need to realize a source at one horizon and a sink at the other; this subsonic, non-relativistic, cyclic (non-homoclinic, for it does not pass through the CP) flow is maintained by the high, rather divergent (115), pressure at both horizons. If the fluid is hot, a two-temperature ion (plasma) would form and the cyclic flow becomes the source of energy radiation [87]. If the fluid is multi-specie, each component would radiate at different frequency, resulting in a spectrum characteristic of the fluid composition. The higher the value of the Hamiltonian the lower is the speed of flow along the closed branch.

From our above formulas we can make a good estimate of the proper period and frequency of such a cyclic flow. Assuming $v^2 \ll 1$, that is, a relatively higher value of the Hamiltonian, then (107) reduces to

$$(v\sqrt{f})^{\gamma-1} \simeq \frac{Y}{r^{2(\gamma-1)}(\sqrt{\mathcal{H}_{\rm cyc}/f} - 1)}, \tag{116}$$

where $\mathcal{H}_{\rm cyc}$ is the value of the Hamiltonian that generates the cyclic flow between the event and cosmological horizons. The first equation in (24) leads to

$$Y^{\frac{1}{\gamma-1}} {\rm d}\tau \simeq r^2\Big(\sqrt{\mathcal{H}_{\rm cyc}/f} - 1\Big)^{\frac{1}{\gamma-1}} {\rm d}r. \tag{117}$$

The integral of the rhs of (117), with the limits being ($r_{\rm eh}, r_{\rm ch}$), converges if $\gamma > 3/2$ (recall that we are assuming that each horizon ($r_{\rm eh}, r_{\rm ch}$), being a single root of $f = 0$, is non-extremal) and diverges as $\ln|r - r_h|$ if $\gamma = 3/2$. For the values of Fig. 6, $\mathcal{H}_{\rm cyc} = \mathcal{H}_c + 0.29 \simeq 0.680248$, we find the proper period to be

$$\tau \simeq 2Y^{\frac{1}{1-\gamma}} \int_{r_{\rm eh}}^{r_{\rm ch}} r^2\Big(\sqrt{\mathcal{H}_{\rm cyc}/f} - 1\Big)^{\frac{1}{\gamma-1}} {\rm d}r \simeq 26761.9.$$

7 Hu–Sawicki and Starobinsky models of f(R) gravity

Two more solution curves are provided in this section and concern two of the most popular models of f(R) gravity: the Hu–Sawicki and Starobinsky models [8,51].

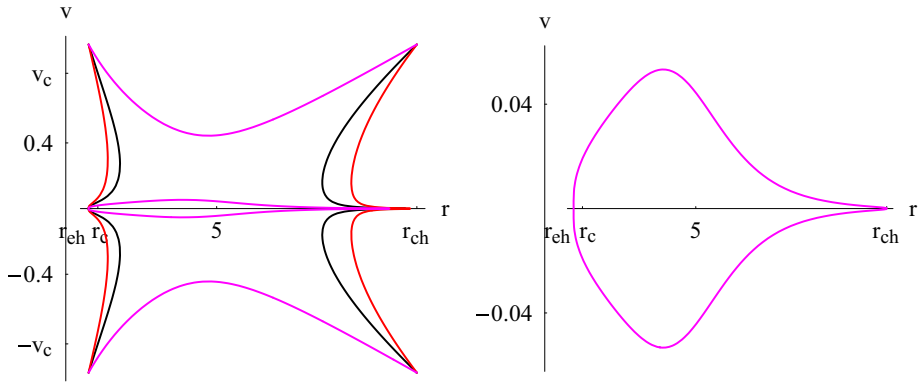

Fig. 6 *Left plot* is a contour plot of $\mathcal{H}$ (107) for a de Sitter-like f(R) black hole with $M = 1$, $\beta = 0.05$, $\Lambda = 0.04$, $\gamma = 1.7$, $Y = 1/8$, $n_c = 0.001$. The parameters are $r_{\rm eh} \simeq 1.91048$, $r_{\rm ch} \simeq 9.8282$, $r_c \simeq 2.13406$, $v_c \simeq 0.824282$. *Black plot* the solution curve through the CPs (r_c, v_c) and $(r_c, -v_c)$ for which $\mathcal{H} = \mathcal{H}_c \simeq 0.390248$. *Red plot* the solution curve corresponding to $\mathcal{H} = \mathcal{H}_c - 0.1$. *Magenta plot* the solution curve corresponding to $\mathcal{H} = \mathcal{H}_c + 0.29$. *Right* plot is a zoomed in plot of the cyclic flow corresponding to $\mathcal{H} = \mathcal{H}_c + 0.29$

There is a variety of black hole solutions of f(R) gravity models, the most treated in the literature are constant curvature, $R = R_0$, solutions. If R is the constant R_0, the field equations take the form

$$R_{\mu\nu}[1 + \mathrm{f}'(R_0)] - \tfrac{1}{2} g_{\mu\nu}[R_0 + \mathrm{f}(R_0)] = -8\pi T_{\mu\nu}. \quad (118)$$

For an electromagnetic source,

$$T^{\mu}_{\nu} = -\tfrac{1}{4\pi}\left(F^{\mu\alpha}F_{\nu\alpha} - \tfrac{1}{4}\delta^{\mu}_{\nu}F^{\alpha\beta}F_{\alpha\beta}\right),$$

(with $F_{\mu\nu} = \partial_\mu A_\nu - \partial_\nu A_\mu$) we have $T^{\mu}_{\mu} \equiv 0$. The trace of (118) yields

$$R_0 + \mathrm{f}(R_0) = [1 + \mathrm{f}'(R_0)]R_0/2, \quad (119)$$

reducing (118) to

$$\underbrace{R_{\mu\nu} - \tfrac{1}{2}R_0 g_{\mu\nu}}_{G_{\mu\nu}} + \frac{R_0}{4} g_{\mu\nu} = -8\pi \, \frac{T_{\mu\nu}}{1 + \mathrm{f}'(R_0)}, \quad (120)$$

where $G_{\mu\nu}$ is the Einstein tensor. On comparing (120) with the field equations of general relativity, we see that $R_0/4$ plays the role of an effective cosmological constant and $T_{\mu\nu}/[1 + \mathrm{f}'(R_0)]$ is an effective SET. If the vector potential $A_\mu = (-Q/r, 0, 0, 0)$, we obtain the spherically symmetric solution given by (1) with[5]

$$f(r) = 1 - \frac{2M}{r} + \frac{Q^2}{[1 + \mathrm{f}'(R_0)]r^2} - \frac{R_0}{12} r^2. \quad (121)$$

[5] Equation (121) provides the correct expression of $f(r)$ of the solution given by Eq. (32) of Ref. [53].

7.1 Starobinsky model

This is the model with $\mathrm{f}(R) = R^2/(6\mathcal{M}^2)$ where the constant $\mathcal{M}$ has value corresponding to the mass scale for quantum gravity. The only existing solution to (119) is $R_0 = 0$, reducing (121) to a Reissner–Nordström black hole the fluid accretion onto which has already been investigated in the literature [89] and is similar to the Schwarzschild case [34]; therefore we shall not comment on this case.

7.2 Hu–Sawicki model

This corresponds to

$$\mathrm{f}(R) = -\mathcal{M}^2 \frac{c_1 (R/\mathcal{M}^2)^n}{c_2 (R/\mathcal{M}^2)^n + 1}, \quad (122)$$

where $n > 0$, (c_1, c_2) are proportional constants [51]

$$\frac{c_1}{c_2} \equiv q_2 \approx 6 \, \frac{\Omega_\Lambda}{\Omega_m} = 6 \, \frac{0.76}{0.24} = 19, \quad (123)$$

and the mass scale

$$\mathcal{M}^2 = (8315\mathrm{Mpc})^{-2} \left(\frac{\Omega_m h^2}{0.13}\right).$$

At the present epoch [51]

$$\frac{R_0}{\mathcal{M}^2} \equiv q_1 \approx \frac{12}{\Omega_m} - 9 = 41. \quad (124)$$

For $n > 0$, Eq. (119) always has the root $R_0 = 0$. Notice that the model (122) has been introduced in order to keep $|\mathrm{f}'(R_0)| \ll 1$, which ensures stability. Hence, we rule out the case $0 < n < 1$, which would yield $|\mathrm{f}'(R_0)| \to \infty$

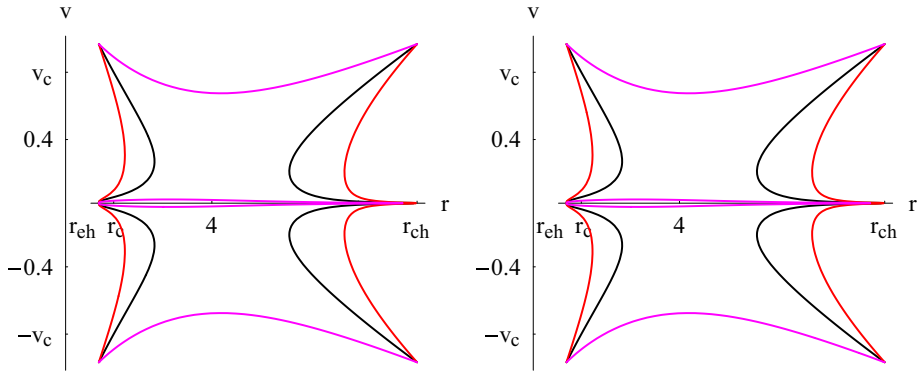

Fig. 7 Contour plot of $\mathcal{H}$ (107) for a de Sitter-like f(R) black hole with f(R) given by Hu–Sawicki formula (122). We took $M = 1$, $Q = 0.01$, $R_0 = 0.16$, $\gamma = 1.7$, $Y = 1/8$, $n_c = 0.001$, $q_1 = 41$, $q_2 = 19$, and c_1 and c_2 are given by (127). *Left plot* For c_2 we took the upper sign in (127), $\mathrm{f}'(R_0) \simeq 1.96272$, $r_{\mathrm{eh}} \simeq 2.12857$, $r_{\mathrm{ch}} \simeq 7.39749$, $r_c \simeq 2.37452$, $v_c \simeq 0.822763$, and $\mathcal{H} = \mathcal{H}_c \simeq 0.291918$. *Right plot* For c_2 we took the lower sign in (127), $\mathrm{f}'(R_0) \simeq 0.0372803$, $r_{\mathrm{eh}} \simeq 2.12854$, $r_{ch} \simeq 7.3975$, $r_c \simeq 2.37448$, $v_c \simeq 0.822764$, and $\mathcal{H} = \mathcal{H}_c \simeq 0.291918$

as $R_0 \to 0$. For $n \geq 1$, the root $R_0 = 0$ reduces (121) to Reissner–Nordström black hole.

From now on we take $n = 2$. Since we want one of the other roots of (119) to be $R_0 = q_1\mathcal{M}^2$, we substitute (123) and (124) into (119) to obtain

$$q_1^3(q_1 - 2q_2)c_2^2 + 2q_1^2c_2 + 1 = 0, \tag{125}$$

yielding

$$c_1 = q_2c_2, \quad c_2 = -\frac{1}{q_1^{3/2}(\sqrt{q_1} \pm \sqrt{2q_2})}. \tag{126}$$

With the numerical values in (123) and (124), the four values of c_1 and c_2 are all negative and one should keep those values that ensure $|\mathrm{f}'(R_0)| \ll 1$

$$c_1 = q_2c_2, \quad c_2 = -\frac{1}{q_1^{3/2}(\sqrt{q_1} \pm \sqrt{2q_2})}. \tag{127}$$

With $f(r)$ given by (121), the rhs of (113) reads

$$v_c^2 = \frac{\left(1 + \mathrm{f}'(R_0)\right)\left(R_0r_c^3 - 12M\right)r_c + 12Q^2}{3\left[\left(1 + \mathrm{f}'(R_0)\right)\left(R_0r_c^3 - 8r_c + 12M\right)r_c - 4Q^2\right]}. \tag{128}$$

For the plots of Fig. 7, we used Eqs. (112) and (128) to find the critical points. The graphs show that accretion is insensitive to the values of the constants (c_1, c_2) and to the value of $\mathrm{f}'(R_0)$ whose effect is to modify the value of the charge in (121).

8 Conclusion

We have developed a Hamiltonian dynamic system for tackling a variety of problems ranging from accretions, matter jets, particle emissions to cosmological and astrophysical applications whenever conservation laws apply. There are several choices for the dynamical variables arguments of the Hamiltonian. The advantage of using the three-velocity is that this entity is bounded (by -1 and 1) and it does not diverge, in contrast with the pressure and the baryon number density, and other densities, which may diverge on the horizons. Throughout the paper we kept using the metric coefficient $f(r)$ to emphasize the general character of the derived mathematical expressions. Since the scope of the model of accretion is fairly wide and applies to all static spherically symmetric solutions (asymptotically flat or else), the present analysis can also be done for other f(R) black holes as well as f(T) black holes [54]. Due to the generality of our work, further analysis will be trivial.

Our general results that applies to all metrics of the form (1) and to all perfect fluids, independently of the form of the EOS, are as follows. The Michel-type accretion of a perfect fluid is characterized by:

- The thermodynamic state functions are determined upon integrating a first order differential equation.
- If the three-velocity vanishes on the horizon(s), the particle number density n diverges there independently of the expression of f and of that of the EOS. Since the specific enthalpy h is never zero for ordinary matter, this implies that the sum $e + p$ diverges there at least as fast as n.
- The fluid may become ultra-stiff as it approaches the horizon(s).

By applying the Hamiltonian dynamic system to f(R) gravity we have performed a detailed analysis of the Michel-type accretion onto a static spherically symmetric black hole in f(R) gravity. Not every model of f(R) theory can predict black holes unless the function f(R) satisfies certain viability conditions such as $f'(R) > 0$ and $f''(R) > 0$, and asymptotically de Sitter phase at present time (see further details in [90]).

To understand the nature of the f(R) black hole and to distinguish it from the known General Relativity black holes, it is worthwhile to study their astrophysical features such as the accretion of various kinds of fluids and their dynamics near them. Using the isothermal and polytropic equations of state, we showed that the standard method employed for tackling the accretion problem has masked some important properties of the fluid flow.

Accretion of isothermal perfect fluids is characterized by the following:

- We have the existence of subsonic flows for all values of the radial coordinate. These solutions represent neither transonic nor supersonic flows as the fluid approaches the horizon.
- We have the existence of solutions with vanishing three-velocity as the fluid approaches the horizon. As $v \to 0$, the fluid cumulates near the horizon resulting in a divergent pressure which pushes the fluid backward (flow-out or a wind of the fluid under the effect of its own divergent pressure). These solutions, as the one depicted in Fig. 3, exist even in the case of a Schwarzschild black hole.
- If the CP is a saddle point, the critical solution curve divides the (r, v) plane into regions where the flow is physical in some of them (corresponding to higher values of the Hamiltonian) and unphysical in the others (corresponding to lower values of the Hamiltonian).
- The existence of separatrix heteroclinic orbits is subject to no constraint. We have checked this conclusion for the f(R) model of Ref. [50] and for Schwarzschild black hole and this should apply to all black holes.
- For the f(R) model of Ref. [50], the existence of two CPs (one saddle and one center), with a possibly periodic flow inside a finite region of space, constrains the values of β not to exceed some lower limit.
- We have instability of the critical flow.

The polytropic test fluid has nearly no global solutions for the f(R) model of Ref. [50] unless one can deal with the fine tuning problem consisting in fixing the speed at spatial infinity in terms of the number density. Among the solutions we derived for the polytropic test fluid no saddle CP occurs. Moreover, the subsonic flow appears to be almost non-relativistic. These features appear quite different from the general relativity black holes [88].

De Sitter-like f(R) black holes are characterized by the presence of closed, but non-homoclinic orbits, joining the event horizon to the cosmological horizon. Such cyclic curves are maintained by the high pressure present in the vicinity of the two horizons and do not require the presence of source-sink system for their realization. For $\gamma > 3/2$, the proper period of the cyclic flow converges to a finite value and has a logarithmically divergent limit for $\gamma = 3/2$. Comparison of the solutions (Figs. 6, 7) show that the accretion is insensitive to the f(R) model.

Acknowledgments We thank both anonymous reviewers for their very constructive comments and suggestions.

Funded by SCOAP^3.

Appendix A: Roots of the Weierstrass polynomial

The Weierstrass polynomial is defined by

$$w(z) \equiv 4z^3 - g_2 z - g_3 = 4(z - e_1)(z - e_2)(z - e_3). \tag{A.1}$$

Let Δ be the parameter

$$\Delta \equiv g_2^3 - 27 g_3^2 > 0; \tag{A.2}$$

the polynomial has the following properties [58].

Three distinct real roots

The Weierstrass polynomial $w(z)$ will have three real roots if

$$g_2 > 0 \quad \text{and} \quad \Delta > 0. \tag{A.3}$$

We parameterize the (real) roots by the angle $0 \le \eta \le \pi$ as follows [58]:

$$e_3 = -\sqrt{\frac{g_2}{3}} \cos\left(\frac{\pi - \eta}{3}\right) < 0, \quad e_2 = -\sqrt{\frac{g_2}{3}} \cos\left(\frac{\pi + \eta}{3}\right),$$
$$e_1 = \sqrt{\frac{g_2}{3}} \cos\left(\frac{\eta}{3}\right) > 0,$$
$$\cos\eta = \frac{9 g_3}{\sqrt{3 g_2^3}}, \quad \sin\eta = \sqrt{\frac{\Delta}{g_2^3}} > 0. \tag{A.4}$$

With this parametrization it is obvious that $e_3 < e_2 < e_1$. The signs of $e_3 < 0$, $e_1 > 0$, and $\sin\eta > 0$ are well defined, and the sign of e_2 depends on that of g_3 ($g_3 = 4e_1e_2e_3$):

$$e_2 g_3 < 0 \quad (e_2 = 0 \Leftrightarrow g_3 = 0). \tag{A.5}$$

Two distinct real roots

The $w(z)$ will have two real roots if

$$g_2 > 0 \quad \text{and} \quad \Delta = 0. \tag{A.6}$$

This happens when one of the local extreme values of $w(z)$ is zero.

One real root

The polynomial $w(z)$ will have one real root with multiplicity 1 if

$$\Delta < 0. \tag{A.7}$$

The sign of the real root e_r

$$e_r = \frac{1}{2\cdot 9^{1/3}}\left[(9g_3+\sqrt{3}\sqrt{-\Delta})^{1/3} + (9g_3-\sqrt{3}\sqrt{-\Delta})^{1/3}\right] \tag{A.8}$$

is related to that of g_3 by

$$e_r g_3 > 0 \quad (e_r = 0 \Leftrightarrow g_3 = 0). \tag{A.9}$$

Appendix B: Re-derivation of the critical points with $\mathcal{H} = \mathcal{H}(r, n)$

With $\mathcal{H}(r, n)$ given by (31), the dynamical system reads

$$\dot{r} = \mathcal{H}_{,n}, \quad \dot{n} = -\mathcal{H}_{,r}. \tag{B.1}$$

Evaluating the derivatives we obtain

$$\begin{aligned}\mathcal{H}_{,v} &= 2h^2\left[\left(f + \frac{C_1^2}{r^4n^2}\right)(\ln h)_{,n} - \frac{C_1^2}{r^4n^3}\right],\\ \mathcal{H}_{,r} &= h^2\left(f_{,r} - \frac{4C_1^2}{r^5n^2}\right).\end{aligned} \tag{B.2}$$

Using $(\ln h)_{,n} = a^2/n$ (20), the system (B.2) reads

$$\dot{r} = \frac{2h^2}{r^4n^3}\left[a^2r^4n^2f + C_1^2(a^2-1)\right], \tag{B.3}$$

$$\dot{n} = -\frac{h^2}{r^5n^2}\left[r^5n^2f_{,r} - 4C_1^2\right]. \tag{B.4}$$

Setting the rhs to zero we obtain

$$a_c^2 = \frac{C_1^2}{r_c^4n_c^2f + C_1^2}, \tag{B.5}$$

$$f_{c,r_c} = \frac{4C_1^2}{r_cr_c^4n_c^2}. \tag{B.6}$$

Now, using (25) in (B.5) and in (B.6) we obtain $a_c^2 = v_c^2$ and $r_c(1-v_c^2)f_{c,r_c} = 4f_cv_c^2$, respectively. Since $a_c^2 = v_c^2$, the equation $r_c(1-v_c^2)f_{c,r_c} = 4f_cv_c^2$ is just the rightmost formula in (41).

For the other sonic point, $f_c = 0$ and $a_c^2 = 1$, the rhs of (B.5) is manifestly zero. The rhs of (B.6) is also zero by (25) and (41). The latter provides the value of f_{c,r_c} as the limit $r_c \to r_f$ and $a_c^2 \to 1$.

References

1. A.G. Riess et al., Astron. J. **116**, 1009 (1998)
2. J.L. Tonry et al., Astrophys. J. **594**, 1 (2003)
3. C.L. Bennett et al., Astrophys. J. Suppl. **148**, 1 (2003)
4. S. Weinberg, Rev. Mod. Phys. **61**, 1 (1989)
5. T. Padmanabhan, Phys. Rept. **380**, 235 (2003)
6. J. Polchinski. arXiv:hep-th/0603249
7. J. Martin, Comptes Rendus Phys. **13**, 566 (2012)
8. A.A. Starobinsky, Phys. Lett. B **91**, 99 (1980)
9. N. Ohta, R. Percacci, G.P. Vacca, Phys. Rev. D **92**, 061501 (2015)
10. M.U. Farooq, M. Jamil, D. Momeni, R. Myrzakulov, Can. J. Phys. **91**, 703 (2013)
11. M.R. Setare, M. Jamil, Gen. Relativ. Gravit. **43**, 293 (2011)
12. I. Hussain, M. Jamil, F.M. Mahomed, Astrophys. Space Sci. **337**, 373 (2012)
13. T. Clifton, P.G. Ferreira, A. Padilla, C. Skordis, Phys. Rep. **513**, 1 (2011)
14. S. Nojiri, S.D. Odintsov, Phys. Rep. **505**, 59 (2011)
15. M. Jamil, F.M. Mahomed, D. Momeni, Phys. Lett. B **702**, 315 (2011)
16. V. Kagramanova, J. Kunz, C. Lämmerzahl, Phys. Lett. B **634**, 465 (2006)
17. E. Hackmann, C. Lämmerzahl, Phys. Rev. D **78**, 024035 (2008)
18. L. Lombriser, F. Simpson, A. Mead, Phys. Rev. Lett. **114**, 251101 (2015)
19. S. Chakraborty, Class. Quantum. Grav **31**, 055005 (2014)
20. L. Sebastiani, S. Zerbini, Eur. Phys. J C **71**, 1591 (2011)
21. S.H. Hendi, D. Momeni, Eur. Phys. J C **71**, 1823 (2011)
22. T. Moon, Y.S. Myung, E.J. Son, Gen. Rel. Grav. **43**, 3079 (2011)
23. A. Sheykhi, Phys. Rev. D **86**, 024013 (2012)
24. M.E. Rodrigues, E.L.B. Junior, G.T. Marques, V.T. Zanchin. arXiv:1511.00569v1 [gr-qc]
25. Y.S. Myung. arXiv:1503.03559v1 [gr-qc]
26. J.M. Hoff da Silva, M. Dias, Phys. Rev. D **84**, 066011 (2011)
27. T.R.P. Carames, M.E. Guimaraes, J.M. Hoff da Silva, Phys. Rev. D **87**, 106011 (2013)
28. Z. Xiao-Ying, H. Jian-Hua, Chin. Phys. Lett. **31**, 09 (2014)
29. S.K. Chakrabarti, Phys. Rept. **266**, 229 (1996)
30. T. Matsuda, M. Inoue, K. Sawada, Mon. Not. R. Astron. Soc. **226**, 785 (1987)
31. R. Taam, B. Fryxall, Astrophys. J. **331**, L117 (1988)
32. E. Shima et al., Mon. Not. R. Astron. Soc. **217**, 367 (1985)
33. H. Bondi, Mon. Not. R. Astron. Soc. **112**, 195 (1952)

34. F.C. Michel, Astrophys. Space Sci. **15**, 153 (1972)
35. K.S. Thorne, R.A. Flammang, A.N. Zytkow, Mon. Not. R. Astron. Soc. **194**, 475 (1981)
36. S.L. Shapiro, Astrophys. J. **185**, 69 (1973)
37. S.L. Shapiro, Astrophys. J. **189**, 343 (1974)
38. W. Brinkmann, Astron. Astrophys. **85**, 146 (1980)
39. G.R. Blumenthal, W.G. Mathews, Astrophys. J. **203**, 714 (1976)
40. J. Karkowski, E. Malec, Phys. Rev. D **87**, 044007 (2013)
41. P. Mach, E. Malec, Phys. Rev. D **88**, 084055 (2013)
42. F. Ficek, Class. Quantum Grav. **32**, 235008 (2015)
43. M. Jamil, M.A. Rashid, A. Qadir, Eur. Phys. J. C **58**, 325 (2008)
44. B. Nayak, M. Jamil, Phys. Lett. B **709**, 118 (2012)
45. M. Jamil, D. Momeni, K. Bamba, R. Myrzakulov, Int. J. Mod. Phys. D **21**, 1250065 (2012)
46. D. Dwivedee, B. Nayak, M. Jamil, L.P. Singh, J. Astrophys. Astr. **35**, 97 (2014)
47. C.S.J. Pun, Z. Kovacs, T. Harko, Phys. Rev. D **78**, 024043 (2008)
48. S. Chakraborty, Class. Quantum Grav. **32**, 075007 (2015)
49. D. Perez, G.E. Romero, S.E.P. Bergliaffa, Astron. Astrophys. **551**, A4 (2013)
50. S. Soroushfar, R. Saffari, J. Kunz, C. Lämmerzahl, Phys. Rev. D **92**, 044010 (2015)
51. W. Hu, I. Sawicki, Phys. Rev. D **76**, 064004 (2007)
52. R. Saffari, S. Rahvar, Phys. Rev. D **77**, 104028 (2008)
53. A. de la Cruz-Dombriz, A. Dobado, A.L. Maroto, Phys. Rev. D **80**, 124011 (2009)
54. A.K. Ahmed, M. Azreg-Aïnou, S. Bahamonde, S. Capozziello, M. Jamil, Eur. Phys. J. C. arXiv:1602.03523 [gr-qc] **(to appear)**
55. V.V. Kiselev, Class. Quantum Grav. **20**, 1187 (2003)
56. A. Younas, S. Hussain, M. Jamil, S. Bahamonde, Phys. Rev. D **92**, 084042 (2015)
57. A. Ganguly, S.G. Ghosh, S.D. Maharaj, Phys. Rev. D **90**, 064037 (2014)
58. M. Azreg-Aïnou, Phys. Rev. D **87**, 024012 (2013)
59. L. Rezzolla, O. Zanotti, *Relativistic hydrodynamics* (Oxford University Press, Oxford, 2013)
60. E. Gourgoulhon, An introduction to relativistic hydrodynamics, in *Stellar fluid dynamics and numerical simulations: from the sun to neutron stars*, ed. by M. Rieutord, B. Dubrulle, vol. 21 (EAS Publications Series, Aussois and Cargèse, France, 2006), pp. 43–79
61. S. Weinberg, *Gravitation and cosmology: principles and applications of the general theory of relativity* (Wiley, New York, 1972)
62. P. Crawford, I. Tereno, Gen. Relativ. Gravit. **34**, 2075 (2002)
63. G.F.R. Ellis, R. Maartens, M.A.H. MacCallum, *Relativistic cosmology* (Cambridge University Press, Cambridge, 2012)
64. R.T. Jantzen, P. Carini, D. Bini, Ann. Phys. **215**, 1 (1992)
65. E. Chaverra, O. Sarbach, Class. Quantum Grav. **32**, 155006 (2015)
66. S.K. Chakrabarti, Int. J. of Mod. Phys. D **20**, 1723 (2011)
67. I. Novikov, K.S. Thorne, in *Black Holes*, ed. by C. DeWitt, B. DeWitt (Gordon and Breach, New York, 1973), p. 343
68. S.K. Chakrabarti, *Theory of transonic astrophysical flows* (World Scientific, Singapore, 1990)
69. T.P. Sotiriou, Class. Quantum Grav. **23**, 5117 (2006)
70. T. Faulkner, M. Tegmark, E.F. Bunn, Y. Mao, Phys. Rev. D **76**, 063505 (2007)
71. A. Saa, J. Math. Phys. **37**, 2346 (1996)
72. A. Sheykhi, H. Alavirad, Int. J. Mod. Phys. D **18**, 1773 (2009)
73. S. Ghosh, P. Banik, Int. J. Mod. Phys. D **24**, 1550084 (2015)
74. S.L. Shapiro, A.P. Lightman, D.M. Eardley, ApJ **204**, 187 (976)
75. R.K. Nagle, E.B. Saff, A.D. Snider, *Fundamentals of differential equations and boundary value problems*, 6th edn. (Pearson, International Edition, UK, 2012)
76. J. Polking, A. Boggess, D. Arnold, *Diffrential equations with boundary value problems*, 2nd edn. (Prentice Hall, Upper Saddle River, 2006)
77. P. Bugl, *Differential equations: matrices and models* (Prentice Hall, Englewood Cliffs, 1995)
78. M. Azreg-Aïnou, Class. Quantum Grav. **30**, 205001 (2013)
79. P. Mach, Phys. Rev. D **91**, 084016 (2015)
80. M. Jamil, Y. Myzrakulov, O. Razina, R. Myrzakulov, Astrophys. Space Sci. **336**, 315 (2011)
81. U. Debnath, M. Jamil, Astrophys. Space Sci. **335**, 545 (2011)
82. M. Jamil, Int. J. Theor. Phys. **49**, 62 (2010)
83. M. Jamil, M.A. Rashid, Eur. Phys. J. C **58**, 111 (2008)
84. M. Jamil, Int. J. Theor. Phys. **49**, 144 (2010)
85. D.-J. Liu, X.-Z. Li, Chin. Phys. Lett. **22**, 1600 (2005)
86. B.C. Paul, P. Thakur, A. Saha, Phys. Rev. D **85**, 024039 (2012)
87. P.A. Becker, M. Kafatos, Astrophys. J. **453**, 83 (1995)
88. E. Chaverra, P. Mach, O. Sarbach. arXiv:1511.07728v1 (2015)
89. J.A. de Freitas, Pacheco. J. Thermodyn. **2012**, 791–870 (2012)
90. L. Amendola, S. Tsujikawa, *Dark energy: theory and observations* (Cambridge University Press, Cambridge, 2015)

Eur. Phys. J. C (2016) 76:269
DOI 10.1140/epjc/s10052-016-4118-5

THE EUROPEAN PHYSICAL JOURNAL C

Regular Article - Theoretical Physics

Astrophysical flows near $f(T)$ gravity black holes

Ayyesha K. Ahmed[1,a], **Mustapha Azreg-Aïnou**[2,b], **Sebastian Bahamonde**[3,c], **Salvatore Capozziello**[4,5,6,d], **Mubasher Jamil**[1,e]

[1] Department of Mathematics, School of Natural Sciences (SNS), National University of Sciences and Technology (NUST), H-12, Islamabad, Pakistan
[2] Engineering Faculty, Başkent University, Bağlıca Campus, Ankara, Turkey
[3] Department of Mathematics, University College London, Gower Street, London WC1E 6BT, UK
[4] Dipartimento di Fisica, Universitá di Napoli "Federico II" Compl. Univ. di Monte S. Angelo, Edificio G, Via Cinthia, Naples 80126, Italy
[5] Gran Sasso Science Institute (INFN), Via F. Crispi 7, L' Aquila 67100, Italy
[6] INFN Sez. di Napoli Compl. Univ. di Monte S. Angelo Edificio G, Via Cinthia, 80126 Naples, Italy

Received: 13 February 2016 / Accepted: 29 April 2016 / Published online: 13 May 2016

Abstract In this paper, we study the accretion process for fluids flowing near a black hole in the context of $f(T)$ teleparallel gravity. Specifically, by performing a dynamical analysis by a Hamiltonian system, we are able to find the sonic points. After that, we consider different isothermal test fluids in order to study the accretion process when they are falling onto the black hole. We find that these flows can be classified according to the equation of state and the black hole features. Results are compared in $f(T)$ and $f(R)$ gravity.

1 Introduction

One of the most important problems in modern cosmology is the dark energy issue, which is responsible for the accelerated expansion of the observed Universe. Over the last few decades, several studies have been focused on trying to tackle this problem. It is well known that this form of energy is acting as a repulsive gravitational force so that in General Relativity (GR) one needs to consider a further non-standard fluid with a negative pressure to justify this accelerated scenario. The simplest approach is to consider a cosmological constant in order to explain it. However, from quantum considerations, the necessary expected value of it must be extremely much larger than the observed value [1]. Another approach to the cosmic accelerated behavior comes from modified theories of gravities where, instead of searching for new material ingredients, the philosophy is to address cosmic dynamics taking into account possible further degrees of freedom of the gravitational field. A very well-studied approach to modified gravity comes out from the "Teleparallel equivalent to General Relativity" (TEGR). This theory yields the same field equations as in General Relativity, so that TEGR is an alternative and equivalent theory. However, the geometrical interpretations of these theories are different. On the one hand, GR assumes a non-zero curvature and a vanishing torsion by choosing the symmetric Levi-Civita connection. On the other hand, TEGR considers an antisymmetric connection provided with a non-vanishing torsion and a zero curvature (Weitzenböck connection). In other words, one can say that GR uses the curvature to geometrize the space-time, meanwhile TEGR uses torsion to explain gravitational effects. In TEGR, we need to use tetrad fields as the dynamical variables in order to define the Weitzenböck connection (see [2–8,10–13], and also the review [14] for the basis in TEGR).

A natural generalization of TEGR is, instead of using the scalar torsion T, to consider an arbitrary and smooth function of the torsion $f(T)$ in the gravitational action [15–18]. This theory is the so-called "$f(T)$ gravity". The idea comes out naturally exactly as when GR is generalized to $f(R)$ gravity [19–22]. An important problem related to $f(T)$ gravity is that it is no longer invariant under local Lorentz transformations so that different tetrads might give rise to different solutions. Therefore one needs to be very careful choosing the correct tetrad [23]. Although TEGR is equivalent to GR, it is important to mention that $f(R)$ is no longer equivalent to $f(T)$ gravity [24]. One needs to consider a more general theory of gravity, the so-called "$f(T, B)$ gravity" to obtain the teleparallel equivalent to $f(R)$ gravity [25]. In addition, it is important to remark that $f(T)$ gravity contains only second

[a] e-mail: ayyesha.kanwal@sns.nust.edu.pk
[b] e-mail: azreg@baskent.edu.tr
[c] e-mail: sebastian.beltran.14@ucl.ac.uk
[d] e-mail: capozziello@na.infn.it
[e] e-mail: mjamil@sns.nust.edu.pk

order derivative terms; meanwhile $f(R)$ gravity contains up to fourth order derivative terms in the metric formalism.

In the last few years, $f(T)$ gravity acquired a lot of interest in cosmology due to the possibility to explain by it the accelerated expansion of the cosmic Hubble fluid (see [26–35]). In addition, astrophysical studies related with compact objects as black holes has been considered among $f(T)$ gravity such as in [36–40]. However, it is worth noticing that this is not the only solution that can be achieved by the Noether symmetry approach. As shown in [41] for $f(R)$ gravity, the symmetries select the form of the function and several Noether vectors can exist. In the specific case of $f(T)$ gravity, other solutions have been found as discussed in [42,43]. A very well-studied process, known as accretion, occurs when a fluid is situated in the vicinity of a black hole or a massive astrophysical object (see [44–47]). In this process, the compact object takes particles from the fluid and increases its mass. Accretion takes place regularly in the Universe, and it can be used to test gravitational theories using observational measurements [48–50]. The first study of accretion was performed using Newtonian gravity by Bondi [51]. He found transonic solutions for a gas accreting onto compact objects. Michel extended the later work considering GR for a Schwarzschild black hole [52]. An important work in this field has been pursued by Babichev et al., where they showed that the mass of the black hole decreases when a phantom fluid is in accretion onto it [53]. Later, Jamil and Qadir showed that primordial black holes decay earlier when the effect of accretion of phantom energy is considered [54]. In addition, Nayak and Jamil also found that primordial black holes accrete radiation, matter, and vacuum energy when they pass through radiation, matter, and vacuum dominated eras, respectively, with the result that they live longer during the radiation era [55]. After that, several works have been published on accretion onto compact objects (see [56–60]).

Recently, Ahmed et al. studied accretion for cyclic and heteroclinic flows near $f(R)$ black holes [61]. In this paper, we will use a similar formalism in order to study the accretion process in a black hole in the context of $f(T)$ gravity.

This paper is organized as follows: In Sect. 2, we briefly introduce the TEGR and $f(T)$ gravity. In Sect. 3, we discuss the metric representation of black holes in $f(T)$ gravity. Section 4 is devoted to finding the general equations for spherical accretion. In Sect. 5, we perform a dynamical system analysis using the Hamiltonian formalism and we study the system at the critical points (CPs). In Sect. 6, we obtain solutions for isothermal test fluids for different kind of fluids. In Sect. 7, we analyze the accretion process for a polytropic test fluid. Finally, in Sect. 8, we discuss our results and draw conclusions. Throughout the paper we will use the metric signature $(-,+,+,+)$ and the geometric units $G = c = 1$.

2 Teleparallel equivalent of general relativity and $f(T)$ gravity

Let us briefly introduce TEGR and its generalization which is the so-called $f(T)$ gravity. We will adopt the notation used in [25]. In this theory, the dynamical variable is the tetrad field e_a^μ (or vierbein), where Latin and Greek index indicate tangents space and space-time index, respectively. The construction of this theory relies on the relationship between the tetrad field and the metric $g_{\mu\nu}$ in the following way:

$$g_{\mu\nu} = e_\mu^a e_\nu^b \eta_{ab}\,, \tag{1}$$

$$g^{\mu\nu} = E_a^\mu E_b^\nu \eta^{ab}\,, \tag{2}$$

where $g^{\mu\nu}$ is the inverse of the metric, E_a^μ is the inverse tetrad, which satisfies the relation $E_a^\mu e_\nu^a = \delta_\nu^\mu$, and $\eta_{ab} = (-1,1,1,1)$ is the Minkowski metric. Therefore, at each point x^μ of the manifold, the tetrad field forms an orthonormal basis for the tangent space.

As we discussed before, TEGR uses a specific connection (Weitzenböck connection) where the space-time is globally flat but is endowed with a non-zero torsion tensor. This connection is defined by

$$W_\mu{}^\lambda{}_\nu = E_a^\lambda \partial_\mu e_\nu^a\,. \tag{3}$$

Then we can construct the torsion tensor using the antisymmetric part of the Weitzenböck connection as follows:

$$T^\lambda{}_{\mu\nu} = W_\mu{}^\lambda{}_\nu - W_\nu{}^\lambda{}_\mu = E_a^\lambda\left(\partial_\mu e_\nu^a - \partial_\nu e_\mu^a\right). \tag{4}$$

Using the torsion tensor, one can define the contorsion tensor

$$K_\mu{}^\lambda{}_\nu = \frac{1}{2}\left(T^\lambda{}_{\mu\nu} - T_{\nu\mu}{}^\lambda + T_\mu{}^\lambda{}_\nu\right). \tag{5}$$

In addition, it is useful to define

$$S^{\mu\nu\lambda} = \frac{1}{4}(T^{\mu\nu\lambda} - T^{\nu\mu\lambda} - T^{\lambda\mu\nu}) + \frac{1}{2}(g^{\mu\lambda}T^\nu - g^{\mu\nu}T^\lambda)\,, \tag{6}$$

where $T^\mu = T^\lambda{}_\lambda{}^\mu$ is the contraction of the torsion tensor.

Using the above tensor, the torsion scalar T can be defined as

$$T = S_\mu{}^{\nu\lambda} T^\mu{}_{\nu\lambda}. \tag{7}$$

The Riemann tensor can be expressed depending on the contorsion tensor as follows:

$$R^\lambda{}_{\mu\sigma\nu} = \nabla_\nu K_\sigma{}^\lambda{}_\mu - \nabla_\sigma K_\nu{}^\lambda{}_\mu + K_\sigma{}^\rho{}_\mu K_\nu{}^\lambda{}_\rho - K_\sigma{}^\lambda{}_\rho K_\nu{}^\rho{}_\mu\,. \tag{8}$$

Here ∇_μ represents the covariant metric derivative. Therefore, the Ricci scalar R and the torsion scalar T are related by

$$R = -T + \frac{2}{e}\partial_\mu(eT^\mu)\,, \tag{9}$$

where $e = \det(e^a_\mu)$. It is important to remark that $B = \frac{2}{e}\partial_\mu(eT^\mu)$ is a boundary term.

Instead of using the Ricci scalar R as in GR, the TEGR Lagrangian density is described by the torsion scalar T

$$S_{\rm TEGR} = \int T e\,\mathrm{d}^4x\,. \tag{10}$$

Since B is a boundary term, from (9), one can see that the TEGR action will arise to the same field equations as the Einstein–Hilbert action, making these two theories equivalent.

One important and very well-studied generalization of TEGR is to consider an arbitrary smooth function of the scalar torsion to construct the action

$$S_{f(T)} = \int f(T)e\,\mathrm{d}^4x\,. \tag{11}$$

This theory is called "$f(T)$ gravity" and it has numerous and interesting applications, for example in cosmology (see [14] for a comprehensive review of those models). One important feature of this theory is that meanwhile TEGR is an equivalent theory to GR, $f(T)$ does not produce the same field equations as $f(R)$ gravity (due to Eq. (9)) and therefore one needs to consider a generalization of (11) from $f(T) \to f(T, B)$ to find the teleparallel equivalent to $f(R)$ gravity as discussed in [25]. Starting from the action (11), the field equations read

$$\begin{aligned} &4e\Big[f_{TT}(\partial_\mu T)\Big]S_\nu{}^{\mu\lambda} + 4e^a_\nu\partial_\mu(eS_a{}^{\mu\lambda})f_T \\ &\quad - 4ef_T T^\sigma{}_{\mu\nu}S_\sigma{}^{\lambda\mu} - ef\delta^\lambda_\nu = 16\pi e\Theta^\lambda_\nu\,, \end{aligned} \tag{12}$$

where the energy-momentum tensor is defined as follows:

$$\Theta^\lambda_a = \frac{1}{e}\frac{\delta(eL_m)}{\delta e^a_\lambda}\,. \tag{13}$$

With these considerations in mind, let us start our discussion of black holes in $f(T)$ gravity.

3 Black hole in $f(T)$ gravity

The metric for a spherically symmetric black hole with mass M in $f(T)$ gravity is given by [40]

$$\mathrm{d}s^2 = -A\,\mathrm{d}t^2 + \frac{\mathrm{d}r^2}{c_3^2 A} + r^2(\mathrm{d}\theta^2 + \sin^2\theta\mathrm{d}\phi^2), \tag{14}$$

where

$$A \equiv \frac{2c_1r^2}{3c_3} - \frac{2c_5}{c_3r} = \frac{2Xr^2}{3} - \frac{2C_5}{r}, \tag{15}$$

$$\text{where}\quad c_5 \equiv c_1c_4 - c_2c_3, \tag{16}$$

$$\text{and,}\quad X \equiv \frac{c_1}{c_3};\quad C_5 \equiv \frac{c_5}{c_3}. \tag{17}$$

Here, all c_1, c_2, c_3, c_4, and c_5 are constants. The horizon is given by

$$r_h = \left(\frac{3c_5}{c_1}\right)^{1/3} = \left(\frac{3C_5}{X}\right)^{1/3}, \tag{18}$$

where we have introduced the new constants $C_5 = c_5/c_3$ and $X = c_1/c_3$, which will turn out to be very useful in the study of the dynamical system. To ensure that $r_h > 0$, C_5, and X must have the same sign: $C_5/X > 0$. Since A must be positive at spatial infinity, we must have $X > 0$ resulting in $C_5 > 0$. Upon performing the coordinate transformation

$$t = c_3t', \tag{19}$$

we bring the metric (14) to the following form, where $\alpha(r) = c_3^2A(r)$:

$$\mathrm{d}s^2 = -\alpha(r)\mathrm{d}t'^2 + \frac{\mathrm{d}r^2}{\alpha(r)} + r^2(\mathrm{d}\theta^2 + \sin^2\theta\mathrm{d}\phi^2). \tag{20}$$

This is precisely the general form of metric used in Ref. [61] where accretions of samples of $f(R)$ black holes were investigated, among which we find the solution

$$\alpha(r) \equiv 1 - \frac{2M}{r} + \beta r - \frac{\Lambda r^2}{3}. \tag{21}$$

This will serve in Sect. 6.4 as a tool for comparing accretion onto the $f(T)$ black hole (14) with that onto the $f(R)$ black hole (21).

The metric (14) being equivalent to (20), all general equations expressed in terms of α, which were derived in Ref. [61], are thus applicable to our present investigation upon replacing α by c_3^2A. However, because of their importance, we will outline their derivations below.

4 General equations for spherical accretion

Let n be the baryon number density in the fluid rest frame and $u^\mu = \mathrm{d}x^\mu/\mathrm{d}\tau$ be the four velocity of the fluid where τ is the proper time. We define the particle flux or current density by $J^\mu = nu^\mu$ where n is the particle density. From the particle conservation law, we see that the divergence of current density is zero, i.e.

$$\nabla_\mu J^\mu = \nabla_\mu(nu^\mu) = 0, \tag{22}$$

where ∇_μ is the covariant derivative. On the other hand, the energy-momentum tensor is explicitly given by

$$\Theta^{\mu\nu} = (\epsilon + p)u^\mu u^\nu + pg^{\mu\nu}, \tag{23}$$

where ϵ denotes the energy density and p is the pressure. We assume that the fluid is radially flowing in the equatorial plane ($\theta = \pi/2$), therefore $u^\theta = 0$ and $u^\phi = 0$. For the sake of simplicity, we set $u^r = u$. Using the normalization condition $u^\mu u_\mu = -1$ and (14), we obtain

$$u_t = -\frac{\sqrt{c_3^2 A + u^2}}{c_3}. \tag{24}$$

On the equatorial plane ($\theta = \pi/2$), the continuity equation (22) yields

$$\begin{aligned}\nabla_\mu(nu^\mu) &= \frac{1}{\sqrt{-g}}\partial_\mu(\sqrt{-g}nu^\mu)\\ &= \frac{1}{r^2}\partial_r(r^2 nu) = 0;\end{aligned} \tag{25}$$

or, upon integrating,

$$r^2 nu = C_1, \tag{26}$$

where C_1 is a constant of integration. The thermodynamics of simple fluids is described by [62]

$$\mathrm{d}p = n(\mathrm{d}h - T\mathrm{d}s), \quad \mathrm{d}\epsilon = h\mathrm{d}n + nT\mathrm{d}s, \tag{27}$$

where T is the temperature, s is the specific entropy, and

$$h = \frac{\epsilon + p}{n} \tag{28}$$

is the specific enthalpy. On the other hand, a theorem of relativistic hydrodynamics [62] states that the scalar $hu_\mu\xi^\mu$ is conserved along the trajectories of the fluid,

$$u^\nu\nabla_\nu(hu_\mu\xi^\mu) = 0, \tag{29}$$

where ξ^μ is a Killing vector of space-time. Considering the timelike Killing vector $\xi^\mu = (1, 0, 0, 0)$ of the metric (14), we obtain

$$\partial_r(hu_t) = 0 \quad \text{or} \quad h\sqrt{c_3^2 A + u^2} = C_2, \tag{30}$$

where C_2 is a constant of integration. It is easy to show that the specific entropy is conserved along the fluid lines: $u^\mu\nabla_\mu s = 0$. In fact, if we rewrite energy-momentum tensor $\Theta^{\mu\nu}$ (23) as $nhu^\mu u^\nu + (nh - e)g^{\mu\nu}$ [61], and then project the conservation formula of $\Theta^{\mu\nu}$ onto u^μ, we obtain

$$\begin{aligned}u_\nu\nabla_\mu\Theta^{\mu\nu} &= u_\nu\nabla_\mu[nhu^\mu u^\nu + (nh - e)g^{\mu\nu}]\\ &= u^\mu(h\nabla_\mu n - \nabla_\mu e) = -nTu^\mu\nabla_\mu s = 0.\end{aligned} \tag{31}$$

In the special case we are considering in this work where the fluid motion is radial and stationary (no dependence on time), and it conserves the spherical symmetry of the black hole, the latter equation reduces to $\partial_r s = 0$ everywhere, that is, $s \equiv$ const. Thus, the motion of the fluid is isentropic and equations (27) reduce to

$$\mathrm{d}p = n\mathrm{d}h, \quad \mathrm{d}\epsilon = h\mathrm{d}n. \tag{32}$$

Equations (26), (30), and (32) are the main equations that we will use to analyze the flow. Since s is constant, this reduces the canonical form of the equation of state (EOS) of a simple fluid $e = e(n, s)$ to the barotropic form

$$\epsilon = F(n). \tag{33}$$

From the second equation (32), we have $h = \mathrm{d}\epsilon/dn$, which yields

$$h = F'(n), \tag{34}$$

where the prime denotes differentiation with respect to n. Now, the first equation (32) yields $p' = nh'$, with $h = F'$, we obtain

$$p' = nF'', \tag{35}$$

which can be integrated by parts to derive

$$p = nF' - F. \tag{36}$$

We see that an EOS of the form $p = G(n)$ is not independent of an EOS of the form $\epsilon = F(n)$. The relation between F and G can be derived upon integrating the differential equation

$$nF'(n) - F(n) = G(n). \tag{37}$$

The local three-dimensional speed of sound a is defined by $a^2 = (\partial p/\partial\epsilon)_s$. Since the entropy s is constant, this reduces to $a^2 = \mathrm{d}p/\mathrm{d}\epsilon$. Using (32), we derive

$$a^2 = \frac{\mathrm{d}p}{\mathrm{d}\epsilon} = \frac{n\mathrm{d}h}{h\mathrm{d}n} \Rightarrow \frac{\mathrm{d}h}{h} = a^2\frac{\mathrm{d}n}{n}. \tag{38}$$

Using (34), this reduces to

$$a^2 = \frac{n\mathrm{d}h}{h\mathrm{d}n} = \frac{n}{F'}F'' = n(\ln F')'. \tag{39}$$

Since the motion is radial in the plane $\theta = \pi/2$, we have $d\theta = d\phi = 0$ and the metric (14) implies the decomposition

$$\mathrm{d}s^2 = -(\sqrt{A}\mathrm{d}t)^2 + (\mathrm{d}r/c_3\sqrt{A})^2.$$

The ordinary three-dimensional speed v is defined by $v \equiv \frac{dr/\sqrt{A}}{c_3\sqrt{A}dt}$ and yields

$$v^2 = \left(\frac{u}{c_3 A u^t}\right)^2 = \frac{u^2}{c_3^2 A + u^2}, \tag{40}$$

where we have used $u^r = u = dr/d\tau$, $u^t = dt/d\tau$, $u_t = -Au^t$, and (24). This implies

$$u^2 = \frac{c_3^2 A v^2}{1-v^2} \quad \text{and} \quad (u_t)^2 = \frac{A^2}{1-v^2}, \tag{41}$$

and (26) becomes

$$\frac{r^4 n^2 c_3^2 A v^2}{1-v^2} = C_1^2. \tag{42}$$

These results will be used in the following Hamiltonian analysis.

5 Hamiltonian systems

We have derived two integrals of motion (C_1, C_2) given in (26) and (30). Let $\mathcal{H}$ be the square of the left-hand side of (30):

$$\mathcal{H} = h^2(c_3^2 A + u^2). \tag{43}$$

Using (41) the Hamiltonian (43) of the dynamical system reads

$$\mathcal{H}(r, v) = \frac{h(r, v)^2 c_3^2 A}{1-v^2}, \tag{44}$$

as derived in Ref. [61] where f has been replaced by $c_3^2 A$. We can absorb the constant c_3^2 into a redefinition of the Hamiltonian, however, we will do that in a further step of our derivation.

5.1 Sonic points

With $\mathcal{H}$ given by (44), the dynamical system reads

$$\dot{r} = \mathcal{H}_{,v}\,, \qquad \dot{v} = -\mathcal{H}_{,r} \tag{45}$$

(here the dot denotes the $\bar{t}$ derivative). Evaluating the right-hand sides we find

$$\mathcal{H}_{,v} = \frac{2c_3^2 h^2 A v}{(1-v^2)^2}\left[1 + \frac{1-v^2}{v}(\ln h)_{,v}\right], \tag{46}$$

$$\mathcal{H}_{,r} = \frac{c_3^2 h^2}{1-v^2}\left[A_{,r} + 2A(\ln h)_{,r}\right]. \tag{47}$$

Following the same approach as in Ref. [61], we arrive at

$$\dot{r} = \frac{2c_3^2 h^2 A}{v(1-v^2)^2}(v^2 - a^2), \tag{48}$$

$$\dot{v} = -\frac{c_3^2 h^2}{r(1-v^2)}[r A_{,r}(1-a^2) - 4Aa^2]. \tag{49}$$

For the CP, the right-hand sides vanish if the conditions

$$v_c^2 = a_c^2 \quad \text{and} \quad r_c(1-a_c^2)A_{c,r_c} = 4A_c a_c^2 \tag{50}$$

hold. Here $A_c \equiv A(r_c)$ and $A_{c,r_c} \equiv A_{,r}|_{r=r_c}$. They lead to

$$a_c^2 = \frac{r_c A_{c,r_c}}{r_c A_{c,r_c} + 4A_c}. \tag{51}$$

If solutions to the system of equations (50) exist, we rewrite the constant C_1^2 in (42) as

$$C_1^2 = r_c^4 n_c^2 c_3^2 v_c^2 \frac{A_c}{1-v_c^2} = \frac{r_c^5 n_c^2 c_3^2 A_{c,r_c}}{4}, \tag{52}$$

where we have used the second equation in (50). Using this in (42) we obtain the result

$$\left(\frac{n}{n_c}\right)^2 = \frac{r_c^5 A_{c,r_c}}{4}\,\frac{1-v^2}{r^4 A v^2}. \tag{53}$$

If no solution to (50), we can keep (42) as it is or introduce any point (r_0, v_0) from the phase portrait to obtain

$$n^2 = \left(\frac{C_1}{c_3}\right)^2 \frac{1-v^2}{r^4 A v^2} \quad \text{or} \quad \left(\frac{n}{n_0}\right)^2 = \frac{r_0^4 A_0 v_0^2}{1-v_0^2}\,\frac{1-v^2}{r^4 A v^2}. \tag{54}$$

The above dynamical system allows one to perform the analysis of the fluids that we are considering.

6 Isothermal test fluids

Isothermal flow is often referred to the fluid flowing at a constant temperature. In this section we find the general solution of the isothermal EOS of the form $p = k\epsilon$, that is, of the form $p = kF(n)$ (33) with $G(n) = kF(n)$ (37). Here k is the state parameter such that $(0 < k \leq 1)$ [63]. The differential equation (37) reads

$$nF'(n) - F(n) = kF(n), \tag{55}$$

yielding

$$\epsilon = F = \frac{\epsilon_c}{n_c^{k+1}}\, n^{k+1} = \frac{\epsilon_0}{n_0^{k+1}}\, n^{k+1}, \tag{56}$$

where we have chosen the constant of integration[1] so that (28) and (34) lead to the same expression for h:

$$h = \frac{(k+1)\epsilon_c}{n_c^{k+1}} n^k = \frac{(k+1)\epsilon_c}{n_c} \left(\frac{n}{n_c}\right)^k. \tag{57}$$

Using (53) or (54), we obtain

$$h^2 \propto \left(\frac{1-v^2}{v^2 r^4 A}\right)^k \tag{58}$$

and

$$\mathcal{H}(r, v) = \frac{A^{1-k}}{(1-v^2)^{1-k} v^{2k} r^{4k}}, \tag{59}$$

where all the constant factors have been absorbed into the redefinition of the time $\bar{t}$ and the Hamiltonian $\mathcal{H}$. Now we will analyze the behavior of the fluid by taking different cases for the state parameter k. For instance, we have $k = 1$ (ultra-stiff fluid), $k = 1/2$ (ultra-relativistic fluid), $k = 1/3$ (radiation fluid) and $k = 1/4$ (sub-relativistic fluid). In the case of the metric (14), Eq. (51) reduces to

$$k = \frac{2c_1 r_c^3 + 3c_5}{6c_1 r_c^3 - 9c_5} = \frac{2Xr_c^3 + 3C_5}{6Xr_c^3 - 9C_5} \tag{60}$$

and yields

$$r_c = \left(\frac{3k+1}{2(3k-1)}\right)^{1/3} r_h, \tag{61}$$

where r_h is given by (18). It is easy to see that, in order to have $r_c > r_h > 0$, we must have $C_5/X > 0$ and $1/3 < k < 1$. This fixes the values of k that yield a critical flow with the presence of a CP given by (61) and $v_c^2 = k$. In Ref. [61] we have shown that if the flow approaches the horizon with a vanishing three-dimensional speed, the pressure must diverge as

$$p \sim (r - r_h)^{-\frac{k+1}{2k}}, \tag{62}$$

if $A(r) = 0$ has a single root.

6.1 Solution for ultra-stiff fluid ($k = 1$)

The equation of state for the ultra-stiff fluids is $p = k\epsilon$ i.e. the value of state parameter is defined as $k = 1$. The Hamiltonian (59) reduces to

$$\mathcal{H} = \frac{1}{v^2 r^4}. \tag{63}$$

[1] This constant, ϵ_c/n_c^{k+1}, in (56) can be chosen as $\epsilon_\infty/n_\infty^{k+1}$ or ϵ_0/n_0^{k+1} where (ϵ_0, n_0) are energy density and number density.

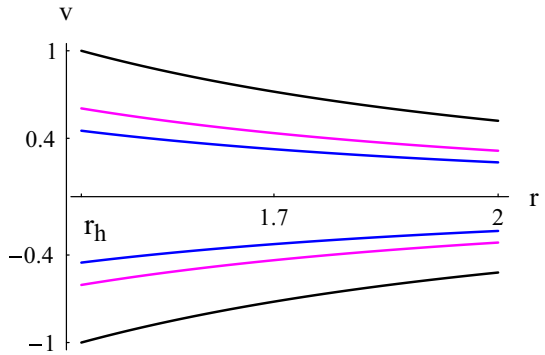

Fig. 1 Case $k = 1$. Plot of $\mathcal{H}$ (63) for $C_5 = X = 1$. The event horizon (18) is at $r_h = 3^{1/3}$. *Black plot* the solution curve corresponding to $\mathcal{H} = \mathcal{H}_{\min} = r_h^{-4}$. The *magenta and blue plots* correspond to $\mathcal{H} > \mathcal{H}_{\min}$

From (63) we see that, for physical flows ($|v| < 1$), the lower value of $\mathcal{H}$ is $\mathcal{H}_{\min} = 1/r_h^4$: $\mathcal{H} > \mathcal{H}_{\min}$. As shown in Fig. 1, physical flows are represented by the curves sandwiched by the two black curves, which are contour plots of $\mathcal{H}(r, v) = \mathcal{H}_{\min}$. The upper curves, where $v > 0$, correspond to fluid outflow or particle emission and the lower curves, where $v < 0$, correspond to fluid accretion. From (63) we see that for the global solutions, shown in Fig. 1, which are the only existing solutions for $k = 1$, the speed v behaves asymptotically as $v \sim 1/r^2$. Using this and the fact that $A \sim r^2$ in (42), we obtain $n \sim 1/r$.

6.2 Solution for ultra-relativistic fluid ($k = 1/2$)

Ultra-relativistic fluids are those fluids whose isotropic pressure is less than the energy density. In this case, the equation of state is defined as $p = \frac{\epsilon}{2}$, yielding $k = 1/2$. Using this expression in (61) reduces to $r_c = 5r_h/2$. Thus, we have two CPs given by

$$\begin{aligned} r_c &= 5r_h/2, \quad v_c = \sqrt{1/2}, \\ r_c &= 5r_h/2, \quad v_c = -\sqrt{1/2}. \end{aligned} \tag{64}$$

The Hamiltonian (59) takes the simple form

$$\mathcal{H} = \frac{\sqrt{A}}{r^2 |v| \sqrt{1-v^2}}. \tag{65}$$

For some given value of $\mathcal{H} = \mathcal{H}_0$, Eq. (65) can be solved for v^2. Another way to represent the flow is to use contour plots, as shown in Fig. 2. For the global solutions depicted in the figure, the speed v has two different asymptotic behaviors. Since $\mathcal{H}$ retains the same constant value and $A \sim r^2$, we have either (a) $v \to 0$ as $v \sim cst/r$ or (b) $v \to 1$ such that $r^2(1-v^2) \sim cst$ yielding $v \sim 1 - cst/(2r^2)$. Using these in (42), we obtain (a) $n \sim 1/r^2$ and (b) $n \sim 1/r^4$.

The plot shows three main types of fluid motion:

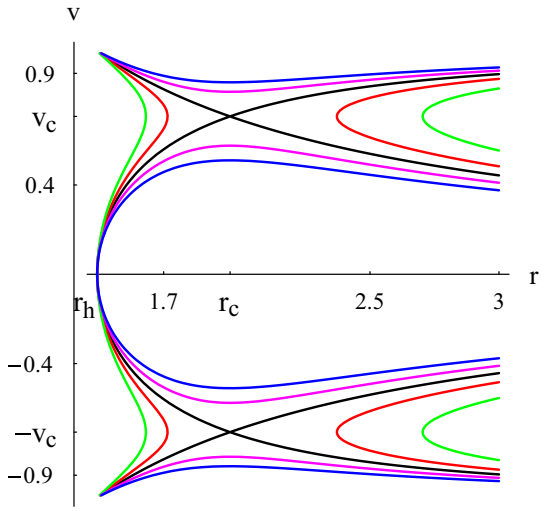

Fig. 2 Case $k = 1/2$. Plot of $\mathcal{H}$ (65) for $C_5 = X = 1$. The event horizon (18) is at $r_h = 3^{1/3}$ and $r_c = 5r_h/2$. *Black plot* the solution curve through the saddle CPs (r_c, v_c) and $(r_c, -v_c)$ corresponding to $\mathcal{H} = \mathcal{H}_c \simeq 0.646209$. The *magenta* and *blue plots* correspond to $\mathcal{H} > \mathcal{H}_c$ and the *red* and *green plots* to $\mathcal{H} < \mathcal{H}_c$

1. Purely supersonic accretion ($v < -v_c$), which ends inside the horizon, or purely supersonic outflow ($v > v_c$).
2. Purely subsonic accretion followed by subsonic flowout; this is the case of the branches of the blue and magenta solution curves corresponding to $-v_c < v < v_c$. Notice that for this motion the fluid reaches the horizon, $A(r_h) = 0$, with a vanishing speed, ensuring that the Hamiltonian (65) remains constant. The critical black solution curve reveals two types of motions: if we assume that $\mathrm{d}v/\mathrm{d}r$ is continuous at the CPs.
3. a. Supersonic accretion until $(r_c, -v_c)$, followed by a subsonic accretion until $(r_h, 0)$, where the speed vanishes, then a subsonic flowout until (r_c, v_c), followed by a supersonic flowout.
   b. Subsonic accretion followed by a supersonic accretion which ends inside the horizon. In the upper plot, we have a supersonic outflow followed by a subsonic motion.

The fluid flow in Type (3) from $(r_c, -v_c)$ to (r_c, v_c) describes a heteroclinic orbit that passes through two different saddle CPs: $(r_c, -v_c)$ and (r_c, v_c). It is easy to show that the solution curve from $(r_c, -v_c)$ to (r_c, v_c) reaches (r_c, v_c) as $\bar{t} \to -\infty$, and the curve from (r_c, v_c) to $(r_c, -v_c)$ reaches $(r_c, -v_c)$ as $\bar{t} \to +\infty$; we can change the signs of these two limits upon performing the transformation $\bar{t} \to -\bar{t}$ and $\mathcal{H} \to -\mathcal{H}$. The flowout of the fluid, which starts at the horizon, is caused by the high pressure of the fluid, which diverges there (62): The fluid under the effects of its own pressure flows back to spatial infinity. Not all solution curves shown in Fig. 2 are physical. Recall that the analysis made in this paper considers the fluid elements as test particles not modifying the geometry of the $f(T)$ black hole. It is thus assumed that the accretion does not modify the mass of the black hole nor its other intrinsic properties. The flow, being non-geodesic, however, still obeys the simple rule that if r increases, v must be positive, and if r decreases, v must be negative. For instance, for $v > 0$, we see from Fig. 2 that the red plot has two branches. Consider the branch on the right of the vertical line $r = r_c$. The flow along the segment of that branch along which v increases and r decreases is unphysical, for this is neither an accretion nor a flowout.

6.3 Solutions for radiation fluid ($k = 1/3$) and sub-relativistic fluid ($k = 1/4$)

Radiation fluids ($k = 1/3$) are the fluids which absorb the radiation emitted by the black hole. It is the most interesting case in astrophysics and sub-relativistic fluids ($k = 1/4$) are those fluids whose energy density exceeds their isotropic pressure. The Hamiltonian (59) for these fluids takes the following expressions, respectively:

$$\mathcal{H} = \frac{A^{2/3}}{r^{4/3}|v|^{2/3}(1-v^2)^{2/3}} \qquad (k = 1/3), \tag{66}$$

$$\mathcal{H} = \frac{A^{3/4}}{r\sqrt{|v|}(1-v^2)^{3/4}} \qquad (k = 1/4). \tag{67}$$

As we concluded earlier in this section, there is no critical flow for these fluids and for all fluid cases where $k \leq 1/3$; rather, simple fluid flow characterizes this class of fluids. Moreover, the fluid flow for this class of fluids is not global, in that it does not extend to spatial infinity except in the case $k = 1/3$ where the flow can be global and non-global. This conclusion can be derived from (59) as follows. If the flow is global, v behaves asymptotically as

$$v \simeq v_0 r^{-\alpha} + v_\infty, \tag{68}$$

where $\alpha > 0$, v_0, and $|v_\infty| \leq 1$ are constants. If we assume that the flow is global, that is, r may go to infinity, the Hamiltonian (59) behaves in the limit $r \to \infty$ as

$$\begin{aligned} &\mathcal{H} \propto r^{2(1-3k+k\alpha)} && (v_\infty = 0), \\ &\mathcal{H} \propto r^{2(1-3k)} && (0 < |v_\infty| < 1), \\ &\mathcal{H} \propto r^{2(1-3k)+(1-k)\alpha} && (|v_\infty| = 1). \end{aligned} \tag{69}$$

Thus, in the case $k < 1/3$, the Hamiltonian diverges at spatial infinity. Since the Hamiltonian is a constant of motion, the assumption that r goes to infinity is not valid. For $k = 1/3$ global flow is possible, as we shall justify below; however, non-global flow is also realizable. Figure 3 depicts typical non-global fluid flows for this class of fluids where $k \leq 1/3$. Let r_{rm} be the r coordinate of the rightmost point on the solution curve. We observe:

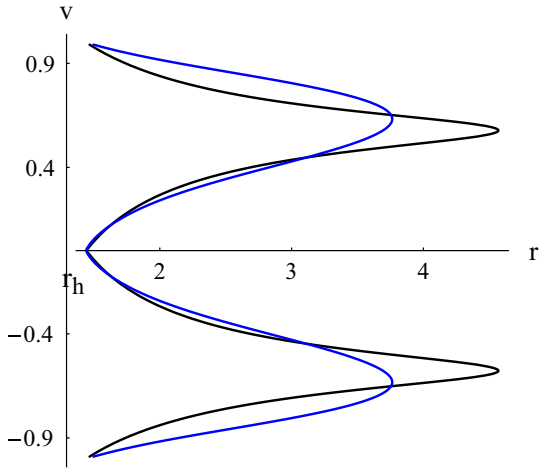

Fig. 3 Case $k \leq 1/3$. *Black plot* contour plots of $\mathcal{H}$ (66) for $C_5 = X = 1$ (k=1/3). *Blue plot* contour plots of $\mathcal{H}$ (67) for $C_5 = X = 1$ (k=1/4). The event horizon (18) is at $r_h = 3^{1/3}$

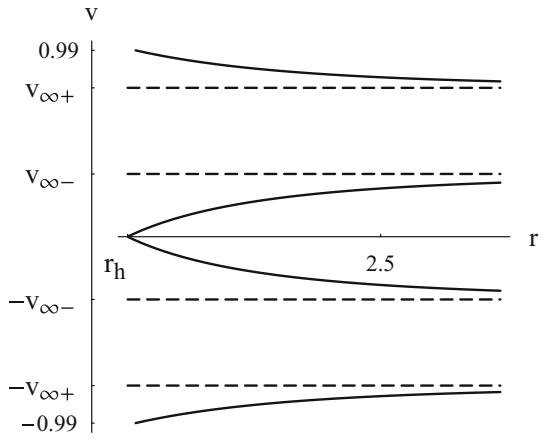

Fig. 4 Case $k = 1/3$. Contour plots of the Hamiltonian (66) with value (70) $\mathcal{H} = 2.25(2X/3)^{2/3} > (3X^2)^{1/3}$ for $C_5 = X = 1$ showing a global solution. The event horizon (18) is at $r_h = 3^{1/3}$, $v_{\infty-} = 1/3$, and $v_{\infty+} = \sqrt{(17 - \sqrt{33})/18} \simeq 0.79076$

1. (Generally supersonic) accretion from $r_{\rm rm}$ that crosses the horizon with the speed of light. Such a flow is possible if a fluid source is available at $r_{\rm rm}$ that injects fluid particles with a non-vanishing speed.
2. (Almost subsonic) accretion from $r_{\rm rm}$ that reaches the horizon with a vanishing speed, followed by a (almost subsonic) flowout back to $r_{\rm rm}$. Such a flow could be made possible if a source-sink system is available at $r_{\rm rm}$.
3. (Generally supersonic) flowout that emanates from the horizon with the speed of light and reaches $r_{\rm rm}$ with a non-vanishing speed. Such a flow is possible if a sink is available at $r_{\rm rm}$.

Now, if $k = 1/3$ and $0 < |v_\infty| < 1$, the Hamiltonian (69) has a finite limit as $r \to \infty$, so global flow is possible. To achieve it, that is, to determine such global flow solutions, notice that the value of the Hamiltonian (66) in this case is

$$\mathcal{H} = \frac{1}{|v_\infty|^{2/3}(1 - v_\infty^2)^{2/3}} \left(\frac{2X}{3}\right)^{2/3} \qquad (0 < |v_\infty| < 1). \tag{70}$$

Since $0 < |v_\infty| < 1$, we have $0 < |v_\infty|^{2/3}(1 - v_\infty^2)^{2/3} \leq 4^{1/3}/3$. Hence, to have such global flow solutions, we must restrict the value of the Hamiltonian by

$$\mathcal{H} \geq \frac{3}{4^{1/3}} \left(\frac{2X}{3}\right)^{2/3} = (3X^2)^{1/3}. \tag{71}$$

Non-global solutions correspond to $0 < \mathcal{H} < (3X^2)^{1/3}$. Notice also that for a given value of $\mathcal{H} > (3X^2)^{1/3}$, there are two possible values of $|v_\infty|$, denoted by $(v_{\infty-}, v_{\infty+})$, such that $v_{\infty-}^2 < 1/3$ and $v_{\infty-}^2 > 1/3$; for $\mathcal{H} = (3X^2)^{1/3}$ we have $v_{\infty-}^2 = v_{\infty+}^2 = 1/3$. It is easy to show that for $v_\infty = v_{\infty-}$, $v_0 < 0$, and that for $v_\infty = v_{\infty+}$, $v_0 > 0$, as shown in Fig. 4. Figure 4 depicts a typical global fluid flow for $k = 1/3$. We observe three types of flow:

1. (Supersonic) accretion with an initial velocity $-v_{\infty+}$ that crosses the horizon with the speed of light.
2. (Subsonic) accretion with an initial velocity $-v_{\infty-}$ that reaches the horizon with a vanishing speed, followed by a (subsonic) flowout that reaches spatial infinity with the same speed $v_{\infty-}$.
3. (Supersonic) flowout that emanates from the horizon with the speed of light and reaches spatial infinity with a speed $v_{\infty+}$.

For the global flow, we determine the particle density n as follows. Equation (70) with $\mathcal{H}$ given by the right-hand side of (66) yields

$$A = \frac{2X}{3} \frac{|v|(1 - v^2)}{|v_\infty|(1 - v_\infty^2)} r^2. \tag{72}$$

Substituting this in (42) we obtain

$$n^2 = \frac{N^2}{|v|^3 r^6}, \tag{73}$$

where all constants (X, c_3, v_∞) have been grouped or absorbed into the new constant N^2. Since asymptotically $|v| \to v_{\infty\pm}$, which is a non-zero constant, $n \sim r^{-3}$.

6.4 Accretions in $f(T)$ and $f(R)$ gravities

We draw a comparison between accretions in $f(T)$ and $f(R)$ gravities. For that end we select from $f(R)$ gravity black

holes a similar solution (21) to the one considered here (14), that is, an anti-de Sitter-like $f(R)$ black hole [61]. The following enumeration shows similarities and differences.

1. The accretion of an isothermal perfect fluid with $k = 1$ is characterized by the presence of global solutions, which are the only existing solutions with no CPs. The speed v and the particle density n behave asymptotically as $v \sim 0$ and $n \sim 1/r$ for both gravities.
2. If the isothermal perfect fluid has $k = 1/2$, the accretion is characterized by the presence of two CPs and critical flow for both gravities. For the global solutions we have either $v \sim 0$ and $n \sim 1/r^2$ or $v \sim 1$ and $n \sim 1/r^4$.
3. (a) For $f(T)$ gravity the accretion of an isothermal perfect fluid with $k = 1/3$ has no CP nor critical flow while for $f(R)$ gravity the fluid flow has two CPs. For the global solutions of both gravities $v \sim cst$, where cst may assume any value between 0 and 1, and $n \sim 1/r^3$.
   (b) For $k < 1/3$, the accretion onto an $f(T)$ gravity black hole is again noncritical, with no CP, while that onto an $f(R)$ gravity black hole may have four CPs, as was shown in Ref. [61] for the isothermal perfect fluid with $k = 1/4$. For both gravities there are no global solutions.

This, however, is just a qualitative comparison. First of all notice that the black hole (21) of the $f(R)$ gravity reduces to that of GR and the theory itself reduces to GR, $f(R) = R + \Lambda$, if the $f(R)$-parameter $\beta = 0$. This is not the case with the black hole (14) of the $f(T)$ gravity which does not reduce to any of the known GR black holes no matter how the $f(T)$-parameters (X, C_5) are chosen.

A deeper investigation should focus on the evaluation of the rates of accretion and efficiencies of the outgoing spectra for different black holes and different gravity theories.

The efficiency of the conversion of gravitational (potential) energy into radiation is one of the open problems of radial accretion onto a black hole; this is if one assumes, as most workers concluded, that the infall velocity scales almost as the free fall velocity (the case of Fig. 1 or the case of the critical subsonic accretion followed by a supersonic accretion of Fig. 2). This efficiency problem becomes more involved if we consider the critical accretion of Fig. 2 along the branch where v vanishes as $r \to r_h$ or accretions along the blue and magenta branches of the same figure. Here the three velocity has a deceleration phase from r_c to r_h and it does not scale as a free fall velocity. This is the main discovery in this work and in [61]. The deceleration of the fluid increases by far the conversion efficiency; moreover, the efficiency is roughly proportional to n^2 [64], which diverges by (54) as $r \to r_h$.

All that is out of the scope of this work and could be the aim and task of subsequent works. In a first step one may consider the simplest cases of the $f(T) = T$ [$f(R) = R$ or GR] gravity theory. We believe that, when all these tasks are performed (most likely numerically), the result that will be at hand will confirm the equivalence of these gravity theories.

7 Polytropic test fluids

The polytropic equation of state is

$$p = G(n) = Kn^{\gamma}, \tag{74}$$

where K and γ are constants. For ordinary matter, one generally works with the constraint $\gamma > 1$. Inserting (74) into the differential equation (37), it is easy to establish [61] the following expressions of the specific enthalpy:

$$h = m + \frac{K\gamma n^{\gamma-1}}{\gamma - 1}, \tag{75}$$

by integration, and the three-dimensional speed of sound from (39)

$$a^2 = \frac{(\gamma - 1)Y}{m(\gamma - 1) + Y} \qquad (Y \equiv K\gamma n^{\gamma-1}), \tag{76}$$

where we have introduced the baryonic mass m. Since $\gamma > 1$, this implies $a^2 < \gamma - 1$ and, particularly, $v_c^2 < \gamma - 1$.

Using (53) or, preferably, the general expression (54), in (76) we arrive at

$$h = m\Big[1 + Z\Big(\frac{1 - v^2}{r^4 A v^2}\Big)^{(\gamma-1)/2}\Big], \tag{77}$$

where

$$Z \equiv \frac{K\gamma}{m(\gamma - 1)}\Big|\frac{C_1}{c_3}\Big|^{\gamma-1} = \text{const.} > 0; \tag{78}$$

so we have a positive constant. If the CPs exist, Z takes the special form

$$Z \equiv \frac{K\gamma n_c^{\gamma-1}}{m(\gamma - 1)}\Big(\frac{r_c^5 A_{c,r_c}}{4}\Big)^{(\gamma-1)/2} = \text{const.} > 0. \tag{79}$$

Inserting (77) into (44) we evaluate the Hamiltonian by

$$\mathcal{H} = \frac{A}{1 - v^2}\Big[1 + Z\Big(\frac{1 - v^2}{r^4 A v^2}\Big)^{(\gamma-1)/2}\Big]^2, \tag{80}$$

where $(c_3 m)^2$ has been absorbed into a redefinition of $(\bar{t}, \mathcal{H})$.

The constraint $X > 0$, in (14), yields $A_{,r} > 0$ for all r, and this implies that the constant $Z > 0$ (recall that $\gamma > 1$).

Thus, the sum of the terms inside the square parentheses in (80) is positive, while the coefficient $A/(1-v^2)$ diverges as $r \to \infty$ ($0 \leq 1-v^2 < 1$). So, the Hamiltonian too diverges as r approaches spatial infinity. Since the Hamiltonian has to remain constant on a solution curve, we conclude that there are no global solutions (solutions that extend to, or emanate from, spatial infinity). This conclusion is general and it extends to all anti-de Sitter-like solutions [61].

Since $\gamma > 1$, the solution curves do not cross the r axis at points where $v = 0$ and $r \neq r_h$, for otherwise the Hamiltonian (80) would diverge there. The curves may cross the r axis at $r = r_h$ only. The horizon (18) being a single root to $A(r) = 0$, if we assume $v \propto |r - r_h|^{\delta}$ and $\delta > 0$ near the horizon, it is easy to show that

$$|v| \propto |r - r_h|^{\frac{2-\gamma}{2(\gamma-1)}}, \tag{81}$$

that is, $\delta = (2-\gamma)/[2(\gamma-1)]$. Equation (81) being *valid* for $\delta > 0$, we see that only physical solutions with $1 < \gamma < 2$ may cross the r axis. For these values of γ, the pressure $p = Kn^{\gamma}$ diverges at the horizon as

$$p \propto |r - r_h|^{\frac{-\gamma}{2(\gamma-1)}} \qquad (1 < \gamma < 2). \tag{82}$$

Now, substituting

$$Y = m(\gamma - 1)Z\Big(\frac{1-v^2}{r^4 A v^2}\Big)^{(\gamma-1)/2}$$

into (76), we arrive at

$$a^2 = Z(\gamma - 1 - a^2)\Big(\frac{1-v^2}{r^4 A v^2}\Big)^{(\gamma-1)/2}, \tag{83}$$

which along with Eq. (51) takes the form of the following expressions at the CPs:

$$v_c^2 = Z(\gamma - 1 - v_c^2)\Big(\frac{1-v_c^2}{r_c^4 A_c v_c^2}\Big)^{(\gamma-1)/2}, \tag{84}$$

$$v_c^2 = \frac{2Xr_c^3 + 3C_5}{6Xr_c^3 - 9C_5}, \tag{85}$$

where we have used (14) to reduce the right-hand side of (51). For a given value of the positive constant Z, the resolution of this system of equations in (r_c, v_c) provides all the CPs, if there are any; the values of these are then used to determine n_c from (79).

Numerical solutions to the system of Eqs. (84) and (85) are shown in Figs. 5 and 6. The constant Z is a collection of parameters depending on the black hole and the barotropic fluid. For a given black hole solution, Z is roughly proportional to Kn_c/m. For the physical case one is generally interested in in astrophysics, $1 < \gamma < 2$, the solution curve has two CPs of the same sign of v for large values of Z (in total four CPs as in the left plot of Fig. 5). As Z reaches some critical value, Z_0, each couple of CPs of the same sign of v merge as in the middle plot of Fig. 5. Below that critical value of Z there are no CPs as in the right plot of Fig. 5. For $Z \geq Z_0$, we have heteroclinic flow between two CPs of same value of r_c and opposite values of v_c.

The critical flow in the left plot of Fig. 5 is no difference of that of Fig. 2 (black plot). The only different feature is that the former flow is non-global while the latter flow is global. Similarly, the magenta and blue curves (corresponding to $\mathcal{H} > \mathcal{H}_c$) of the left and middle plots of Fig. 5 have branches which are subsonic for the whole process of accretion-flowout as is the case of the curves of Fig. 2 corresponding to $\mathcal{H} > \mathcal{H}_c$. Another similarity emerges upon comparing the solutions with no CPs corresponding to $Z < Z_0$ (right plot of Fig. 5) with those of Fig. 3 where no CPs occur too.

A common conclusion we can draw upon comparing the solutions of this section with those of the previous one is that low pressure fluids (k and K small) do not develop critical flows (no CPs) and high pressure fluids develop critical flows but they may maintain purely subsonic, even non-relativistic, flows.

Barotropic fluids with $\gamma > 2$, if there are any, may have CPs but no critical flow and their accretion velocity never vanishes as depicted in Fig. 6. The accretion make take place along two different paths starting from rightmost point of the lower branch of Fig. 6. For large values of the Hamiltonian (this would be the case if Z is large, n, or K), the accretion along one of these two paths is almost non-relativistic for $r > r_c$, then the velocity jumps to supersonic and relativistic values as r approaches r_h. For lower values of the Hamiltonian, the accretion takes place near the CP and the polytropic fluid never reaches the horizon.

As the title of this section indicates, the analysis made in this section and in the previous ones concern accretion of *test* fluids neglecting all back-reaction effects. This rules out any homoclinic flow and motion along closed paths, as those shown in Fig. 6, where v conserves the same sign but r increases and decreases.

8 Conclusions

In this paper, we discussed in detail the accretion process of a spherically symmetric black hole in the context of $f(T)$ gravity. In order to select the form of $f(T)$ model, we adopted the Noether symmetry approach, following [40]. In particular, we discussed spherically symmetric solutions coming from $f(T) = T^m$ models (and, in general, analytic $f(T)$ models) that give rise to metrics of the form (20) and related gravitational potentials of the form (21); see [40] for details.

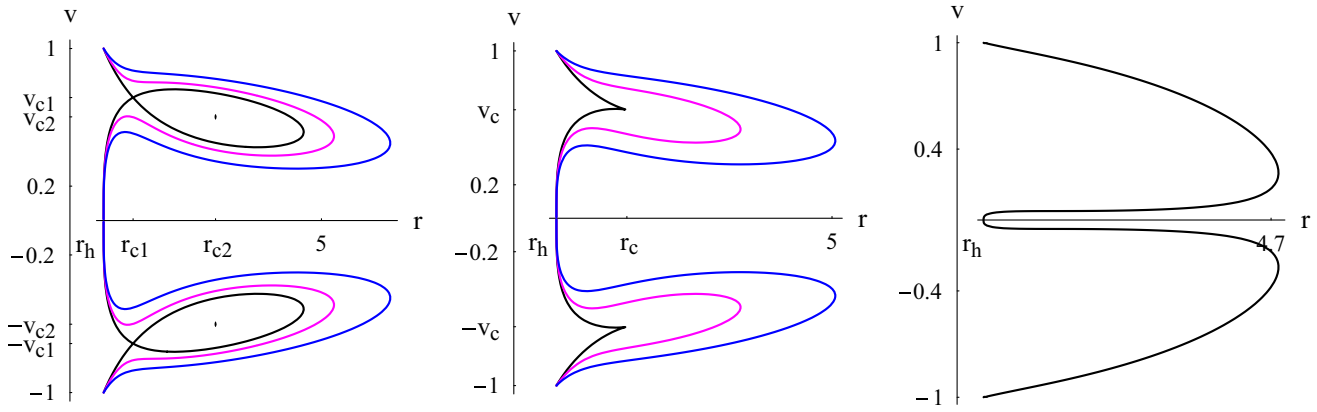

Fig. 5 Accretion of a polytropic test fluid. Contour plots of the Hamiltonian (80) for $C_5 = X = 1$, and $1 < \gamma = 5/3 < 2$ showing non-global solutions. The solutions cross the r axis at $r = r_h = 3^{1/3}$ (81). The *left plot* corresponds to $Z = 9$, $\mathcal{H} = \mathcal{H}_{c1} = 53.7813$ and the four CPs are $(r_{c1} = 1.92371, v_{c1} = 0.715054)$, $(r_{c1}, -v_{c1})$, $(r_{c2} = 3.27018, v_{c2} = 0.602669)$, and $(r_{c2}, -v_{c2})$. The CPs (r_{c2}, v_{c2}) and $(r_{c2}, -v_{c2})$ are not part of the solution curve $\mathcal{H} = \mathcal{H}_{c1}$, for $\mathcal{H}_{c2} \neq \mathcal{H}_{c1}$. The *middle plot* corresponds to $Z = Z_0 = 6.78181083$ for which each couple of CPs of the same sign of v merge with $\mathcal{H}_c = 35.8097$ and $(r_c = 2.351, v_c = 0.6482)$. The *black, magenta, and blue curves* correspond to $\mathcal{H} = \mathcal{H}_c, \mathcal{H} = \mathcal{H}_c + 3$, and $\mathcal{H} = \mathcal{H}_c + 10$, respectively. The *right plot* corresponds to $Z = 1$ and $\mathcal{H} = 20$ with no CPs

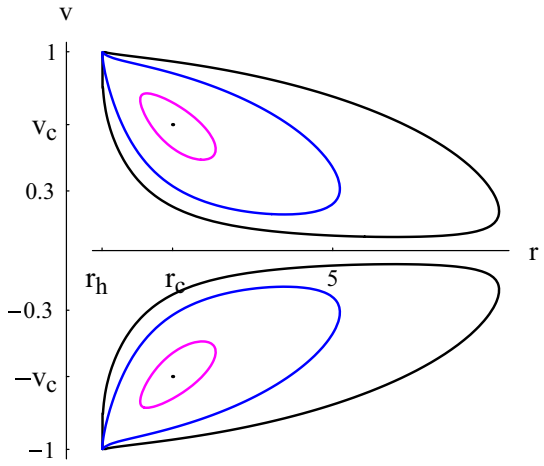

Fig. 6 Accretion of a polytropic test fluid. Contour plots of the Hamiltonian (80) for $C_5 = X = 1$, $Z = 9$, and $\gamma = 7/3 > 2$. The solution does not cross the r axis. The *magenta*, *blue*, and *black curves* correspond to $\mathcal{H} = \mathcal{H}_c + 1$, $\mathcal{H} = \mathcal{H}_c + 10$, and $\mathcal{H} = \mathcal{H}_c + 30$, respectively, with $\mathcal{H}_c = 11.8888$. The plot of $\mathcal{H} = \mathcal{H}_c$ is made of the two CPs $(r_c = 2.53004, v_c = 0.633548)$ and $(r_c, -v_c)$

We have analyzed the motion of isothermal relativistic and ultra-relativistic fluids by means of a Hamiltonian dynamical system capable of representing hydrodynamics around the black hole. The thermodynamical properties of the fluids have been discussed according to the suitable EOS. Furthermore, conserved quantities and CPs have been selected for any fluid. Roughly, the accretion mechanism can be classified as subsonic and supersonic according to the features of the black hole and the EOS. In particular, the three-dimensional velocity flow strictly depends on the EOS, the radius, and the CPs on the phase space. Finally, the results have been compared to the analog results in $f(R)$ gravity putting in evidence similarities and differences.

Clearly, the accretion process of the fluids flowing the black holes strictly depends on the conserved quantities (Noether's symmetries) and the structure of CPs, as shown above. If conserved quantities are not identified, it could become extremely difficult to define the phase space structure of the dynamical problem and consequently the features of CPs. In conclusion, identifying the Noether symmetries allows one to fix the model (i.e. the form of $f(T)$), to derive the metric and the gravitational potentials, thanks to the reduction of the dynamical system, to define the form of the space phase. Models without these features are very difficult to handle.

From a very genuinely observational point of view, these studies could be related to the possible observable features of $f(T)$ black holes. In particular, the possibility to investigate $f(T)$ vs. $f(R)$ black holes could be a powerful tool to discriminate between the curvature (GR) and torsional (TEGR) formulation of theories of gravity (see [14] for a detailed discussion). Specifically, the accretion process onto a black hole could be the feature capable of discriminating among competing models and, in general, between a curvature or a torsional formulation. A main role in this discussion is played by the stability conditions. For example, as discussed in [65] for the case of $f(R)$ gravity, the stability conditions for any self gravitating object strictly depend on the theory. There it is demonstrated that the Jeans stability criterion is different if one considers $f(R)$ instead of GR because effective mass, stability radius, Jeans wave length, and the other parameters characterizing any astrophysical object slightly change according to the underlying model. In general, if the accretor

has a mass M and a radius $\mathcal{R}$, the gravitational energy release is

$$\Delta E_{\rm acc} = \frac{GM}{\mathcal{R}}. \tag{86}$$

Clearly the accretion yield increases with the compactness $M/\mathcal{R}$, that is, given a mass M, the yields depend on the accretor radius. Considering alternative theories of gravity, the above relation can be written as

$$\Delta E_{\rm acc} = \frac{G_{\rm eff} M}{\mathcal{R}}, \tag{87}$$

where the features of the given model can be summarized using the effective gravitational coupling $G_{\rm eff}$. This means that the effective potential (related, for example, to the g_{00} component of the metric), determines the accretion process. For example, the potential (21) indicates that the extra terms with respect to the Newtonian one contribute to any accretion process by modifying the accretion yield. As discussed in Sect. 6D, differences and similarities between the $f(T)$ and $f(R)$ pictures can be put in evidence by a detailed study of the accretion process. In particular, the number of CPs, the state parameter k and other features, besides the effective potential, can discriminate among competing models. From a genuine observational point of view, luminous phenomena powered by black holes could contain features capable of discriminating among theories as soon as the parameters G, M, and $\mathcal{R}$ are combined into a gravitational potential. For example, the accretion luminosity,

$$L_{\rm acc} = \frac{GM}{\mathcal{R}}\dot{M} = \eta c^2 \dot{M}, \tag{88}$$

is a feature directly related to these phenomena. Here $\dot{M}$ is the mass variation with time. If one considers a gamma ray burst, we have $L \sim 10^{52}$ erg/s with $\dot{M} \sim 0.1 M_{\odot}/s$. As shown in [66], this huge amount of energy can be addressed in a strong field regime by curvature corrections. In other words, the role of $G_{\rm eff}$ for the adopted underlying model is crucial. Furthermore, other characterizing parameters, besides $G_{\rm eff}$, can be identified to discriminate observationally concurring accretion models: e.g. the Salpeter timescale [67], the blackbody temperature T_b for thermalization, the Eddington limit [68], and so on. These arguments will be the topic of a forthcoming paper.

Acknowledgments S.B. is supported by the Comisión Nacional de Investigación Científica y Tecnológica (Becas Chile Grant No. 72150066). S.C. is supported by INFN (*iniziativa specifica* TEONGRAV) and acknowledges the COST Action CA15117 (CANTATA).

References

1. J. Martin, Comptes Rendus Physique **13**, 566 (2012)
2. Y.N. Obukhov, J.G. Pereira, Phys. Rev. D **67**, 044016 (2003)
3. H.I. Arcos, J.G. Pereira, Int. J. Mod. Phys. D **13**, 2193 (2004)
4. R. Weitzenböck, *Invarianten Theorie* (Nordhoff, Groningen, 1923)
5. Y.M. Cho, Phys. Rev. D **14**, 2521 (1976)
6. Y.M. Cho, Phys. Rev. D **14**, 3335 (1976)
7. K. Hayashi, Phys. Lett. B **69**, 441 (1977)
8. K. Hayashi, T. Shirafuji, Phys. Rev. D **19**, 3524 (1979)
9. K. Hayashi, T. Shirafuji, Phys. Rev. D **24**, 3312 (1981)
10. W. Kopczyński, J. Phys. A **15**, 493 (1982)
11. R.T. Hammond, Rept. Prog. Phys. **65**, 599 (2002)
12. J.W. Maluf, Annalen Phys. **525**, 339 (2013)
13. R. Aldrovandi and J. G. Pereira, *Teleparallel Gravity : An Introduction*. Fundamental Theories of Physics, Vol. 173. Springer Dodrecht, Heidelberg (2013)
14. Y.F. Cai, S. Capozziello, M. De Laurentis, E. N. Saridakis. arXiv:1511.07586 [gr-qc]
15. R. Ferraro, F. Fiorini, Phys. Rev. D **75**, 084031 (2007)
16. G.R. Bengochea, R. Ferraro, Phys. Rev. D **79**, 124019 (2009)
17. B. Li, T.P. Sotiriou, J.D. Barrow, Phys. Rev. D **83**, 064035 (2011)
18. T.P. Sotiriou, B. Li, J.D. Barrow, Phys. Rev. D **83**, 104030 (2011)
19. T.P. Sotiriou, V. Faraoni, Rev. Mod. Phys. **82**, 451 (2010)
20. S. Capozziello, Int. J. Mod. Phys. D **11**, 483 (2002)
21. S. Capozziello, M. De Laurentis, Phys. Rept. **509**, 167 (2011)
22. S. Nojiri, S.D. Odintsov, Phys. Rept. **505**, 59 (2011)
23. N. Tamanini, C.G. Böhmer, Phys. Rev. D **86**, 044009 (2012)
24. K. Bamba, S. Capozziello, M. De Laurentis, S. Nojiri, D. Saez-Gomez, Phys. Lett. B **727**, 194 (2013)
25. S. Bahamonde, C.G. Böhmer, M. Wright, Phys. Rev. D **92**(10), 104042 (2015)
26. R. Myrzakulov, Eur. Phys. J. C **71**, 1752 (2011)
27. S.H. Chen, J.B. Dent, S. Dutta, E.N. Saridakis, Phys. Rev. D **83**, 023508 (2011)
28. P. Wu, H.W. Yu, Phys. Lett. B **693**, 415 (2010)
29. K. Bamba, C.Q. Geng, C.C. Lee, L.W. Luo, JCAP **1101**, 021 (2011)
30. H. Farajollahi, A. Ravanpak, P. Wu, Astrophys. Space Sci. **338**, 23 (2012)
31. G.R. Bengochea, Phys. Lett. B **695**, 405 (2011)
32. M. Jamil, D. Momeni, R. Myrzakulov, Eur. Phys. J. C **72**, 1959 (2012)
33. M. Jamil, D. Momeni, R. Myrzakulov, Eur. Phys. J. C **72**, 2075 (2012)
34. M. Jamil, D. Momeni, R. Myrzakulov, Eur. Phys. J. C **72**, 2137 (2012)
35. K. Bamba, M. Jamil, D. Momeni, R. Myrzakulov, Astrophys. Space Sci. **344**, 259 (2013)
36. R. Ferraro, F. Fiorini, Phys. Rev. D **84**, 083518 (2011)
37. T. Wang, Phys. Rev. D **84**, 024042 (2011)
38. C.G. Böhmer, A. Mussa, N. Tamanini, Class. Quant. Grav. **28**, 245020 (2011)
39. M. Hamani Daouda, M.E. Rodrigues, M.J.S. Houndjo, Eur. Phys. J. C **71**, 1817 (2011)
40. A. Paliathanasis, S. Basilakos, E.N. Saridakis, S. Capozziello, K. Atazadeh, F. Darabi, M. Tsamparlis, Phys. Rev. D **89**, 104042 (2014)
41. S. Capozziello, A. De Felice, JCAP **0808**, 016 (2008)

42. P.A. Gonzalez, E.N. Saridakis, Y. Vasquez, J. High Ener. Phys. **53** (2012)
43. S. Capozziello, P.A. Gonzalez, E.N. Saridakis, Y. Vasquez, J. High Energy Phys. **39**, 1302 (2013)
44. E. Shima, T. Matsuda, T. Hidenori, K. Sawada, MNRAS **217**, 367 (1985)
45. T. Matsuda, M. Inoue, K. Sawada, MNRAS **226**, 785 (1987)
46. S.K. Chakrabarti, Phys. Rept. **266**, 229 (1996)
47. R. Taam, B. Fryxall, Astrophys. J. **331**, L117 (1988)
48. T. Harko, Z. Kovacs, F.S.N. Lobo, Phys. Rev. D **80**, 044021 (2009)
49. C.S.J. Pun, Z. Kovacs, T. Harko, Phys. Rev. D **78**, 024043 (2008)
50. D. Perez, G.E. Romero, S.E.P. Bergliaffa, Astron. Astrophys. **551**, A4 (2013)
51. H. Bondi, MNRAS **112**, 195 (1952)
52. F.C. Michel, Astrophys. Space Sci. **15**, 153 (1972)
53. E. Babichev, V. Dokuchaev, Y. Eroshenko, Phys. Rev. Lett. **93**, 021102 (2004)
54. M. Jamil, A. Qadir, Gen. Rel. Grav. **43**, 1069 (2011)
55. B. Nayak, M. Jamil, Phys. Lett. B **709**, 118 (2012)
56. T.K. Das, A. Sarkar, Astron. Astrophys. **374**, 1150 (2001)
57. S.K. Chakrabarti, S.A. Sahu, Astron. Astrophys. **323**, 382 (1997)
58. U. Debnath, Eur. Phys. J. C **75**, 129 (2015)
59. S. Bahamonde, M. Jamil, Eur. Phys. J. C **75**, 508 (2015)
60. G.Z. Babar, M. Jamil, Y.K. Lim, Int. J. Mod. Phys. D **25**, 1650024 (2016)
61. A.K. Ahmed, M. Azreg-Aïnou, M. Faizal, M. Jamil, Eur. Phys. J. C (2016). doi:10.1140/epjc/s10052-016-4112-y. arXiv:1512.02065 [gr-qc]
62. L. Rezzolla, O. Zanotti, *Relativistic Hydrodynamics* (Oxford University Press, NY, 2013)
63. P. Mach, E. Malec, Phys. Rev. D **88**, 084055 (2013)
64. A. Treves, L. Maraschi, M. Abramowicz, Astron. Soc. Pacif. **100**, 427 (1988)
65. S. Capozziello, M. De Laurentis, I. De Martino, M. Formisano, S.D. Odintsov, Phys. Rev. D **85**, 044022 (2012)
66. S. Capozziello, G. Lambiase, Phys. Lett. B **750**, 344 (2015)
67. E.E. Salpeter, Ap. J. **140**, 796 (1964)
68. G.B. Rybicki, A.P. Lightman, *Radiative Processes in Astrophysics* (Wiley, New York, 1979)